PULSATILE VISCOUS FLOW IN FLEXIBLE-ELASTIC TUBES

A Dissertation

Presented to

the Faculty of the Graduate School

University of Missouri

In Partial Fulfillment

of the Requirements for the Degree

Doctor of Philosophy

---

by

Melvin Richard Brashears

December 1971

The undersigned, appointed by the Dean of the Graduate Faculty, have examined a thesis entitled

PULSATILE VISCOUS FLOW IN FLEXIBLE-ELASTIC TUBES

presented by Melvin Richard Brashears

a candidate for the degree of Doctor of Philosophy

and [redacted] on it is worthy of acceptance.

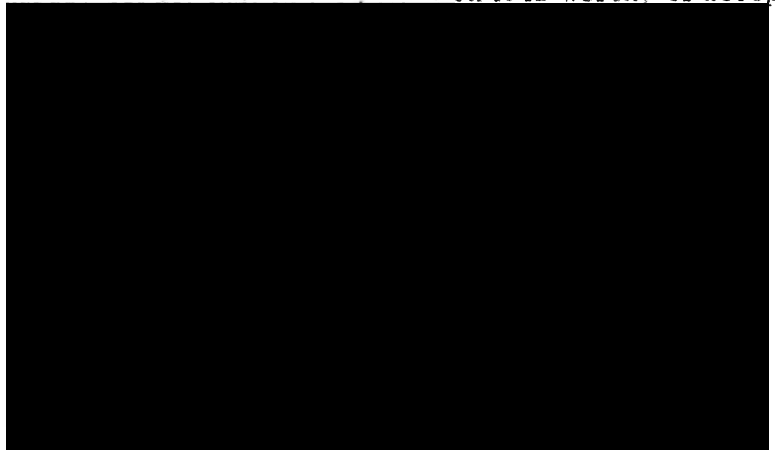

ACKNOWLEDGMENTS

The author would like to express his appreciation to Drs. F. D. Harris and J. B. Miles for the opportunity to pursue his studies at the University of Missouri at Columbia.

The assistance given the author by fellow graduate students, Messrs. W. A. Decker, J. L. Harlow, D. A. Johnson and K. B. Unklesbay is gratefully acknowledged.

Finally, the author would like to acknowledge the financial support provided by the National Science Foundation, National Aeronautics and Space Administration, and the Mechanical Engineering Department of the University of Missouri at Columbia.

This investigation was supported in part by PHS Research Grant No. US PHS-RM-00009-02 from the division of Regional Medical Programs, which is under the direction of Missouri Regional Medical Programs; the author would like to express his appreciation for this support.

TABLE OF CONTENTS

Chapter Page

Chapter Page

LIST OF TABLES

LIST OF FIGURES

Figure Page

LIST OF SYMBOLS

A	Modulus and phase of the negative of the pressure gradient
A_1	Modulus and phase of the pressure
a_o	Fourier coefficient corresponding to the mean value of the function
a_n, b_n	Fourier coefficients for the nth harmonic
C_1	Constant of integration defined in Equation (2.30)
c	Complex phase velocity
c_o	Inviscid wave velocity or modulus of the mean Fourier coefficient
c_1	Phase velocity
D	Diameter or physical constant defined in Equation (2.58).
D_1	Displacement constant defined in Equation (2.32)
E	Elastic modulus
E_c	Complex elastic modulus whose real part is E

E_1	Displacement constant defined in Equation (2.31)
E_{pk}	Slope of pressure-diameter at peak pulse value
e_{rr}	Radial strain
$e_{\theta\theta}$	Tangential strain
e_{zz}	Longitudinal strain
F_{10}	Ratio of Bessel functions, Equation (2.49)
$F(t)$, $f(t)$	Arbitrary function of time
G	Complex parameter defined in Equation (2.27)
H	Weighted wall thickness equal to h with no external constraint
H'	Complex parameter defined in Equation (2.28)
h	Wall thickness or step size for numerical integration
h_o	Zero-pressure wall thickness
i	Imaginary unit
J	Number of harmonics
J_o	Zero order Bessel function of the first kind
J_1	First order Bessel function of the first kind

K	Spring constant, per unit inner vessel wall area, of any external constraint or the number of digital points per cycle less the end point
k'	Constant defined in Equation (2.29)
L	Fluid inductance
L_1, L_2	Length of tube at states one and two
n	Harmonic number
P, p	Pressure
Q	Volumetric flow
R	Radius
r	Radial coordinate
R_i	Inner radius
R_o	Outer radius
R_s	Fluid resistance
r_{i1}, r_{i2}	Inside radius at states one and two
r_{o1}, r_{o2}	Outside radius at states one and two
T	Temperature of fluid or period of one cycle
t	time

u_r	Radial displacement
u	Tangential displacement
u_z	Axial displacement
V	Mean velocity
V_1, V_2	Volume of tube wall at states one and two
v_r	Radial velocity
v	Tangential velocity
v_z	Axial velocity
$\bar{v}_z$	Mean instantaneous axial velocity
X	Real part of c_o/c - i.e., c_o/c_1
X_1	Real part of time derivative
x	Complex parameter defined by Equation (2.26)
Y	The negative of the imaginary part of c_o/c
Y_1	Imaginary part of time derivative
z	Axial coordinate

GREEK SYMBOLS

α	Pulsatile parameter - or damping constant
β	Phase constant
γ	Complex propagation constant
η	Complex parameter defined in Equation (2.33)
θ	Angular displacement
μ	Absolute viscosity
ν	Kinematic viscosity
ρ	Fluid density
ρ_w	Tube density
σ	Poisson's ratio
σ_c	Complex Poisson's ratio of which the real part is σ
τ_{rr}	Radial stress
$\tau_{\theta\theta}$	Hoop stress
τ_{zz}	Longitudinal stress
ϕ_n	Fourier phase
ω	Radian frequency

CHAPTER I

INTRODUCTION

1.1 General

The flow of an incompressible viscous fluid through a circular tube has received considerable attention during the past fifteen years, both for steady flow [1-5] and for pulsatile flow.[6-12] The practical application of blood flow through vascular channels has served as impetus for these studies.[13-22] For the case of steady flow through an elastic tube, there is a pressure drop along the longitudinal axis due to viscous energy dissipation. The diameter of this tube is theoretically determined by the equality of the pressure difference across the wall and the elastic stress. Due to this equality there would be an expected variation in the diameter of the tube along the flow axis. However, it has been shown that this variation can be neglected for the case of laminar flow when the physical properties of the system are in the ranges of the physiological counterparts.[23]

The non-steady flow field is a much more complicated one, both theoretically and experimentally. The mathematical model describing the system consists of the usual Navier-Stokes equations, and equations of continuity, and, in addition, the equations of motion of the boundary. This

is a simultaneous set of non-linear, second order, partial differential equations representing the flow field and boundary displacement field. The boundary conditions complicate matters as the no-slip condition for velocity must be applied to a moving wall whose position is unknown. Thus a complete unsimplified theoretical solution would be very difficult and at the present time has not been obtained.

The first major progress was made in 1955 by two mathematicians working independently, Womersley and Uchida.[25] They obtained exact solutions of the Navier-Stokes equations for the case of pulsatile flow in rigid tubes. This greatly simplifies the mathematical model as the system reduces to one linear ordinary differential equation which can be integrated. In 1957 Womersley[26] obtained an approximate solution for the case of a non-rigid tube. To date, this remains as the most comprehensive solution to the problem, although there have been many variations on Womersley's original model.

The main disadvantage to these solutions is that they are very laborious to apply. The solutions are given in terms of complex Bessel functions and in general require considerable calculation. To overcome this hardship another model was proposed by Fry.[27,28] He proposed a simplified model to which a solution can be conveniently obtained to the differential equation instantaneously on

an analog computer or can be found in closed form with one integration.

One of the main objectives of this study will be to investigate the aforementioned models by comparing them to experimentally measured flow fields and determine the merits and/or, disadvantages of each.

1.2 The Scope of the Investigation

This report is primarily an experimental study of the laminar pulsatile flow of an incompressible viscous fluid through a horizontal elastic tube. The three major mathematical models will be investigated to determine the applicability of each. The tendency is to apply these models directly to complicated in-vivo systems without in-vivo experimentation to determine the accuracy of the fluid mechanic assumption needed to arrive at these models.

An experimental system will be designed that does not inherently violate some of the simplifying assumptions, namely

(1) Newtonian fluid

(2) Cyclindrical symmetry

(3) Flow through "straight" tubes

(4) No body forces

(5) Isotropic wall properties

(6) Uniform geometry

(7) Laminar flow

(8) Wall thickness much smaller than radius

With these assumptions not violated, some quantitative information on the fluid mechanics assumptions can be made; e.g., the magnitude of the convective acceleration terms, second order terms and size of the radial velocity components.

The pressure gradient will also be investigated to see if a correlation exists between it and

(1) The time derivative of pressure, e.g.

$$\frac{\Delta P}{\Delta z} \simeq \frac{\Delta P}{\Delta t}\frac{\Delta t}{\Delta z} = -\frac{\Delta P}{\Delta t}\frac{1}{c}$$

(2) The diameter gradient, e.g.

$$\frac{\Delta P}{\Delta t} \simeq F\frac{\Delta D}{\Delta z}$$

where F may be a function (or perhaps a constant)

(3) The time derivative of diameter, e.g.,

$$\frac{\Delta P}{\Delta t} \simeq F\frac{\Delta D}{\Delta z} \simeq F\frac{\Delta D}{\Delta t}\frac{\Delta t}{\Delta z} = -F\frac{\Delta D}{\Delta t}\frac{1}{c}$$

These functional relationships are only suggested at this point, but will be tested experimentally to determine the applicability.

The various flow fields, calculated from the aforementioned methods of obtaining the pressure gradient, will be compared to experimentally measured flow fields. This will reveal the advantages and/or disadvantages of the theoretical solutions.

1.3 The Importance of the Study

For the application of the mentioned models, the pressure gradient must be measured. This can be done by the simultaneous measurement of pressure at two locations and the gradient found by subtracting the upstream pressure from the downstream reading and dividing by the distance between the taps. This requires two internal (inside a vessel) measurements. Thus if the number of measurements of pressure could be reduced from two to one, a considerable simplification in experimental technique would be achieved. This could be accomplished if the pressure gradient could be calculated from the time derivative of pressure. However this still requires one internal measurement (namely pressure at one position).

To alleviate internal measurements, the diameter gradient will be investigated to see if it can be correlated with the pressure gradient. This would reduce the measurements from two internal to two external. Then, as with the pressure curves, the diameter gradient-time derivative relationships will be investigated to see if the pressure gradient can be obtained from the one external measurement of diameter.

In recent years there has been considerable progress in electronic devices that can be used to monitor vessel positions. In-vitro measurements do not present near the difficulties as in-vivo ones. In the past such techniques

as x-ray, plethysmographic devices, acoustical echo systems and pulsed Doppler electronics have been used to measure vessel size both in-vitro and in-vivo. Recently pressure sensitive p-n junctions and pressure sensitive transistors are making it possible to continuously monitor vessel position very accurately. With the realistic electrical progress, a correlation of vessel position to internal flow characteristics would be very desirable.

CHAPTER II

REVIEW OF LITERATURE

2.1 Introduction

In considering the steady flow of a viscous fluid in a rigid tube, one need only be concerned with the pressure drop along the flow axis as this difference is proportional to the volume flow. This condition gives rise to "Poiseuille flow" with the familiar parabolic velocity profile. Thus the difference in pressure is the determining factor and the absolute level of pressure is immaterial. It has also been shown[23] that the Poiseuille law can be applied successfully to steady flow in elastic tubes if an "operating diameter" is used to replace the zero-pressure diameter of the tube. The flow field then becomes a strong function of the absolute pressure, as well as the pressure gradient, since the size of the tube is a function of that absolute pressure.

In an artery the flow is far from "steady" even though the direct application of the steady flow solution to certain portions of the vascular systems gives very good results. The properties of non-steady flow will be discussed in detail after an appropriate theoretical foundation has been laid.

The complete mathematical model for pulsatile flow in non-rigid tubes will be stated and then appropriate

assumptions will be made to derive the various theoretical solutions.

As was stated before, the flow field is described by the Navier-Stokes equations and equation of continuity, i.e., v_θ equal zero and all gradients in circumfrential direction vanish. This then gives rise to two Navier-Stokes equations plus continuity as the governing equations of the motion of the fluid.

Radial Navier-Stokes Equation

$$\frac{\partial v_r}{\partial t} + v_r\frac{\partial v_r}{\partial r} + v_z\frac{\partial v_r}{\partial r} = \frac{-1}{\rho}\frac{\partial P}{\partial r} + \nu\left[\frac{\partial^2 v_r}{\partial r^2} + \frac{1}{r}\frac{\partial v_r}{\partial r} + \frac{\partial^2 v_r}{\partial z^2} - \frac{v_r}{r^2}\right] \tag{2.1}$$

Axial Navier-Stokes Equation

$$\frac{\partial v_z}{\partial t} + v_r\frac{\partial v_z}{\partial r} + v_z\frac{\partial v_z}{\partial z} = \frac{-1}{\rho}\frac{\partial P}{\partial z} + \nu\left[\frac{\partial^2 v_z}{\partial r^2} + \frac{1}{r}\frac{\partial v_z}{\partial r} + \frac{\partial^2 v_z}{\partial z^2}\right] \tag{2.2}$$

Continuity

$$\frac{\partial v_r}{\partial r} + \frac{v_r}{r} + \frac{\partial v_z}{\partial z} = 0 \tag{2.3}$$

The equations of motion used for the tube wall have most often been the membrane equations.[26, 30] They are

Radial Equation of Motion

$$P - \frac{E_c h}{1 - \sigma_c^2}\left[\frac{\sigma_c}{R}\frac{\partial u_z}{\partial z} + \frac{u_r}{R^2}\right] - \rho_w H\frac{\partial^2 u_r}{\partial t^2} = 0 \tag{2.4}$$

Axial Equation of Motion

$$-\mu\left(\frac{\partial v_z}{\partial r}+\frac{\partial v_r}{\partial z}\right)+\frac{E_c h}{1-\sigma_c^2}\left(\frac{\partial^2 u_z}{\partial z^2}+\frac{\sigma_c}{R}\frac{\partial u_r}{\partial z}\right)-Ku_z-\rho_w H\frac{\partial^2 u_z}{\partial t^2}=0 \tag{2.5}$$

The coupling boundary conditions for the motion of the liquid are

$$v_r=\frac{\partial u_r}{\partial t} \quad @ \quad r=R \tag{2.6}$$

$$v_z=\frac{\partial u_z}{\partial t} \quad @ \quad r=R \tag{2.7}$$

This is a system of five simultaneous, non-linear, second order partial differential equations in the unknowns v_r, v_z, P, u_r and u_z and to date have not been solved in this complete form.

2.2 Womersley and Uchida's Rigid Solution[24, 25]

For the assumption of fully developed flow in a rigid tube under the influence of a periodic pressure gradient, the system of equations (2.1) through (2.5) reduce to the axial Navier-Stokes equation,

$$\frac{\partial v_z}{\partial t}=\frac{-1}{\rho}\frac{\partial P}{\partial z}+\nu\left(\frac{\partial^2 v_z}{\partial r^2}+\frac{1}{r}\frac{\partial v_z}{\partial r}\right) \tag{2.8}$$

Assuming the pressure gradient can be written as

$$-\frac{\partial P}{\partial z} = Ae^{in\omega t} \tag{2.9}$$

and that the velocity can be expressed in the same form, namely

$$v_z = v_1(r)e^{in\omega t} \tag{2.10}$$

equation 2.8 becomes

$$\frac{dv_1}{dr^2} + \frac{1}{r}\frac{dv_1}{dr} - \frac{in\omega v_1}{\nu} = \frac{A}{\mu} \tag{2.11}$$

The solution to this equation is

$$v_1 = \frac{A}{\rho}\frac{1}{in\omega}\left[1 - \frac{J_o\left(r\sqrt{n\omega/\nu}\, i^{3/2}\right)}{J_o\left(r\sqrt{n\omega/\nu}\, i^{3/2}\right)}\right] \tag{2.12}$$

and therefore

$$v_z = \frac{A}{\rho}\frac{1}{in\omega}\left[1 - \frac{J_o\left(\alpha i^{3/2} r/R\right)}{J_o\left(\alpha i^{3/2}\right)}\right] \tag{2.13}$$

where

$$\alpha = R\sqrt{n\omega/\nu}\ . \tag{2.14}$$

If the actual measured pressure gradient is taken as the real part of equation (2.9), the real part of equation (2.13) is the velocity profile.

The average instantaneous velocity can be found by integration of v_z across the cross section. Thus

$$\bar{v}_z = \frac{2}{R^2} \int_0^R v_z r dr \tag{2.15}$$

This yields

$$\bar{v}_z = \frac{A}{\rho} \frac{1}{in\omega} \left[1 - F_{10}\right] e^{in\omega t} \tag{2.16}$$

The volumetric flow can then be found as $Q = \pi R^2 \bar{v}_z$.

Thus, the average instantaneous velocity can be found, once the pressure gradient is expressed as the real part of equation (2.9), in terms of the physical properties of the system. Equation (2.16) is referred to as Uchida's theoretical solution in the remainder of this study.

2.3 Womersley's Elastic Solution[26]

Womersley assumes that all of the variables can be expressed as $\exp[in\omega(t - z/c)]$, which represents a traveling sinusoidal wave in complex notation, and that v_r/c, v_z/c, and $n\omega R/c$ are much less than unity. With these assumptions he performs an order of magnitude analysis on the differential equations, and concludes that the non-linear terms are of order 1/c compared with the main terms. This gives rise to

considerable simplification in that the convective acceleration terms vanish completely. He also shows that the second order terms are of order $n^2\omega^2R^2/c^2$ and therefore can be neglected. The assumed forms of the variables are then substituted into the simplified differential equations and integrated to give

$$v_r = \left[\frac{in\omega R}{2c}\left\{C_1\frac{2J_1\left(\alpha i^{3/2}r/R\right)}{\alpha i^{3/2}J_o\left(\alpha i^{3/2}\right)} + \frac{rA_1}{\rho c}\right\}\right]e^{in\omega(t - z/c)} \tag{2.17}$$

$$v_z = \left[C_1\frac{J_o\left(\alpha i^{3/2}r/R\right)}{J_o\left(\alpha i^{3/2}\right)} + \frac{A_1}{\rho c}\right]e^{in\omega(t - z/c)} \tag{2.18}$$

The velocity components are in terms of two unknown quantities at this point, the complex wave velocity c and C_1, a constant of integration.

The linear equations of motion of the boundary may also be solved by assuming the axial and radial displacements are traveling waves of form

$$u_r = D_1e^{in\omega(t - z/c)} \tag{2.19}$$

$$u_z = E_1e^{in\omega(t - z/c)} \tag{2.20}$$

The solutions to the equations of motion in terms of the unknown constants D_1 and E_1 are

$$\rho_w H n^2 \omega^2 D_1 + A_1 - \frac{E_c h}{1 - \sigma_c 2}\left(\frac{D_1}{R^2} - \frac{in\omega\sigma_c E_1}{Rc}\right) = 0 \qquad (2.21)$$

$$\rho_w H n^2 \omega^2 E_1 - KE_1 - \frac{\mu}{R}\left(\frac{n^2\omega^2 R^2 A_1}{2c^3\rho} - i^3\frac{c_1\alpha^2}{2}F_{10}\right) - \frac{E_c h}{1 - \sigma_c^2}$$

$$\left(\frac{n^2\omega^2 E_1}{c^2} + \frac{in\omega\sigma_c D_1}{Rc}\right) = 0 \qquad (2.22)$$

The boundary conditions [equations (2.6) and (2.7)] will yield two more equations after substitution of the displacement traveling wave equations into their corresponding fluid motion equation evaluated at the inner surface. After considerable rearrangement this yields

$$in\omega\Xi_1 - C_1 - \frac{A_1}{\rho c} = 0 \qquad (2.23)$$

$$D_1 - \frac{R}{2c}\left(F_{10}C_1 + \frac{A_1}{\rho c}\right) = 0 \qquad (2.24)$$

Thus, equation (2.21) through (2.24) define all the unknown constants C_1, D_1, E_1, and c. These constants can be evaluated by the simultaneous solution of the four equations.

By solving the "vanishing" coefficient determinant of the four equations, Womersley obtained an equation for the complex wave velocity as a function of system parameters and is given by

$$\frac{1}{c} = \left\{\frac{R\rho}{E_c h}\left(1 - \sigma_c^2\right)x\right\}^{1/2} = \frac{1}{c_o}\left\{\frac{E\left(1 - \sigma_c^2\right)x}{2E_c}\right\}^{1/2} = \frac{1}{c_o}(X - iY) \tag{2.25}$$

where

$$\left(1 - \sigma_c^2\right)x = G \pm \sqrt{G^2 - \left(1 - \sigma_c^2\right)H'} \tag{2.26}$$

$$G = \frac{5/4 - \sigma_c}{1 - F_{10}} + \frac{k'}{2} + \sigma_c - \frac{1}{4} \tag{2.27}$$

$$H' = \frac{1 + 2k'}{1 - F_{10}} - 1 \tag{2.28}$$

and

$$k' = \frac{H\rho_w}{R\rho}\left(1 - \frac{K}{\rho H n^2 \omega^2}\right) \tag{2.29}$$

Two important quantities are defined by equation (2.25), the true phase velocity $c_1 = c_o/X$ and the attenuation factor, $\exp(-2\pi Y/X)$.

The remaining constants can now be evaluated from equations (2.21) to (2.24) and they are

$$C_1 = \frac{A_1 \eta}{\rho c} \tag{2.30}$$

$$E_1 = \frac{A_1}{in\omega}\frac{1}{\rho c}(1 + \eta) \tag{2.31}$$

$$D_1 = \frac{R}{2c}\frac{A_1}{\rho c}\left(1 + \eta F_{10}\right) \tag{2.32}$$

where

$$\eta = \frac{2}{x\left(F_{10} - 2\sigma_c\right)} - \frac{1 - 2\sigma_c}{F_{10} - 2\sigma_c} \tag{2.33}$$

Substitution of equation (2.30) into equation (2.18) and integrating across the cross section to obtain the average instantaneous velocity gives

$$\bar{v}_z = \frac{A_1}{\rho c}\left(1 + \eta F_{10}\right)e^{in\omega(t - z/c)} \tag{2.34}$$

A_1 is the modulus and phase of the sinusoidal pressure and is related to the pressure gradient as follows

$$\frac{A_1}{\rho c} = \frac{-in\omega}{c}\frac{1}{\rho}\frac{1}{(-in\omega)}A_1 \tag{2.35}$$

by multiplying numerator and denominator by $-in\omega$. This reduces to

$$\frac{A_1}{\rho c} = \frac{1}{in\omega\rho}A \tag{2.36}$$

where A is the modulus and phase of the negative of the pressure gradient. Thus the end result is

$$\bar{v}_z = \frac{A}{in\omega\rho}\left(1 + \eta F_{10}\right)e^{in\omega(t - z/c)} \tag{2.37}$$

It can be shown that the limiting value of η as the tube becomes rigid is -1. Thus, this solution reduces to the exact rigid solution previously outlined. [see equation (2.16)].

The mean instantaneous velocity can now be calculated in terms of the measured pressure gradient A and system properties as η and F_{10} are only a function of these properties.

2.4 Fry's One-Dimensional Solution[27, 28]

Fry has suggested another model for describing blood flow in arteries. The defining equations (2.1) to (2.5) reduce to

$$\frac{\partial v_z}{\partial t} = \frac{-1}{\rho}\frac{\partial P}{\partial z} + \nu\left[\frac{\partial^2 v_z}{\partial r^2} + \frac{1}{r}\frac{\partial v_z}{\partial r}\right] \tag{2.38}$$

under his assumptions of one-dimensional flow in a rigid tube. He then hypothesizes that the shearing stress can be approximately evaluated from the Poiseuille parabolic profile, namely

$$v_z = \frac{-1}{4\mu}\frac{dP}{dz}\left(R^2 - r^2\right) \tag{2.39}$$

Thus performing the required differentiation on this and substituting the result into equation (2.38) yields

$$\frac{\partial v_z}{\partial t} = \frac{-1}{\rho}\frac{\partial P}{\partial z} - \frac{8\nu V}{R^2} \tag{2.40}$$

where V is the mean velocity. He then allows the profile to remain blunt, i.e., "slug flow" so that the equation becomes

$$\frac{\partial v_z}{\partial t} = \frac{-1}{\rho}\frac{\partial P}{\partial z} - \frac{8\nu v_z}{R^2} \tag{2.41}$$

or in terms of volumetric flow

$$L\frac{\partial Q}{\partial t} = \frac{-\partial P}{\partial z} - R_s Q \tag{2.42}$$

where

$$R_s = \frac{8\mu}{\pi R^4} \tag{2.43}$$

and

$$L = \frac{\rho}{\pi R^2} \tag{2.44}$$

The solution to equation (2.42) in complex notation is

$$Q = \frac{Ae^{in\omega t}}{R_s + in\omega L} \tag{2.45}$$

or

$$\bar{v}_z = \frac{Ae^{in\omega t}}{\pi R^2\left(R_s + in\omega L\right)} \tag{2.46}$$

The real part of equation (2.46) is the actual velocity and can be found easily in terms of the measured pressure gradient and physical properties.

2.5 Summary of Flow Models

All three flow models require the calculation of the complex modulus and phase of the negative of the pressure gradient. Uchida's rigid solution requires the additional calculation of the term F_{10}. This in turn requires the calculation of both zero and first order Bessel functions of complex arguments. Womersley's elastic solution requires all of the aforementioned calculations plus the calculations of the complex phase velocity. Thus the main advantage of Fry's model is the reduction and simplicity in the calculation. Once F_{10} has been calculated for use in Uchida's solution, it is not difficult to calculate the phase velocity for the elastic solution as it is only a function of F_{10} and the physical properties of the system.

The three results are listed here in common nomenclature for future reference.

Uchida

$$\bar{v}_z = \frac{A}{\rho} \frac{1}{in\omega}\left[1 - F_{10}\right]e^{in\omega t} \tag{2.46}$$

Womersley

$$\bar{v}_z = \frac{A}{\rho} \frac{1}{in\omega}\left[1 + \eta F_{10}\right]e^{in\omega(t - z/c)} \tag{2.47}$$

Fry

$$\bar{v}_z = \frac{A}{\pi R^2}\left[\frac{1}{R_s + in\omega L}\right]e^{in\omega t} \tag{2.48}$$

where

$$F_{10} = \frac{2J_1\left(\alpha i^{3/2}\right)}{\alpha i^{3/2} J_o\left(\alpha i^{3/2}\right)} \tag{2.49}$$

and

$$-\frac{\partial P}{\partial z} = Ae^{in\omega t} \tag{2.50}$$

2.6 Pressure-Volume Relationships

For the practical application of Womersley's theory, the elastic properties of the tube must be known. The most widely accepted model for the determination of Young's Modulus E, (i.e., slope of the stress-strain curve) is that given by Love.[32, 33]

$$E = \frac{\Delta P}{\Delta R_o} \frac{2\left(1 - \sigma^2\right) R_i^2 R_o}{R_o^2 - R_i^2} \tag{2.51}$$

This implies that plane strain exists (i.e., the tube does not change in length on inflation) during the stressed condition. Thus to determine pressure versus radius relationships, and the corresponding slope, the size of the vessel must be monitored as a function of static pressure.

Another model used somewhat is based on Laplace's equation for thin walled pressure vessels,[34]

$$\tau_{\theta\theta} = \frac{P}{h} \frac{\left(R_o + R_i\right)}{2} \tag{2.52}$$

Substitution of this equation into the equation for plane strain yields

$$E = \frac{\Delta P}{\Delta R_o} \frac{R_o^2}{h}\left(1 - \sigma^2\right) \tag{2.53}$$

A variation can be obtained by assuming plain stress exists and is found by substitution of Laplace's equation into an appropriate stress equation. This yields

$$E = \frac{\Delta P}{\Delta R_o} \frac{R_o^2}{h} \tag{2.54}$$

It should be noted that these models are all two-dimensional in that they limit either stress or strain in one plane.

2.7 Phase Velocity

The classical defining equation for the velocity of pulse transmission in a simple elastic system is given by the Moens-Korteweg equation

$$c_o = \sqrt{\frac{Eh}{2R\rho}} \tag{2.55}$$

The phase velocity resulting from Womersley's analysis was defined in terms of this elastic pulse velocity as

$$\frac{1}{c} = \frac{1}{c_o}(X - iY) \tag{2.56}$$

Other authors have proposed models for the calculation of the pulse velocity. Morgan and Kiely[9, 10] performed a theoretical analysis on the propogation of pressure waves in liquids and presented equations that modify the Moens-Kortweg equation to take into account the fluid viscosity and the internal dampening of the tube wall.

Cox[35] has extended the work of Womersley for the case of a thick-wall viscoelastic tube. He arrives at a solution for the pulse velocity in terms of a sixth order determinant that can only be solved by an iterative scheme. Furthermore the terms in the determinant require the calculation of zero and first order Bessel functions of both the first and second kind. The Bessel functions are of course frequency dependent and must all be evaluated for each harmonic of interest. For the most part the entire solution does not deviate from Womersley's, however the phase velocity exhibits the greatest departure. This amounts to less than 5% for the worst case; thus it is not very practical to apply.

Other models modify the inviscid pulse wave equation with constant multipliers, or functional parameters, to account for some of the deviations of the models from experiment. For example, Bergel[33] has shown that the equation

$$c_o = \sqrt{\frac{Eh}{2R\rho}} \sqrt{D} \qquad (2.57)$$

where

$$D = \frac{2 - h/R}{2 - 2h/R\left[1 - \sigma - 2\sigma^2\right] + \left[h/R\right]^2\left[1 - \sigma - 2\sigma^2\right] - 2\sigma^2 - 2\sigma^2} \tag{2.58}$$

accounts for finite wall thickness and the wall Poisson's ratio.

Again Womersley's solution represents a mean of most predicted models and can be used as somewhat of a standard.

2.8 Fourier Analysis

There are many techniques for representing a function of time in a quantitative form. For periodic functions of time, (pulsatile viscous flow), Fourier series analysis is ideally suited to represent that function mathematically. Any arbitrary function of time which satisfies Dirichlet's conditions can be represented by a sum of sines and cosines as follows:

$$f(t) = a_o + \sum_{n=1}^{\infty} a_n \cos n\omega t + b_n \sin n\omega t \tag{2.59}$$

where

$$a_o = \frac{1}{T}\int_{-T/2}^{T/2} f(t)\,dt \tag{2.60}$$

$$a_n = \frac{2}{T}\int_{-T/2}^{T/2} f(t) \cos n\omega t\, dt \tag{2.61}$$

$$b_n = \frac{2}{T} \int_{-T/2}^{T/2} f(t) \sin n\omega t \, dt \qquad (2.62)$$

The Dirichlet conditions are a sufficient set of restrictions for the right hand side of equation (2.59) to converge to f(t). They can be stated simply as

(1) f(t) be bounded in the interval

(2) only a finite number of discontinuities occur in the interval

(3) only a finite number of maxima and minima occur in the interval.

Courant[39] has shown that for every piecewise smooth function that is periodic of period 2π, there exists a Fourier series expansion. These conditions are always satisfied for periodic physical systems.

To represent an arbitrary function with this series, the Fourier coefficients defined in equations (2.60) to (2.62) must be found by a numerical integration of the function. This requires digital values of the function at some "small" time increment.

CHAPTER III

EXPERIMENTAL APPARATUS

3.1 Introduction

This chapter describes the experimental apparatus used in this study. The apparatus was designed to

(1) Produce pulsatile flow in the test section with capabilities of superimposing a variable mean flow component of velocity.

(2) Make simultaneous measurements of pressure and diameter at two variable locations, plus determine the corresponding gradients associated with each.

(3) Measure the instantaneous average velocity as well as the steady flow component.

(4) Keep physical parameters and dimensions in line with their physiological counterparts.

3.2 Flow System

The flow system consists of a 4.9 meter test section, which is fed by both a variable "constant head" reservoir (see Figure 3.1) and a positive displacement pulsatile pump. The steady flow component is produced by pumping fluid from the sump to the head tank. The pulsatile pump intakes from the sump and passes fluid through an output ball check valve (heart valve).

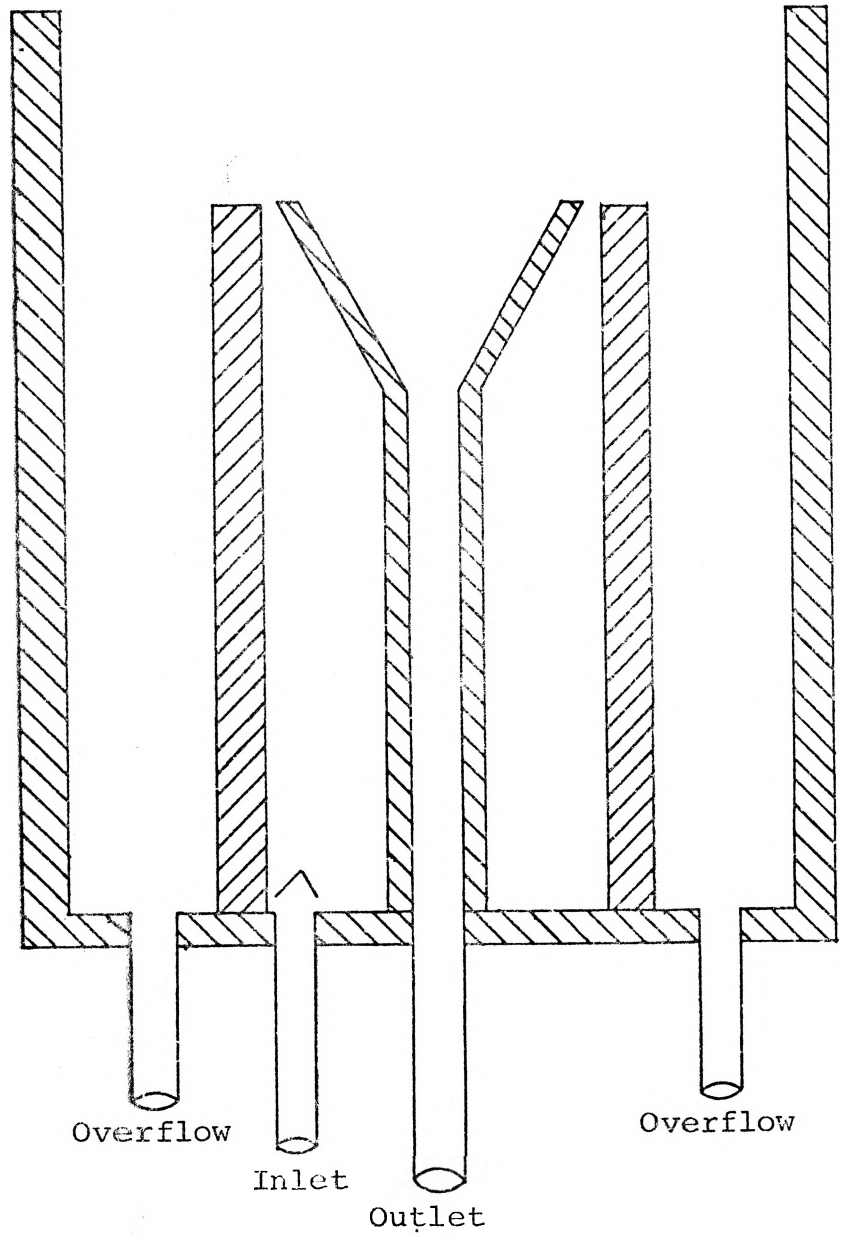

Figure 3.1 Constant Head Tank

Here the mean flow component (if any) is superimposed on the non-steady flow. The total flow now passes through a stilling reservoir, which consists of turbulence dampeners and flow straighteners, to the test section and empties into the flow meter (see Figure 3.2) and returns to the sump for future pumping. A schematic of the flow system is shown in Figure 3.3.

3.3 Pulsatile Pump

The pulsatile pump consists of positive displacement piston that is driven by an eccentric cam and connecting rod supported by a variable position fulcrum. The cam is driven by a DC motor-gear reducer combination that is regulated by a precision motor speed controller. The controller, motor and reducer were purchased from Boston Gear (Ratiotrol), Saint Louis, Missouri.

The head, with intake and output ports, is made of plexiglas and attaches to the cylinder via head bolts and is sealed with a dual purpose Silastic membrane. The piston is sealed with teflon rings. The cylinder volume between the piston and the membrane consists of light weight oil, and is filled when the piston is in bottom dead center position. Thus as positive displacement occurs the membrane is stretched to change the head volume. This gives rise to a pumping action that controls the intake and output ball valves. The frequency can be varied from 0 to 3 cycles per

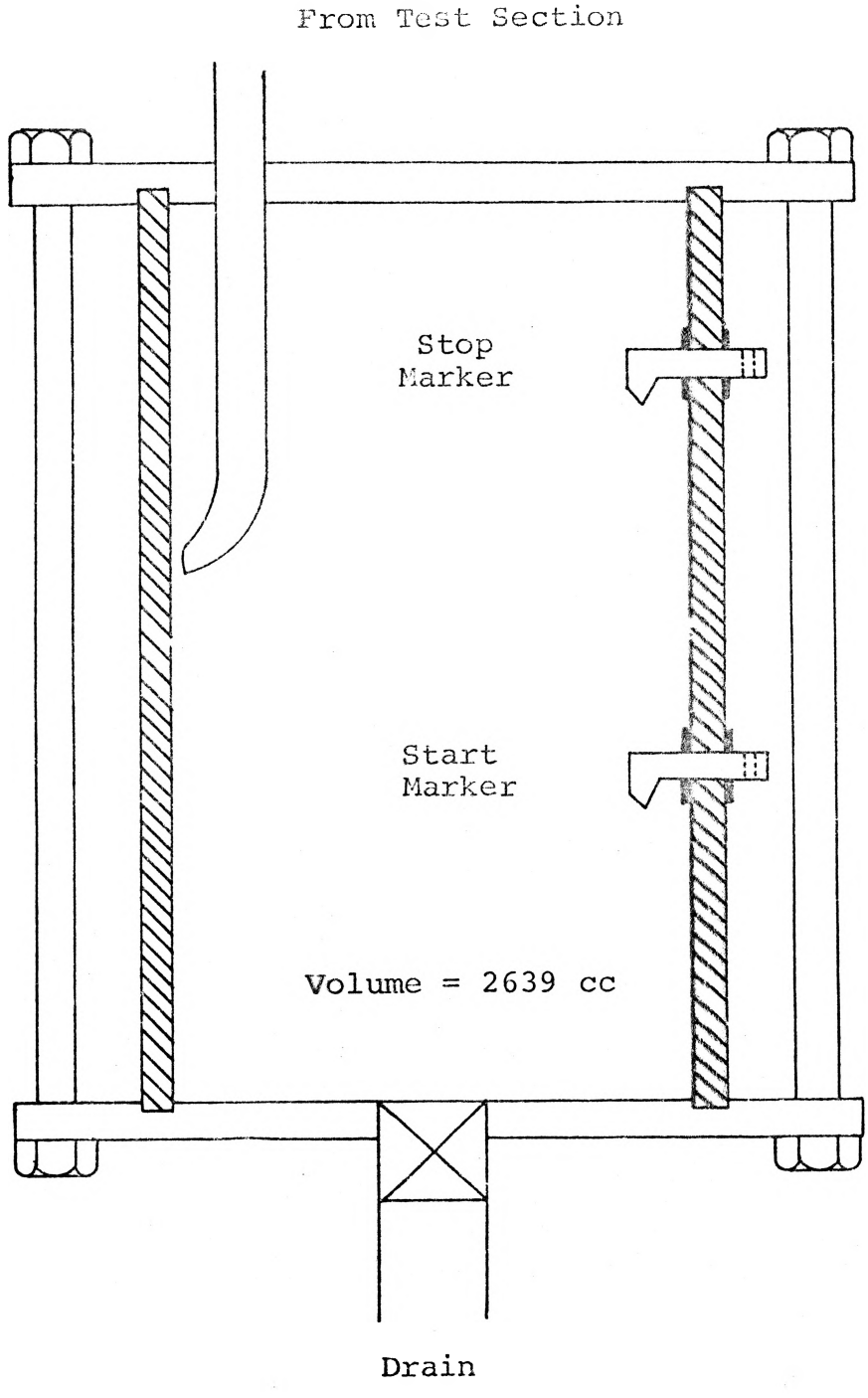

Figure 3.2 Flow Meter

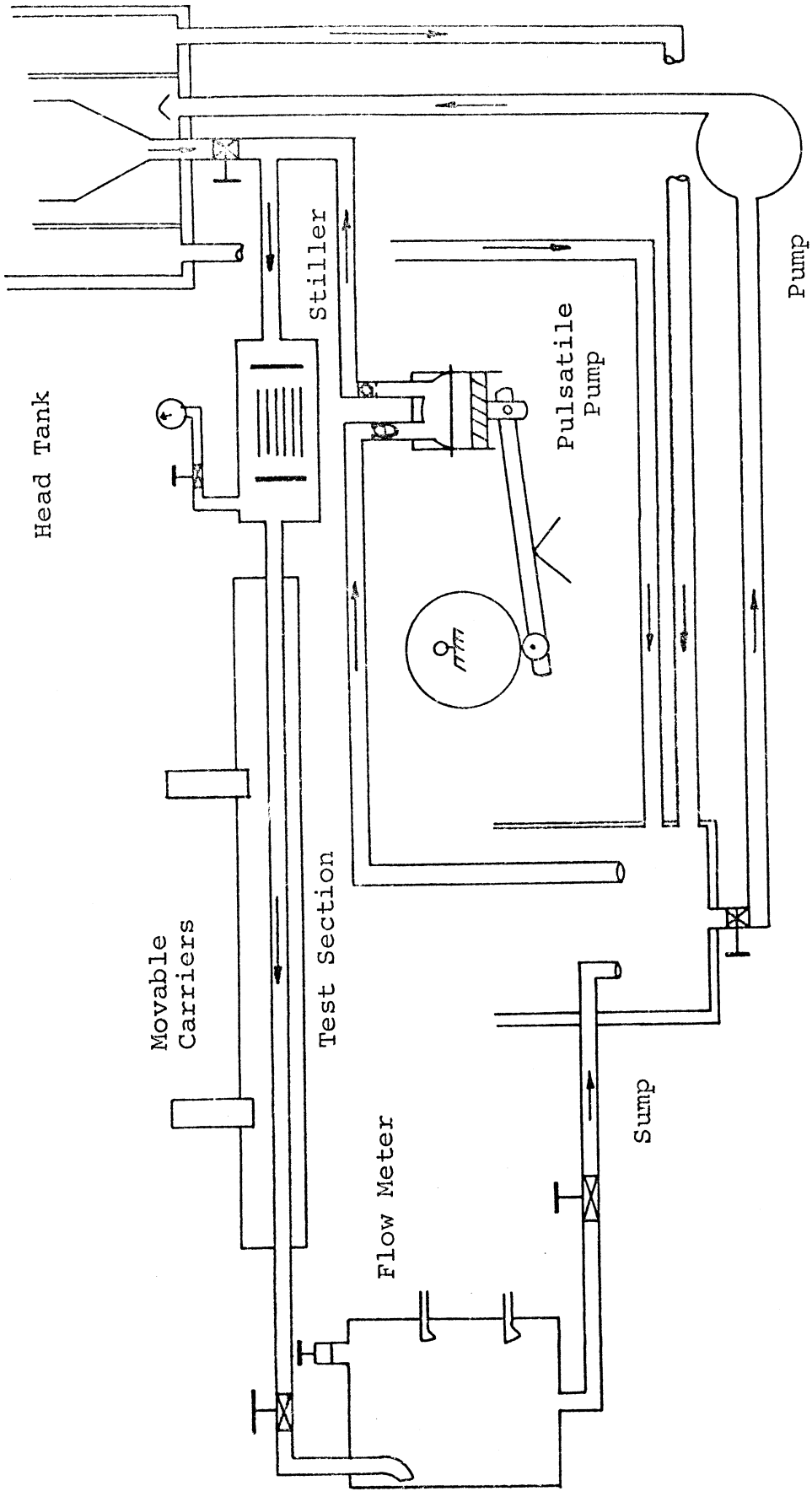

Figure 3.3 Flow System

second and the stroke from 0 to 5 cm by various combinations of cams and/or fulcrum position. However, a nominal value would be around one-half of a centimeter. A schematic is shown in Figure 3.4.

3.4 Pressure and Diameter Measuring Devices

Two identical devices were designed for the simultaneous measurement of pressure and diameter at two variable locations. Pressure was measured by piezoelectric crystal transducers. Their diaphrams are exposed to a cavity, which if fed by hypodermic needles tapped through the wall of the elastic tube. Collars on the needles can be adjusted to the exact wall thickness to ensure no penetration into the flow field.

The diameter of the tube was measured by linear variable differential transformers (LVDT). Their cores are connected to the surface of the horizontal tube. As the tube pulsates a plexiglas connecting rod transfers the motion of the tube to the core of the LVDT. Both pressure transducers and LVDT's are attached to plexiglas carriers, which can be positioned along the channel of the test section to permit measurement at various locations. See Figures 3.5 and 3.6 for sketches of pressure and diameter devices.

3.5 Velocity Measuring Device

A Doppler ultrasonic flowmeter was used to measure instantaneous velocity. The device consists of a "cuff"

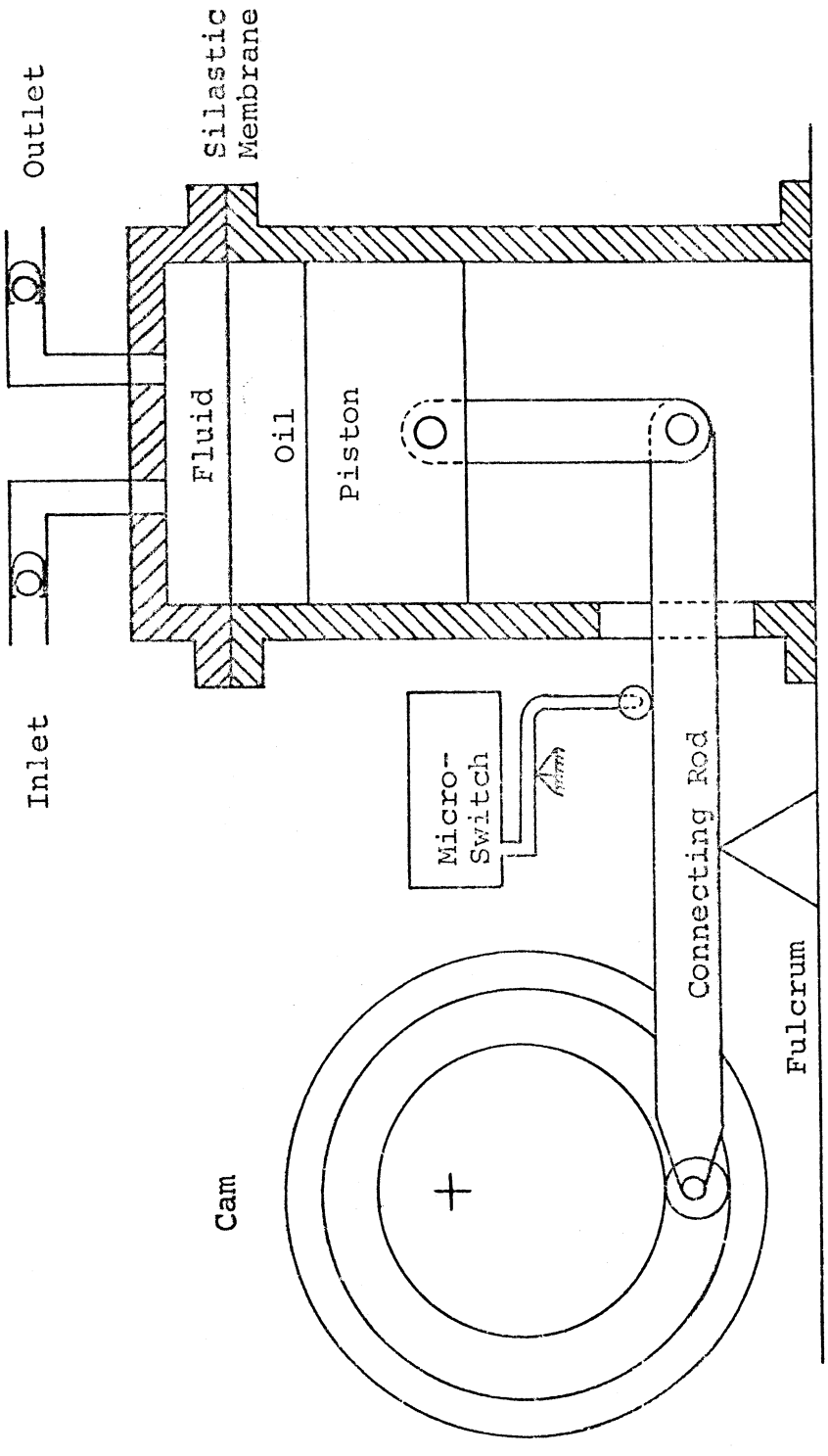

Figure 3.4 Pulsatile Pump

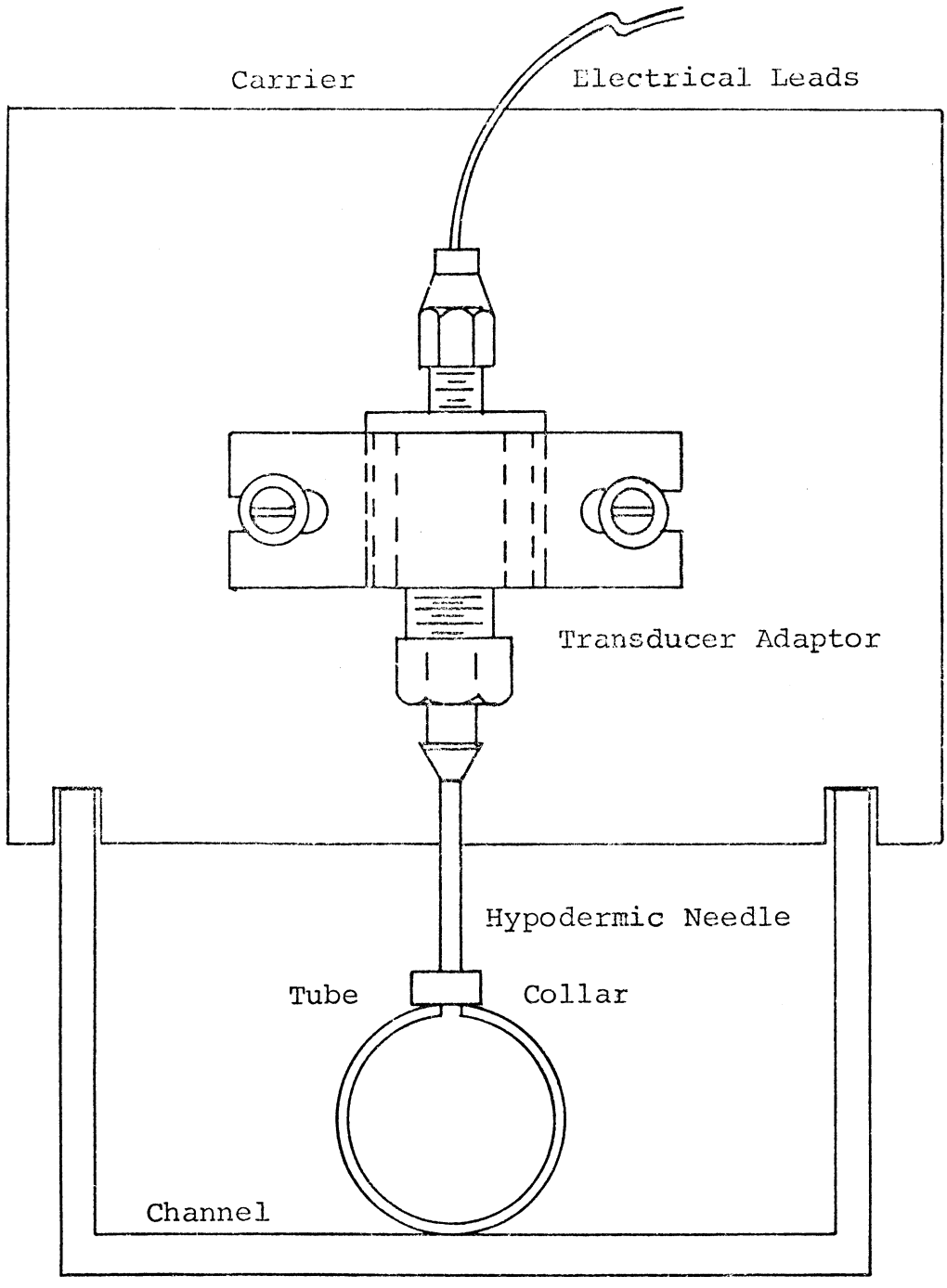

Figure 3.5 Pressure Measuring Device

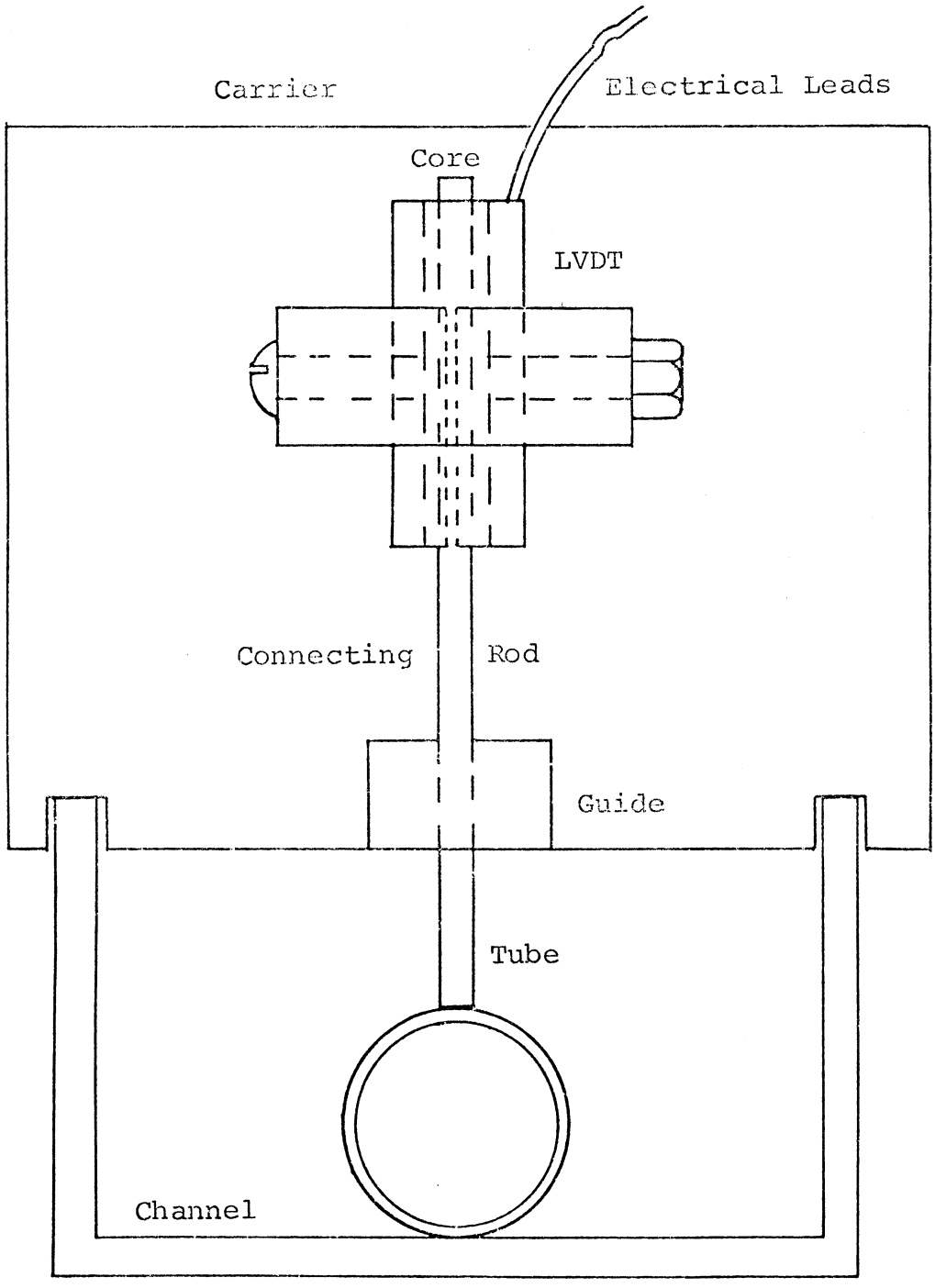

Figure 3.6 Diameter Measuring Device

made of polystyrene with two peizo-electric crystals embedded in it. The transmitting crystal sends out an acoustical wave at an angle of sixty degrees to the flow axis. The receiving crystal "sees" the acoustic velocity as the stationary speed of sound in that liquid plus the stream velocity. Thus the receiving crystal then retransmits a wave to the demodulator equal in frequency to the carrier plus the Doppler shift. The transducer demodulator accepts the varying frequencies from the receiving crystal and detects the differences between these frequencies and that of the exciter. This difference is the Doppler frequency which is then passed to a frequency converter for transformation to a voltage suitable for recording. The electronics of the system will be described in greater detail in the next section.

3.6 Electronic System

A block diagram of the system is shown in Figure 3.7. The measuring system consists of five transducers for the absolute measurement of two pressures, two diameters and instantaneous velocity. This corresponds to P_1, D_1, V, D_2, and P_2 in the diagram.

Pressure was measured with model 701A Kistler quartz pressure transducers accurate to $\pm$ 0.25 mm-hg. The charge signal output of the piezo-electric quartz crystals is then amplified and converted to a voltage in model 503 Kistler

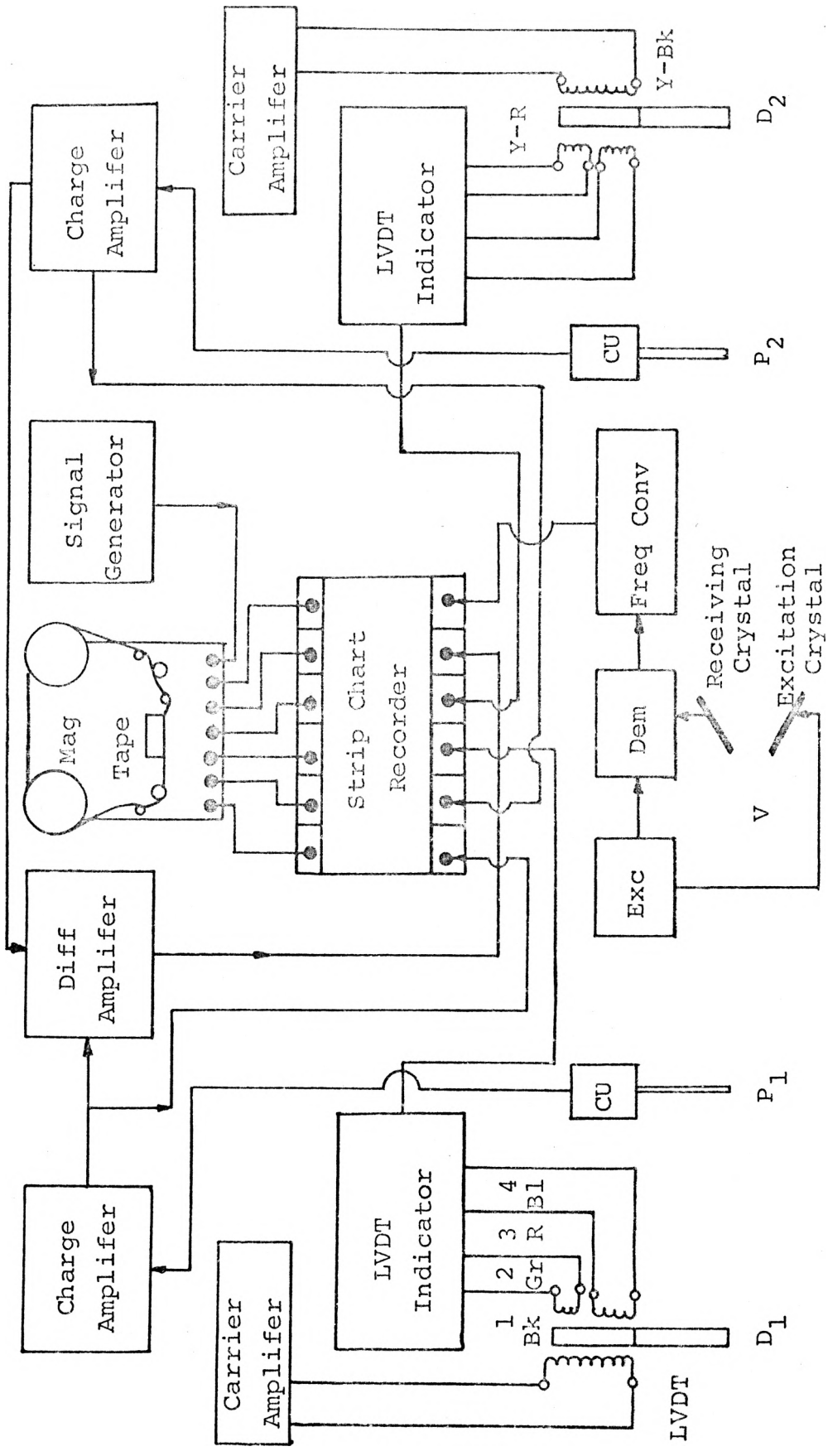

Figure 3.7 Electronic System

charge amplifiers. These analog voltages are then recorded on a strip chart recorder.

Diameter was monitored with model 300 HR Schaevitz linear variable differential transformers (LVDT) accurate to 0.001 cm. The primary excition and indicating electronics are supplied by model 300D Datronic LVDT indicators while balancing and calibrating results from Datronic type 70 input modules.

The gradients are obtained by subtracting the upstream measurement from the downstream. This is done with a Tektronix type 502A dual beam oscilloscope operating in differential mode. These differences are then outputted via the upper and lower beam vertical outputs to the strip chart recorder.

The instantaneous velocity was measured by a Ward model 1502 Doppler ultrasonic blood flowmeter. The exciter supplies a 5 mhz acoustic wave via the transmitting crystal to the integrating volume of the flow field and also to the demodulator. The receiving crystal then delivers the absolute "shifted" frequency to the demodulator which detects the difference between the two waves. This difference is then the Doppler frequency from 0 to 15 khz. The converter then transforms the frequency to a DC voltage in the range of 0 to 1 volt which in turn is recorded on strip chart.

The recorder used was a Beckman type RB 6 channel dynograph direct writing unit. All inputs to the recorder

were in the 0 to 1 volt range for zero point to full scale readings except the two diameters which were 40 mv for full scale output. The master output of the recorder was utilized to relay all six analog signals to a seven channel Ampex SP-300 FM magnetic tape recorder. The master output of the chart recorder was set so full scale stylus deflection corresponded to more than 0.5 vrms. The six signals were then stored on channels 1 to 6 of the 7 channel magnetic tape unit. The seventh channel was used as a signal channel with the input coming from a square wave generating circuit shown in Figure 3.8.

3.7 Tubes and Tube Connector

The tubes used are made of Silastic and have the following physical properties: tube A is 1.842 cm. x 1.588 cm. while tube B is 1.270 cm. x 1.016 cm. They are of the close tolerance type ($\pm$ 0.005 cm.) and were obtained from Dow Corning, Midland, Michigan.

The tube connectors are shown in Figure 3.9. They are located at the inlet and exit of the test section and have bores equal to the zero pressure diameter of the elastic tubes to minimize any pressure loss and creation of reflections.

3.8 Fluid

The fluid used is a mixture of water, pluracol V-10 (obtained from Wyandotte Chemicals, Wyandotte, Michigan) and latex paint. The percentages were varied

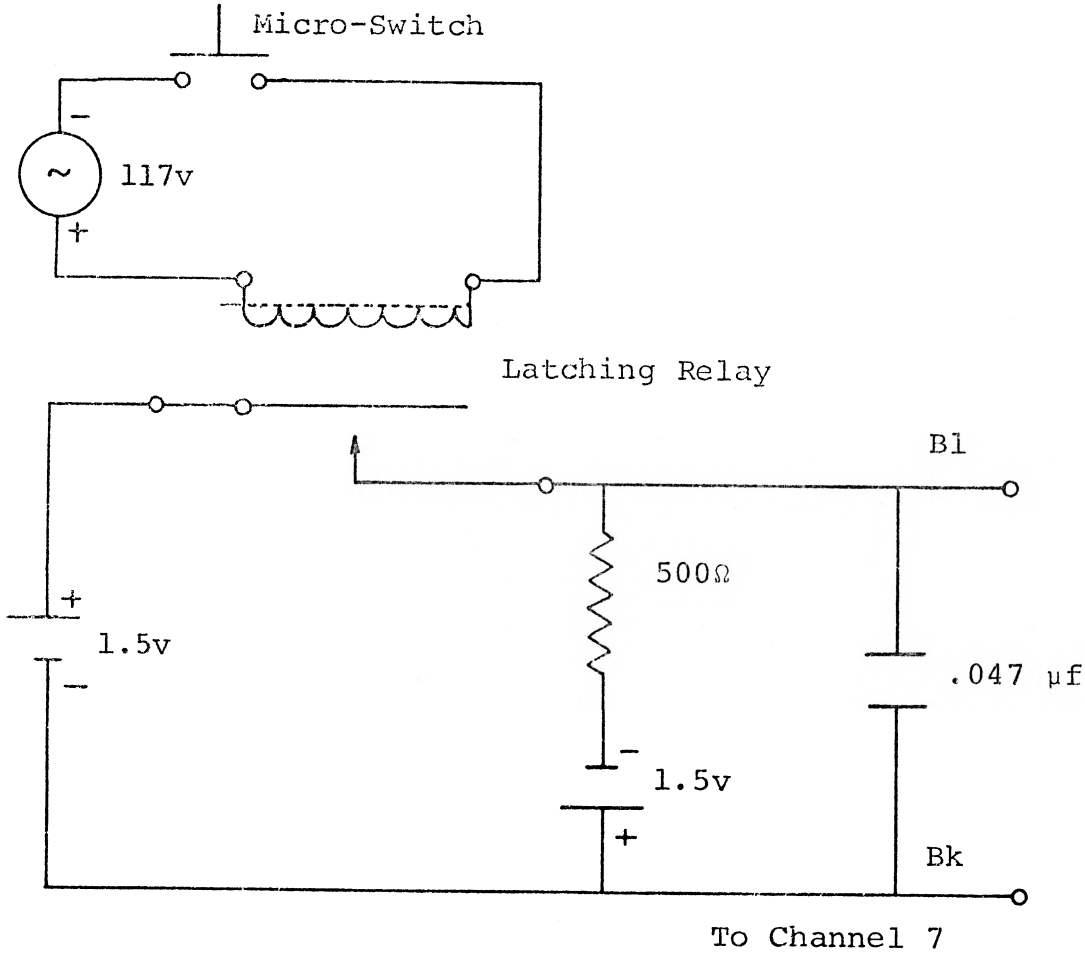

Figure 3.8 Square Wave Generating Circuit

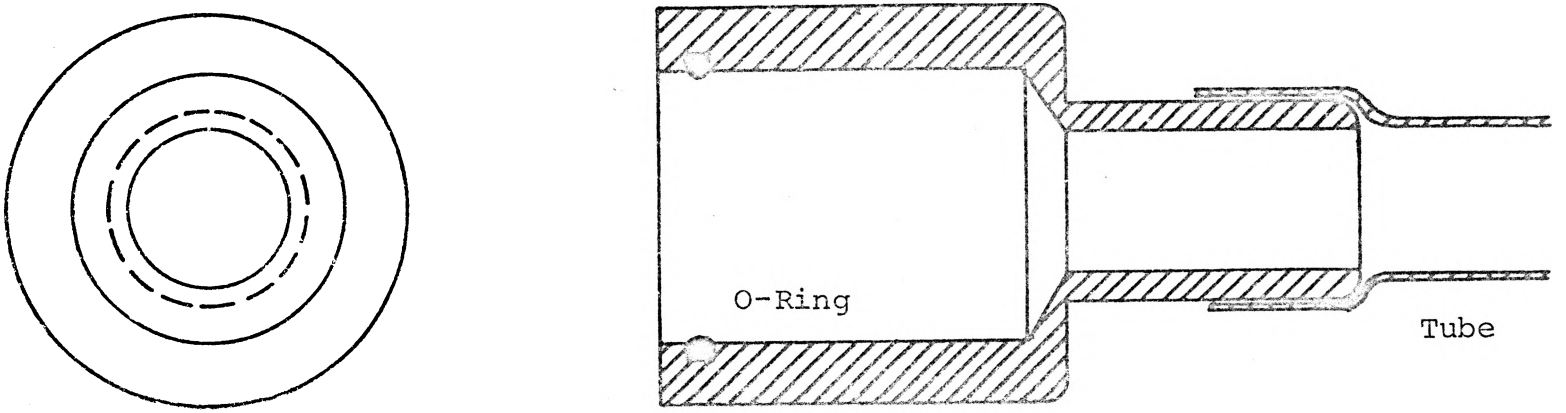

Figure 3.9 Tube Connectors

to allow for different viscosities of the fluid. For each one percent by volume addition of pluracol, the viscosity increased approximately three-fourths of a centistoke at room temperature, i.e., 0% pluracol - 1 cs, 4% pluracol - 3 cs. The latex paint is added to create solid particles in the fluid for scattering of the Doppler acoustic wave. The quantity of paint added was less than 0.2% by volume.

3.9 Viscometer

The viscometer used was an Oswald Pipet and was calibrated with distilled water.

CHAPTER IV

TEST PROCEDURE AND DATA REDUCTION

4.1 Calibration of Equipment

In any attempt to make quantitative experimental measurements, the final result can be no better than the calibration technique employed. For the electronic system described in Figure 3.7, several pieces of equipment are operated in series. This gives rise to accumulating errors and if accurate results (for example less than 2% experimental error) are desired, great care must be taken to ensure this. Thus, the calibration routine will be described in some detail.

Linear variable differential transformers (LVDT) are very reliable measuring devices when properly calibrated. To do this, the LVDT and transformer indicator must have matched sensitivities. This is done, prior to any measurement, by properly nulling the LVDT and adjusting the indicator sensitivity to a known calibration displacement. At the same time all diameter recording equipment (differential amplifiers and recorders) are adjusted to convenient gain settings for the calibration displacement. Thus both diameters and the associated gradient recording equipment are in their calibrated positions.

As with the displacement transducers, the pressure transducer sensitivities must be matched with that of the charge amplifiers. This is done by experimentally obtaining a pressure versus output charge curve. The slope of this curve is the transducer sensitivity and can be set directly on the charge amplifier. A voltage test signal can then be set on the charge amplifier to simulate a full scale pressure for calibration of the remaining recording units for both pressures and the pressure gradient.

The Doppler flowmeter is calibrated in a two-fold manner. First, the converter is adjusted for a precisely known output voltage for a given input frequency supplied by a function generator whose frequency is set against a frequency counter. Secondly, the transducer is calibrated by passing a known volume of fluid through the cuff and monitoring the associated shift in frequency. This ensures the reliability of the entire system, as the components are calibrated separately. The remaining recording equipment can then be calibrated by a simulated test voltage for the required full scale velocity.

To this point all channels of the strip chart recorder are calibrated. However, the master output of the recorder and input adjustments of the magnetic tape recorder are not. To bypass a tedious and lengthy calibration of these components, an alternate scheme is used. The master output of the chart recorder is maximized to

ensure that full scale sinusoidal deflection of the recording pens corresponds to more than 0.707 volts rms. This ensures that the input recording level is sufficient to attain the required modulation for accurate recording and reproducing. The input to the tape is then adjusted to approximately match this level. However, at this point, the signals could not be retrieved very accurately as the "exact" recording level is not known. To alleviate this, the peak to peak values (pulse values) from the calibrated chart recorder are forced onto the pulse values of each channel after the analog to digital process is completed. This will be described in detail in a later section.

4.2 Determination of the Viscosity

An Oswald Pipet was used to determine the kinematic viscosity of the test fluid. The pipet was calibrated with distilled water as the standard. A least square curve fit of the calibration data (time versus temperature) was done so that the relative drain time of the test fluid could be calculated for any temperature. Thus the kinematic viscosity of the test fluid can be calculated from the following equation

$$\nu = \left(\frac{670}{T^{o}F} + .2\right) 10^{-3} \quad \text{(relative time)} \qquad (4.1)$$

which is a least square curve fit of the International Critical Tables, where relative time is the drain time of test fluid divided by drain time of distilled water at the test temperature.

4.3 Determination of Pressure-volume data

For the calculation of elasticity parameters, pressure-displacement measurements need to be made. This was done by pressurizing the system very slowly via the constant head tank and recording the corresponding changes in pressure and diameter. These curves were then digitized for curve fitting and for use as data in the various elasticity models.

Some longitudinal force-length curves were also obtained by hanging weights in the axial direction and recording the corresponding change in length, radius and wall thickness. From this some longitudinal elastic properties, such as Young's modulus and Poisson's ratio, can be calculated to determine the isotropy of the material.

4.4 Frequency Response Considerations

For reliable dynamic measurements, the frequency response of a system must be analyzed. Since the maximum fundamental frequency is 3 cycles per second and if 10 harmonics are used to represent the time varying curves,

the frequency response of the system should be flat to at least 30 cycles per second.

For the pressure transducers and passage lengths, the responses are flat to well above 1500 cps. The charge and differential amplifiers are flat to at least 10^5 cps, so they don't even need to be considered. The LVDT response is determined by the maximum speed at which the core mass can be moved. This was calculated for the physical geometry and stroke of the plexiglas transfer rod and core and found to exceed 30 cps. The LVDT indicating equipment is flat through 400 cps.

The frequency response of the flowmeter is determined by the scattering of the acoustics wave by the solid particles in the fluid. To determine this, the particle size and density must be known. The particles used were titanium dioxide of specific gravity 3.84, calcium carbonate (2.8 sg) potassium silicate (2.4 sg) and magnesium silicate (2.5 sg). The size was determined by a 238X photograph of a glass slide containing a test sample of the fluid. A tracing of this photograph appears in Figure 4.1. Hjelmfelt[37] describes a method of calculating the motion of discrete perticles in a moving fluid. This was done using a particle size of 25 microns, a specific gravity of 4 and a viscosity of that of water. These represent the worst cases for maximum frequency response. After performing the required calculations, it was found that the particles

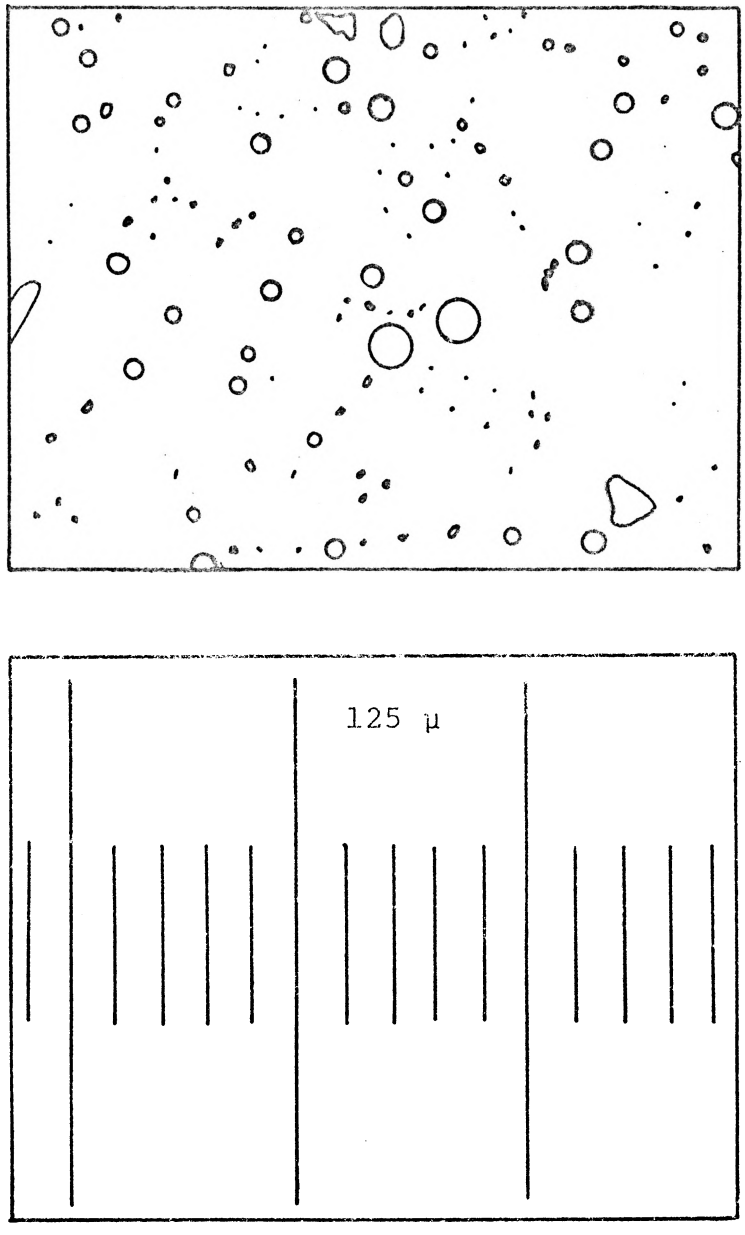

Figure 4.1 238X Sketch of Seeded Test Fluid

would follow the flow to at least 60 cps even for the worst combination of physical properties.

The magnetic tape recorder is specified to have a flat frequency response curve to more than 200 cps, while the chart recorder is flat to at least 60 cps. Thus the total frequency response of the system is well above the required 30 cps maximum.

4.5 Determination of the DC Levels

The DC levels for all channels were not stored on the magnetic tape unit. This was done for two reasons. First, it was desirable to amplify the AC components for full scale stylus deflection to increase the signal to noise ratio on the tape. Secondly, the recorder and the reproducer produce a DC offset during normal operation and these values would have to be determined and subtracted from each channel signal. To do this it would require a DC calibration signal to be put on each channel and then shift all digital points accordingly after the analog to digital process. Also, if the DC component was not suppressed on the chart recorder, the AC waveform (which is of the most interest) would be considerably reduced in amplitude. This would cause degradation of the signal when stored on tape.

To alleviate these problems, the DC levels are determined from the chart recorder. First, the zero DC

points of all galvanometers are marked. The input signals are then amplified so the total signal (AC plus (DC) occupies the full scale. The partial DC component from the absolute zero point to the minimum point on the AC waveform is then recorded. The total DC level is then blocked by introducing a resistor-capacitor network (3 db down at 0.16 cps). The level from the minimum point on the AC waveform to the zero DC point (previously marked) is the additional DC level. The sum of these two levels is then the total mean value of the function. This technique is done on all channels except the one corresponding to velocity.

The mean flow is found by integrating electronically the instantaneous velocity curve (time constant of 5 seconds). The bucket velocity is known from the steady flowmeter and is then forced on the "electronic" mean value (note that this also calibrates the AC components) giving the DC level directly.

The DC levels are then added to the digital points upon input to the Fourier analysis computer program. This returns the data to an absolute value scale.

4.6 Determination of the AC Components

The input AC signals to the chart recorder are amplified for maximum stylus deflection, while the DC values are blocked completely with a RC circuit. The signals are

then recorded on magnetic tape via the master output on the chart recorder. As pointed out in the calibration section (see section 4.1), no great attempt is made to adjust the input level to the exact recording level as the amplitude will be scaled after the analog to digital process.

The signals are now all in analog form and are not very useful for any calculational purposes. Thus the signals are all digitized on a Systems Engineering Laboratories (SEL) 840A computer. During this process the data is stored on digital magnetic tape for input to an IBM 360-50 digital computer for scaling of the digital points and Fourier analysis to determine the AC frequency components. The analog to digital process will be described in detail in appendix A and the Fourier analysis algorithm will be flow charted and described in appendix B.

4.7 Computerized Data Reduction

The output of the Fourier Analysis program (Fourier coefficients) is punched onto cards for input to the various data reduction routines. The pressure gradient is inputted to the flow program shown in Appendix C for comparison of flow theories. The pressure and diameter coefficients are used in the program shown in Appendix D to compute the gradients from the time deratives of the various functions (see section 1.2). All curve fitting was done with the least square program shown in Appendix F.

CHAPTER V

ELASTICITY CONSIDERATIONS

5.1 Introduction

For the practical application of any non-rigid flow model, the elastic properties of the physical system must be known. The models described in section (2.6) are in current use with equation (2.51) the most widely accepted. However, the assumptions of plane strain must be made to express the result in this form. This requires that no length change occur during inflation of the tube. For the freely moving elastic tube this is certainly not the case and the axial strain should be taken into account.

In the practical measurement of strain, the tangential strain is most easily determined since it is only the percentage change in the external diameter. However, when the outside diameter is measured, the inside diameter does not change the same amount because of changing wall thickness, i.e., radial strain. Thus, if a flow area is to be determined from an external diameter, this variation must be taken into account. A three-dimensional elasticity model will be presented here to allow for the aforementioned situations.

5.2 Generalized Elasticity Relations

Love[32] has given the solution for a tube under pressure as

$$\tau_{rr} = \frac{Pr_i^2}{r_o^2 - r_i^2}\left(1 - \frac{r_o^2}{r^2}\right) \tag{5.1}$$

$$\tau_{\theta\theta} = \frac{Pr_i^2}{r_o^2 - r_i^2}\left(1 + \frac{r_o^2}{r^2}\right) \tag{5.2}$$

$$\tau_{zz} = 2\sigma\frac{Pr_i^2}{r_o^2 - r_i^2} + e_{zz}E \tag{5.3}$$

when the external pressure is zero. The generalized stress-strain equations can be written as

$$e_{rr} = \frac{1}{E}\left[\tau_{rr} - \sigma\left(\tau_{\theta\theta} + \tau_{zz}\right)\right] \tag{5.4}$$

$$e_{\theta\theta} = \frac{1}{E}\left[\tau_{\theta\theta} - \sigma\left(\tau_{rr} + \tau_{zz}\right)\right] \tag{5.5}$$

$$e_{zz} = \frac{1}{E}\left[\tau_{zz} - \sigma\left(\tau_{\theta\theta} + \tau_{zz}\right)\right] \tag{5.6}$$

Evaluation of equations (5.1) through (5.3) at the outside surface $r = r_o$ and substitution of these results in the tangential strain equation yields

$$e_{\theta\theta} = \frac{1}{E}\left[\frac{2Pr_i^2}{r_o^2 - r_i^2}\left(1 - \sigma^2\right) - e_{zz}\sigma E\right]$$

Rearranging yields

$$E\left(1 + \frac{e_{zz}}{e_{\theta\theta}}\right) = \frac{2Pr_i^2\left(1 - \sigma^2\right)}{r_o^2 - r_i^2}\,\frac{r_o}{\Delta r_o} \tag{5.7}$$

where

$$e_{\theta\theta} = \frac{\Delta r_o}{r_o} \tag{5.8}$$

For the case of plane strain $\left(e_{zz} \equiv 0\right)$ it is easily seen that this reduces to equation (2.51).

5.3 Determination of Axial Strain

To evaluate equation (5.7) the external diameter must be measured as a function of internal pressure while the axial and radial strain are also determined. A great simplification in experimental technique would be achieved if the latter two strains could be calculated in terms of the measurable tangential strain.

If it is assumed that constant volume occurs upon inflation (Poisson's ratio of one-half) the axial strain can be calculated. Let the volumes at state one and two be

$$V_1 = \pi\left(r_{o1}^2 - r_{i1}^2\right)L_1 \tag{5.9}$$

$$V_2 = \pi\left(r_{o2}^2 - r_{i2}^2\right)L_2 \tag{5.10}$$

Equating the equal volumes and rearranging yields

$$\frac{L_2 - L_1}{L_1} = \frac{r_{o1}^2 - r_{i1}^2 - r_{o2}^2 + r_{i2}^2}{r_{o2}^2 - r_{i2}^2} \tag{5.11}$$

But

$$r_{i1} = r_{o1} - h_1 \tag{5.12}$$

$$r_{i2} = r_{o2} - h_2 \tag{5.13}$$

thus

$$e_{zz} = \frac{L_2 - L_1}{L_1} = \frac{2r_{o1}h_1 - h_1^2}{2r_{o2}h_2 - h_2^2} - 1 \tag{5.14}$$

This allows the calculation of axial strain in terms of outside radius and varying wall of thickness.

5.4 Determination of Wall Thickness

For a three-dimensional strain system, there is a non-zero radial strain. This strain is given by the percentage change in wall thickness at two pressure levels, i.e..

$$h_1 = r_{o1} - r_{i1} \tag{5.15}$$

$$h_2 = r_{o2} - r_{i2} \tag{5.16}$$

Therefore

$$\Delta h = r_{o2} - r_{i2} - r_{o1} + r_{i1} = \Delta r_o - \Delta r_i \qquad (5.17)$$

where Δr_o and Δr_i are the displacements at $r = r_o$ and $r = r_i$. Thus

$$\Delta h = u_{r = r_o} - u_{r = r_i} \qquad (5.18)$$

Love[32] also gives the solution to the displacement field as

$$u = \frac{Pr_i^2}{E\left(r_o^2 - r_i^2\right)}(1 + \sigma)(1 - 2\sigma)\, r - \sigma e_{zz} r + \frac{Pr_o^2 r_i^2 (1 + \sigma)}{E\left(r_o^2 - r_i^2\right) r} \qquad (5.19)$$

Evaluation of equation (5.19) at $r = r_o$ and $r = r_i$ and substitution into equation (5.18) yields

$$\Delta h = -\frac{Pr_i(1 + \sigma)}{E\left(r_o^2 - r_i\right)}\left[r_o^2 - 2(1 - \sigma) r_i r_o + r_i^2 (1 - 2\sigma) - \sigma e_{zz} h\right] \qquad (5.20)$$

But $r_i = r_o - h$ and let Δh be referenced to the original wall thickness h_o. Substitution of these into equation (5.20) results in a cubic when equation (5.14) is substituted for e_{zz}. To reduce this solution to a quadratic an approximate value is substituted for e_{zz} as follows

$$e_{zz} = \frac{2r_{oo}h_o - h_o^2}{2r_o h - h^2} - 1 \simeq \frac{2r_{oo} - h_o}{2r_o - h_o} - 1 \qquad (5.21)$$

Treating e_{zz} as in equation (5.21), equation (5.20) reduces to

$$h^2\left[-E - e_{zz}\sigma E + P\left(2\sigma^2 + \sigma - 1\right)\right] + h\left[h_o E + 2e_{zz}\sigma r_o E - Pr_o\left(2\sigma^2 + \sigma - 1\right) - 2Pr_o\sigma(\sigma + 1) + 2Er_o\right] - \left[2r_o h_o E + 2r_o 2P\sigma(1 + \sigma)\right] = 0 \tag{5.22}$$

This can be non-dimensionalized and solved to yield

$$\frac{h}{h_o} = \frac{-B + \sqrt{B^2 - 4AC}}{2A} \tag{5.23}$$

where

$$B = 1 + \left(\frac{D_o - D}{D - h_o}\right)\sigma\frac{D}{h_o} + \frac{D}{h_o} - \frac{PD}{Eh_o}\left(4\sigma^2 + 3\sigma - 1\right)$$

$$A = \frac{P}{E}\left(2\sigma^2 + \sigma - 1\right) - 1 - \left(\frac{D_o - D}{D - h_o}\right)\sigma$$

$$C = \frac{1}{2}\frac{PD}{Eh_o}\frac{D}{h_o}\sigma(\sigma + 1) - \frac{D}{h_o}$$

and D_o, h_o are the original diameter and wall thickness at zero-pressure.

5.5 Determination of Elastic Modulus

The elastic modulus can be written in terms of tangential strain and the wall thickness as (see equation 5.7)

$$E = \frac{P\left(D^2 - 4Dh + 4h^2\right)}{2\left(D_o h - h^2\right)\left(1 + \sigma\frac{e_{zz}D}{D - D_o}\right)} \qquad (5.24)$$

where

$$h = \frac{h_o}{2A}\left(-B + \sqrt{B^2 - 4AC}\right) \qquad (5.25)$$

[see equation (5.23) for details].

These two equations represent a simultaneous set in the unknowns E and h. To avoid a coupled solution for every pressure, an approximate value for E is substituted into equation (5.25) to evaluate the wall thickness at a given pressure. This wall thickness is then used to calculate the elastic modulus from equation (5.24). The approximate value of E used to calculate h is the slope of the stress strain curve when the stress is predicted by Laplace's equation (equation 2.53 or 2.54). This gives a very good result as h is not as strong a function of E as D/h and the error introduced is negligible.

5.6 Conclusion

A comparison of all of the mentioned models is shown in Figure 5.1 where the slope is given by the mentioned equations. It is seen that Laplace's equation (equation 5.24) yields results very close to the three-dimensional model presented here. At 10% strain, Laplace's equation predicts an elastic modulus 5% high while Bergel's model is approximately 18% low. The plain strain, plain stress models predict 13% and 8% low, respectively.

Throughout the study the three-dimensional model was used for all stress-strain considerations and all flow areas were corrected for the radial strain.

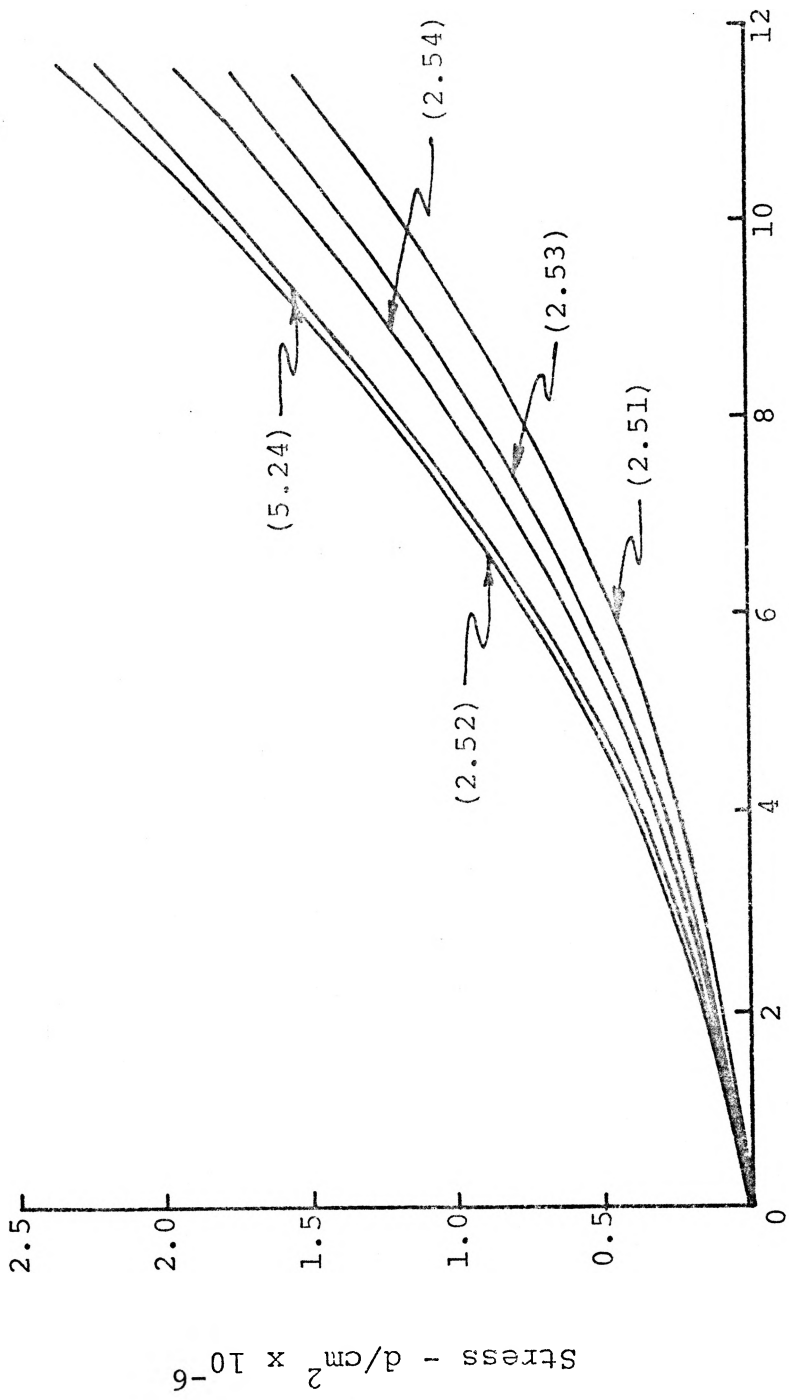

Figure 5.1 Comparison of Stress-Strain Models

CHAPTER VI

DISCUSSION OF RESULTS

6.1 Analysis of Fourier Series Representation

All analog data signals were digitized and curve fitted by Fourier series analysis to obtain a mathematical representation of the function. An error analysis of a curve fit must be performed before an attempt is made to make quantitative use of that representation. To assess the accuracy of a finite number of Fourier harmonics, Parseval's theorem can be used. The total energy content of a curve can be estimated by the variance of that curve which is given by the following

$$\text{Variance} = \frac{1}{K-1} \sum_{i=1}^{K} \left(f_i - \bar{f} \right)^2 \qquad (6.1)$$

where f_i = value of function at point i and

$\bar{f}$ = mean value of the function.

Parseval's theorem states that the variance of a finite number of harmonic components is given by

$$\text{Variance (series)} = \frac{1}{2} \sum_{n=1}^{J} c_n^2 \qquad (6.2)$$

Thus a measure of the accuracy of the fit is a comparison of the series variance to the total variance. Another method of error analysis is to determine the relative amplitudes of each harmonic as a percentage of the pulse value.

Table 6.1 and 6.2 show these results for all of the measurable quantities for one test run. Note that the variance method reaches to within 1% several harmonics before the harmonic content predicts accuracy to the same percentage. This is due to small harmonic content not affecting the total energy significantly, but contributing greatly to the deviation at some time points. However, even though the relative amplitude of the seventh through tenth harmonic may each be 1%, the sum of the total error is not 4% as each harmonic is out of phase to give rise to some cancellation. Thus the actual error of the curve fit is between that predicted by variance and that by relative amplitude. This analysis was performed on all data to ensure accurate representation.

6.2 Measurement of Pressure and Diameter

Pressure and diameter were measured simultaneously at two locations along the length of the tube. As the wave travels from the upstream to downstream recording site, attenuation of the wave occurs due to the viscous pressure loss. This loss occurs both the mean level of the wave as well as the time dependent portion. However, it has been shown[23] that for diameter this attenuation of the mean level can be neglected. There also is an expected phase lag between the waves at the two locations due to the finite transmission time (pulse velocity consideration). These phenomena are shown in Figure 6.1. The upstream pressure peaks at 109.8 mm Hg at 208.4° while the downstream pressure

TABLE 6.1

VARIANCE TABLE (RUN 47)

Through Harmonic	P_1	P_2	D_1	D_2	$-\partial P/\partial z$	$-\partial D/\partial z$	$\overline{v}_z$
1	17.4	81.9	13.1	86.7	38.0	23.7	56.5
2	53.8	83.1	55.5	87.5	58.8	57.6	79.2
3	71.2	90.3	72.9	92.0	70.4	69.3	90.7
4	98.0	99.2	97.4	99.3	98.2	97.2	91.0
5	99.1	99.6	99.0	99.5	99.5	99.0	91.6
6	99.3	99.6	99.5	99.7	99.6	99.4	91.7
7	99.5	99.6	99.7	99.7	99.7	99.6	91.9
8	99.6	99.6	99.7	99.7	99.7	99.6	92.1
9	99.6	99.6	99.7	99.7	99.7	99.6	92.4
10	99.6	99.7	99.8	99.7	99.7	99.6	93.0

TABLE 6.2

HARMONIC CONTENT (RUN 47)

Harmonic	P_1	P_2	D_1	D_2	$-\partial P/\partial z$	$-\partial D/\partial z$	$\overline{v}_z$
1	25.0	71.7	22.7	75.9	39.1	30.0	52.4
2	36.1	8.8	40.7	7.1	29.0	36.2	33.2
3	25.0	21.3	26.1	17.4	21.7	21.3	23.6
4	31.0	23.6	31.0	22.0	33.5	33.2	3.9
5	6.4	5.0	7.8	3.7	7.3	7.1	5.2
6	2.6	0.3	4.3	3.4	1.7	3.8	3.0
7	2.7	0.1	3.0	0.8	1.4	2.6	3.2
8	1.1	1.4	1.4	0.8	0.6	0.4	2.6
9	0.8	1.0	0.3	0.7	0.7	0.6	3.9
10	1.3	1.0	1.0	0.9	1.1	0.8	5.0

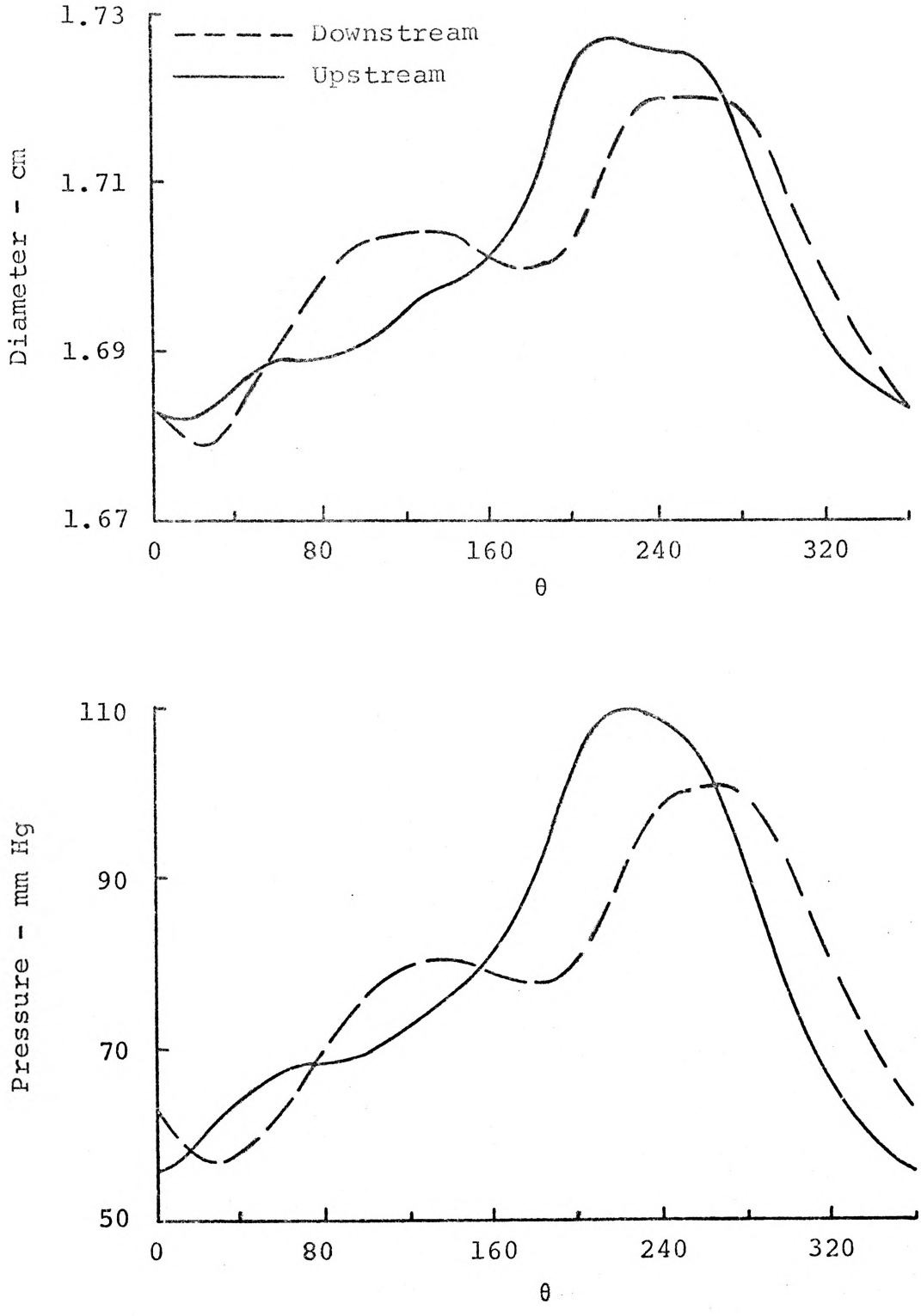

Figure 6.1 Relationship of Upstream to Downstream Conditions - Run 95

has a maximum value of 100.7 mm Hg at 246.3°. This gives rise to a 37.9° phase lag and an attenuation 9.2 mm Hg of which 0.5 mm Hg is the difference in mean values (79 - 78.5 mm Hg). The maximum dilatation occurs at 195.8° and 236.8° with values of 1.727 cm. and 1.719 cm. respectively. Thus, the peak value of the diameter occurs before the peak of the pressure. At first this may seem to be a surprising result as it is customary to consider the pressure as the primary distending force. However this is not the case. Consider the following, the equation of continuity can be written as

$$\frac{\partial v_r}{\partial r} + \frac{v_r}{r} + \frac{\partial v_z}{\partial z} = 0 \tag{6.3}$$

or

$$\frac{1}{r}\frac{\partial}{\partial r}\left(rv_r\right) + \frac{\partial v_z}{\partial z} = 0 \tag{6.4}$$

Integrating across the cross section yields

$$\int_o^R \partial(rv)_r = -\int_o^R r\frac{\partial v_z}{\partial z}\,\partial r \tag{6.5}$$

which can be rewritten as

$$\left[\overline{rv_r}\right]_{r=R} = -\frac{\partial}{\partial z}\int_o^R rv_z\,\partial r \tag{6.6}$$

But the integral is just the mean velocity i.e.,

$$\overline{v}_z = \frac{2}{R^2}\int_o^R v_z r\,\partial r \tag{6.7}$$

and the no-slip condition at the wall yields

$$\left[\overline{rv_r}\right]_{r=R} = R \frac{\partial u_r}{\partial t} \tag{6.8}$$

Thus equation (6.6) reduces to

$$R \frac{\partial u_r}{\partial t} = - \frac{\partial}{\partial z} \left(\frac{R^2}{2} \overline{v_z}\right) \tag{6.9}$$

but $- \frac{\partial}{\partial z} = \frac{1}{c} \frac{\partial}{\partial t}$ (consequence of assumed form for traveling wave).

Therefore

$$R \frac{\partial u_r}{\partial t} = \frac{1}{2c} \frac{\partial}{\partial t} \left(R^2 \overline{v_z}\right) \tag{6.10}$$

Integration with respect to time gives the final result as

$$\frac{u_r}{2R} = \frac{\overline{v_z}}{c} \tag{6.11}$$

This same result can be found directly from equation (2.24) by rearrangement. The phase of $u_r/2R$ can now be found to be $[-\phi_n - \beta z - \tan^{-1}(\alpha/\beta) + \varepsilon_{10}'' - \pi/2]$ where ε_{10}'' is the phase of $(1 + \eta F_{10})$ and $(-\pi/2 + \varepsilon_{10}'')$ is the amount the flow lags the pressure gradient (i.e., the pressure gradient has a phase of $[- \phi_n - \beta z - \tan^{-1}(\alpha/\beta)]$. The phase of the pressure can be found from equation (2.36) and is equal to $[- \phi_n - \beta z + \tan^{-1}(\alpha/\beta) - \pi/2]$. Thus, subtracting this from the phase of the dilatation yields a phase difference of $[\varepsilon_{10}'' - 2\tan^{-1}(\alpha/\beta)]$. Womersley shows that for all finite values of k' (see equation 2.29)), this difference is positive, which gives rise to the phase lead of the diameter to the pressure. As the wall viscosity increases, a

retardation of this phase difference occurs giving rise to two opposing effects that tend to cancel out when both are neglected. This will be discussed in a later section.

Reflections present in the flow field do not present any major obstacles as they can be represented as a retrograde traveling wave. This was taken into account by Womersley and can be included in his final analysis. Figure 6.2 shows the effect of a retrograde wave. For the pressure and diameter curves, the upstream leads the downstream for the first forward wave and is also attenuated. The second portion of the wave has the reverse phase relations. The downstream peak leads the upstream peak to show the effect of a retrograde wave. The third part of the wave is again traveling in the forward direction and the upstream leads the downstream. This reflection occurs at the inlet to the test section. The last reflection is attenuated greatly but does lead the downstream wave in phase. From a wave pattern of this form the group velocity can be found very accurately as the wave travels several lengths of the test section. This is a way of checking the conventional method which is calculated from the phase difference between the foot of the wave at two locations.

6.3 Calculation of Pressure From Diameter

Even though the distension of the tube leads the pressure in phase, the curves representing each are extremely similar. From Figures 6.1 and 6.2, the similarity

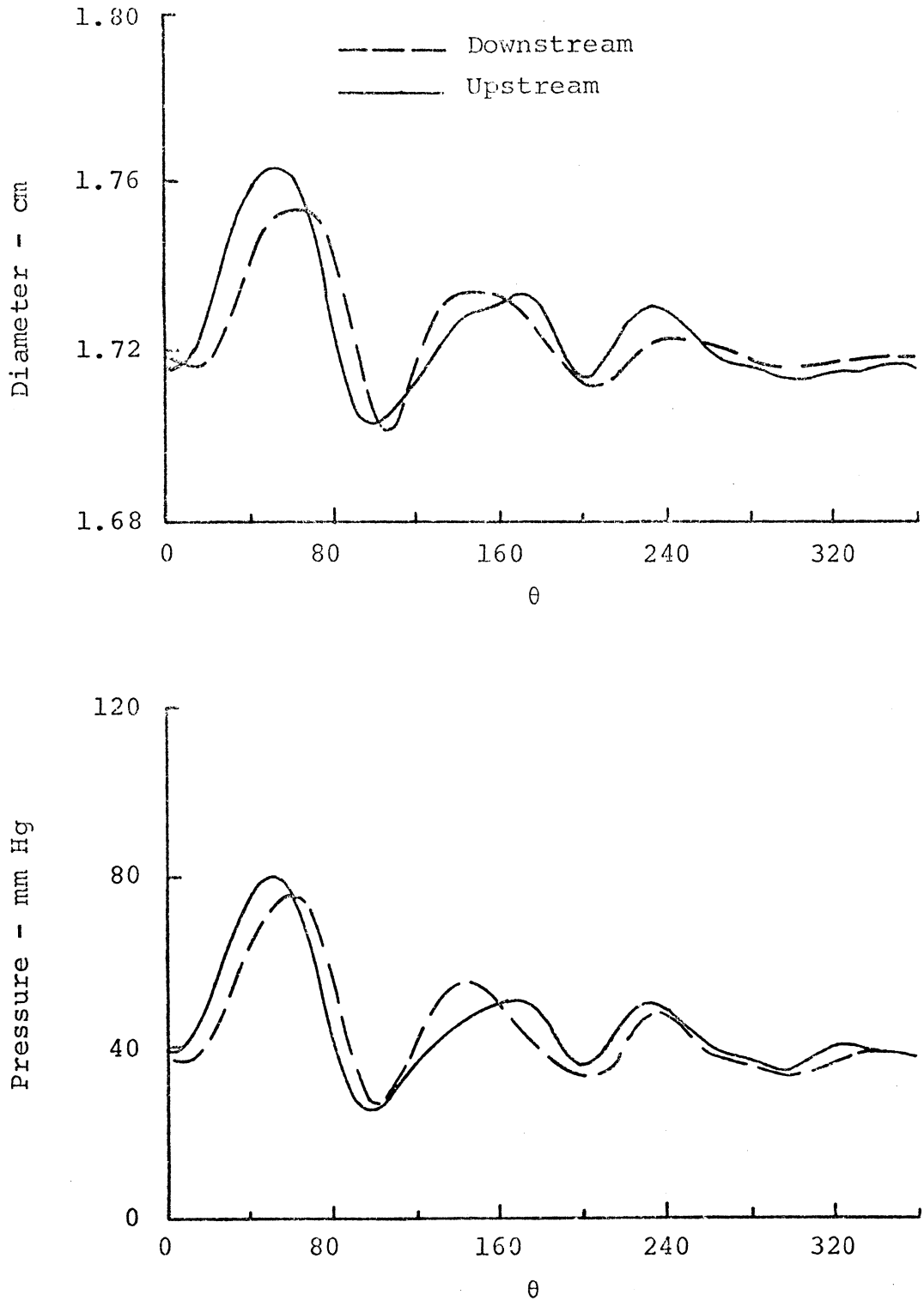

Figure 6.2 Relationship of Upstream to Downstream Conditions - Run 75

can be seen between the pressure and diameter at both recording sites. Figure 6.3 shows the envelope of the discrete frequency spectrum for pressure and diameter both at the upstream and downstream measurement. This similarity can also be seen in Table 6.1 and Table 6.2. In both tables, P_1 and D_1 values are approximately the same as are P_2 and D_2.

The pressure can be related to the diameter by an elastic pressure modulus; i.e.

$$P(t)=E_p\left(D_{pk}\right) D(t) \tag{6.12}$$

where $E_p\left(D_{pk}\right)$ is the slope of the pressure-diameter curve at the peak value of the dilatation. This allows for non-linearity of the curve but assumes that the elastic pressure modulus is constant over the pulse value (i.e., for a complete cycle). Also, no correction is made in the time domain for phase differences. Figures 6.4 through 6.6 compare pressure calculated from Equation 6.12 to the measured pressure. The phase difference is present though never more than a few degrees. The amplitude agrees very well through the full 360° cycle with the greatest deviation occurring in the secondary portion of the cycle.

A more accurate representation of the pressure can be obtained if the elastic pressure modulus is not assumed to be constant over the pulse value and by shifting the

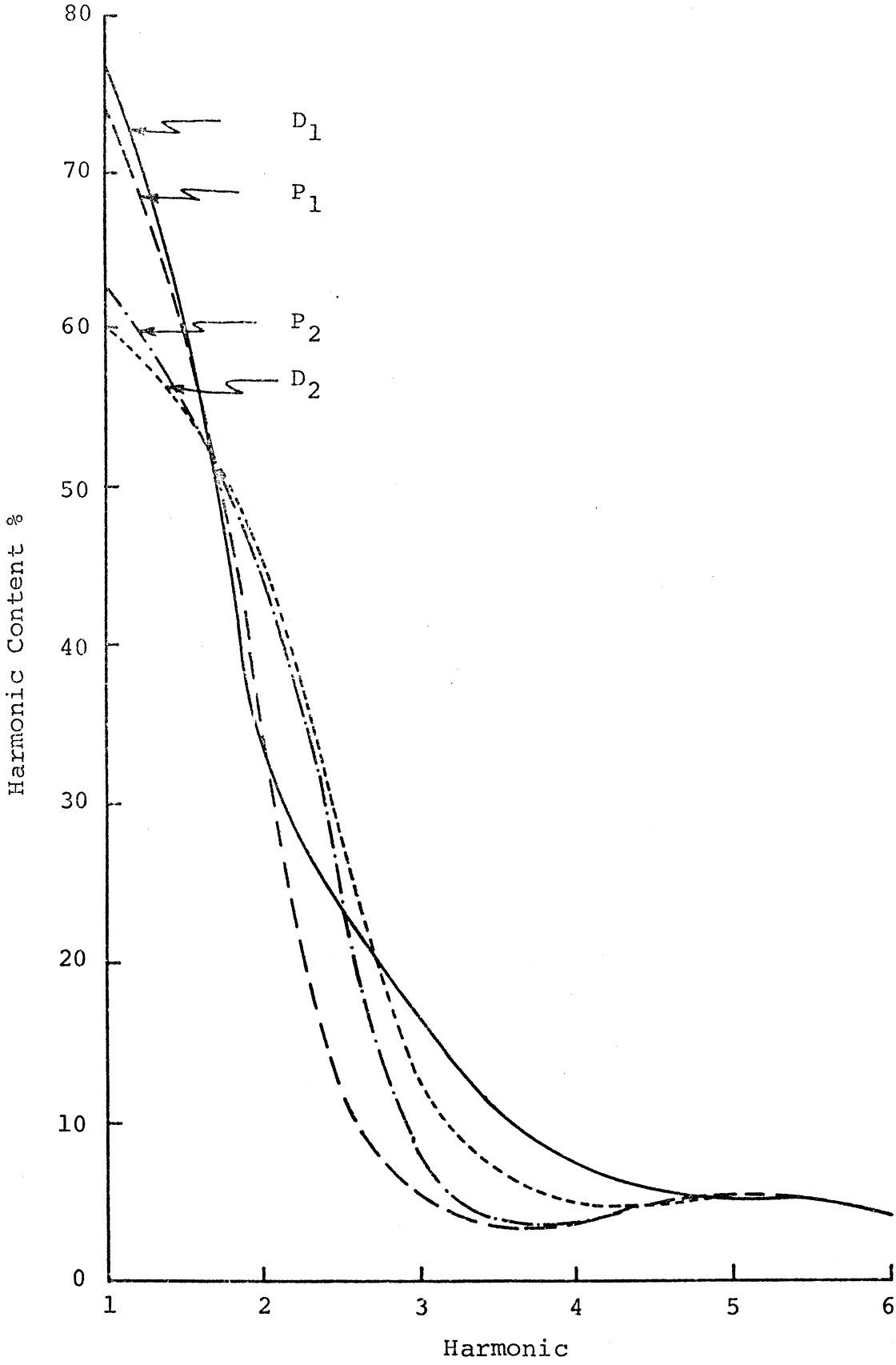

Figure 6.3 Envelope of Discrete Fourier Spectrum - Run 1

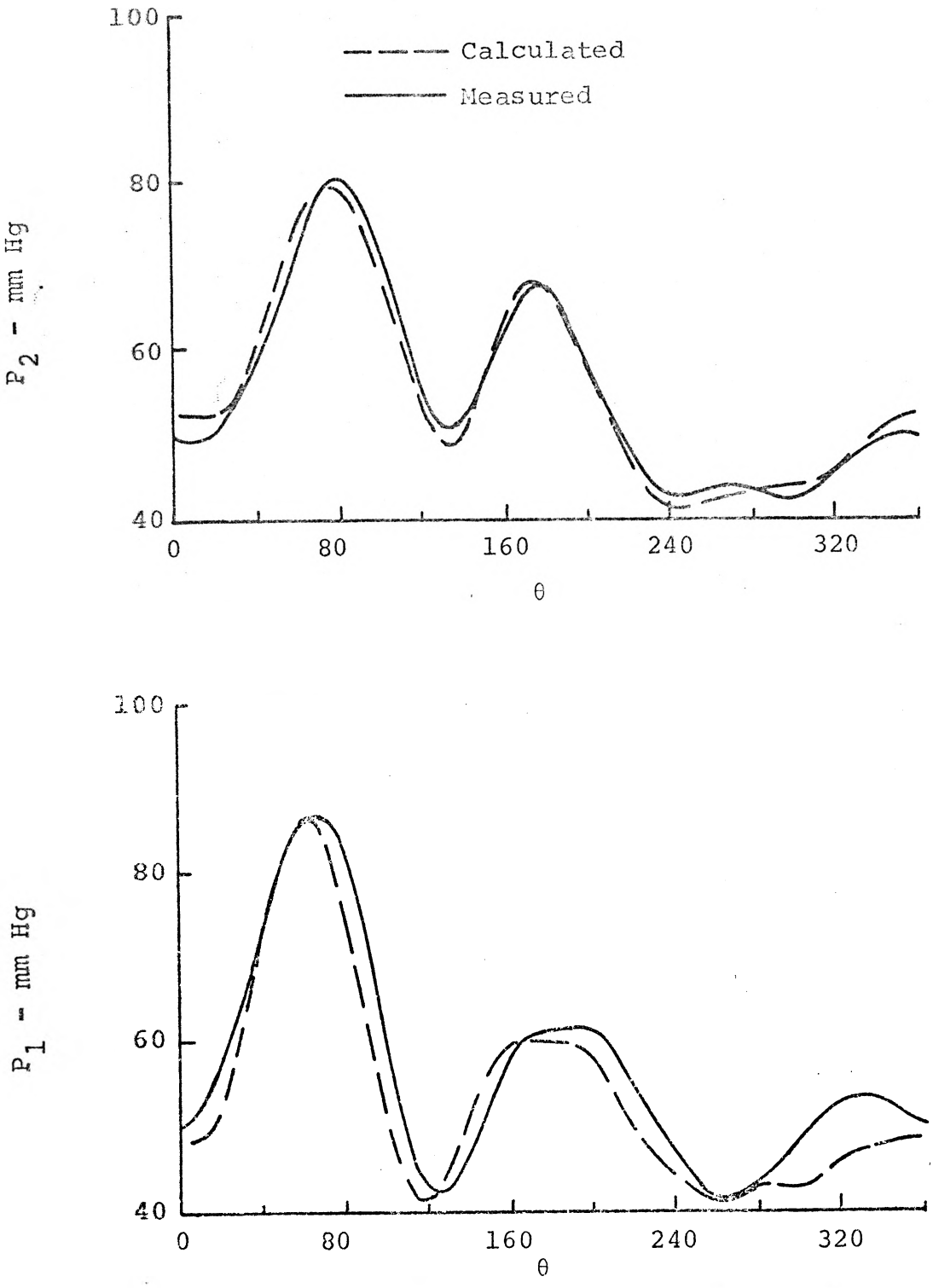

Figure 6.4 Comparison of Calculated to Measured Pressure - Run 32

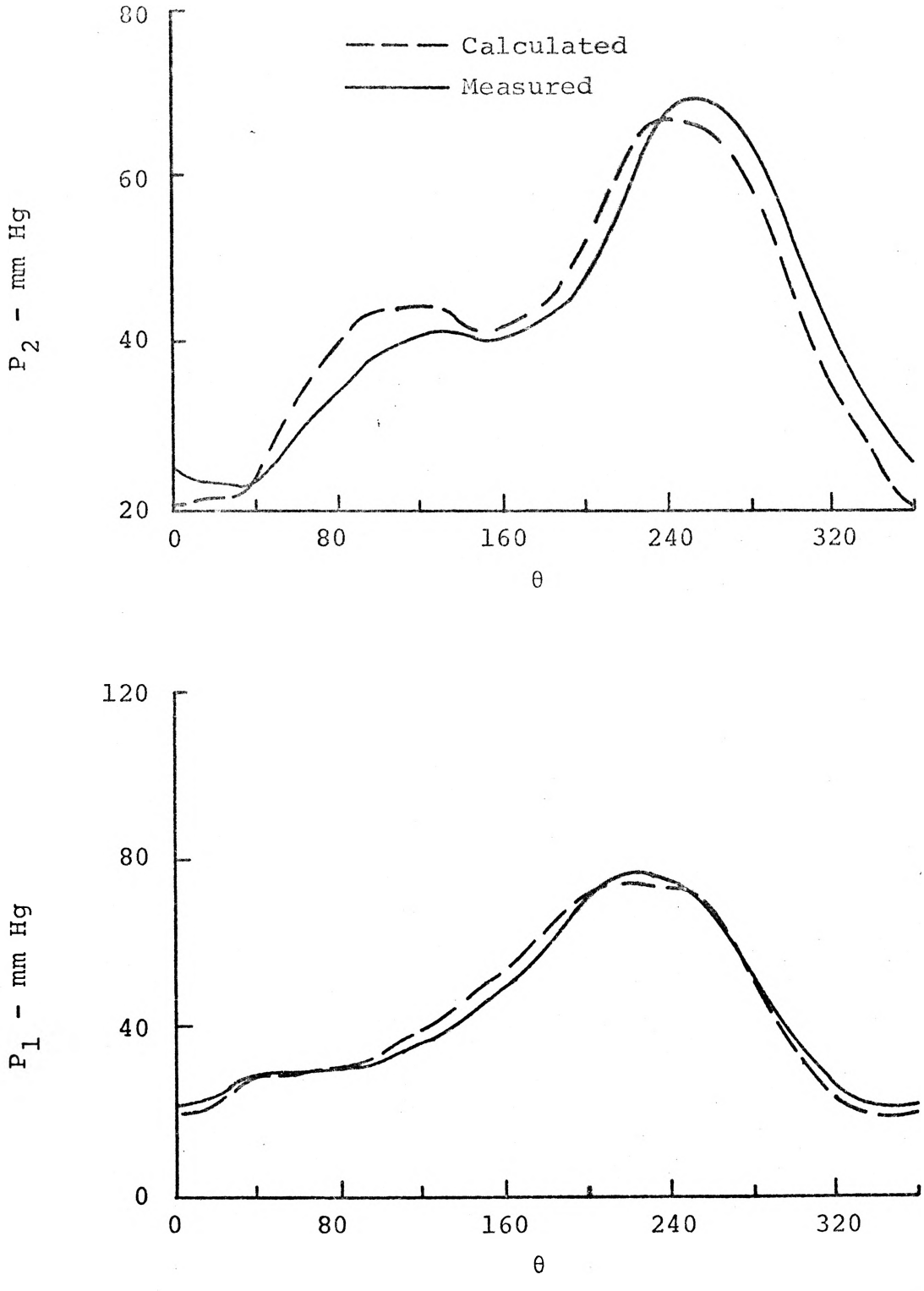

Figure 6.5 Comparison of Calculated to Measured Pressure - Run 87

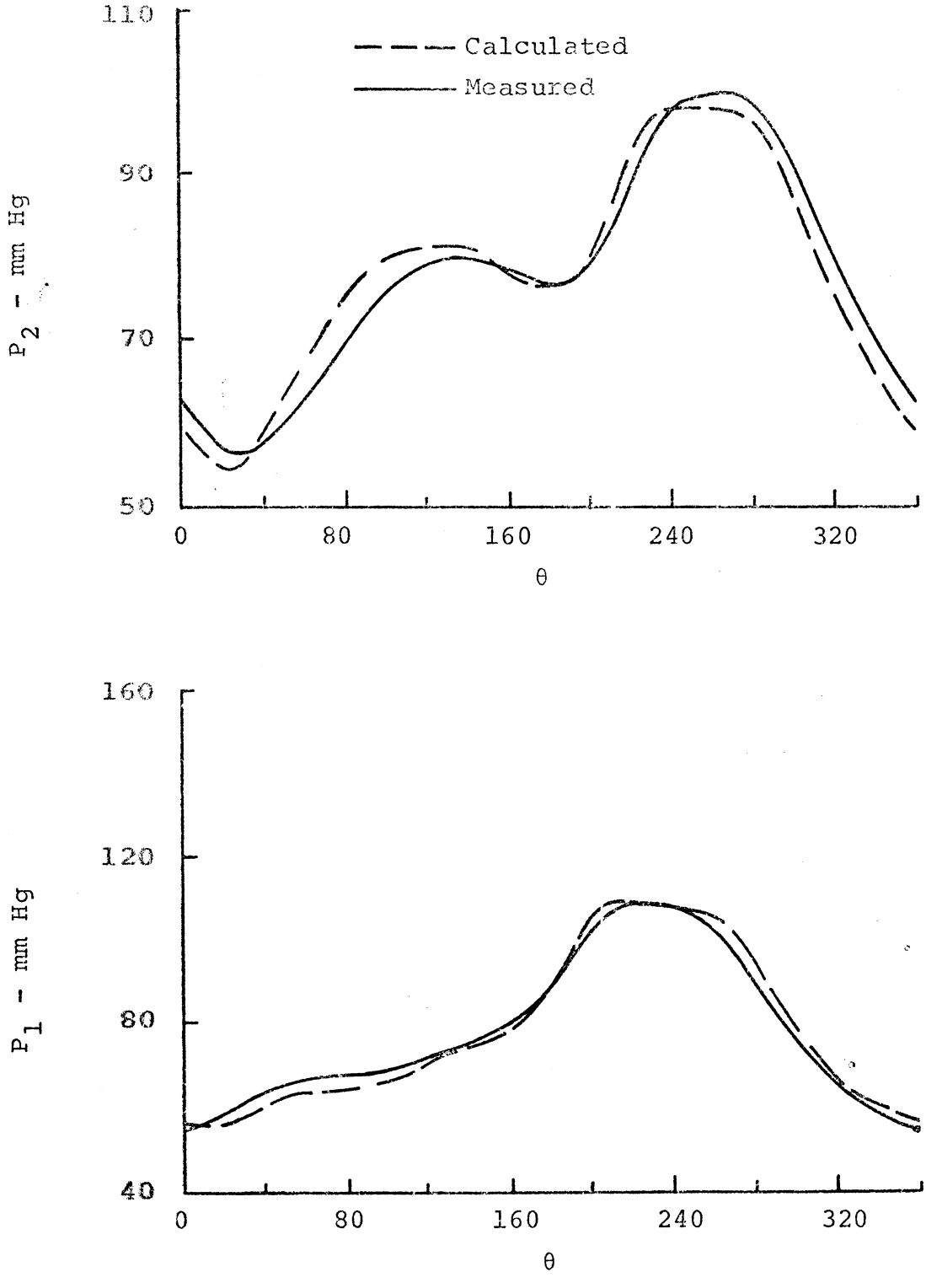

Figure 6.6 Comparison of Calculated to Measured Pressure - Run 95

curves in the time domain to remove the diameter leading affect. This can be represented as

$$P(t) = E_p(D)\ D\left[t + t_s\right] \tag{6.13}$$

where $E_p(D)$ is the instantaneous slope of the pressure-diameter curve and t_s is given by

$$t_s = \text{fundamental shift in time domain.} \tag{6.14}$$

Figures 6.7 through 6.9 compare the measured pressure to the pressure computed from the external measurement of diameter by equation (6.14). The curves show better agreement than the curves computed from equation (6.12). The peak of the calculated upstream pressure in Figure 6.7 and the downstream curve in Figure 6.8 are still 6% and 9% in error respectively. However, note that the entire curve is in error in the same direction. Errors of this type are by far the largest experimental failing. These errors are caused by difficulty in obtaining the mean values as accurately as the AC components (see section 4.5). If only the AC components are displayed graphically this problem is alleviated, but since the elastic properties of the tube are a strong function of these mean values, a plot of this sort would leave something to be desired. It is true though, that the pulsatile flow field is only a function of these AC components and are thus of primary interest.

6.4 Calculation of Pressure Gradient from Diameter Gradient

The spatial gradient of displacement may be related to the pressure gradient by similar reasoning as in the case

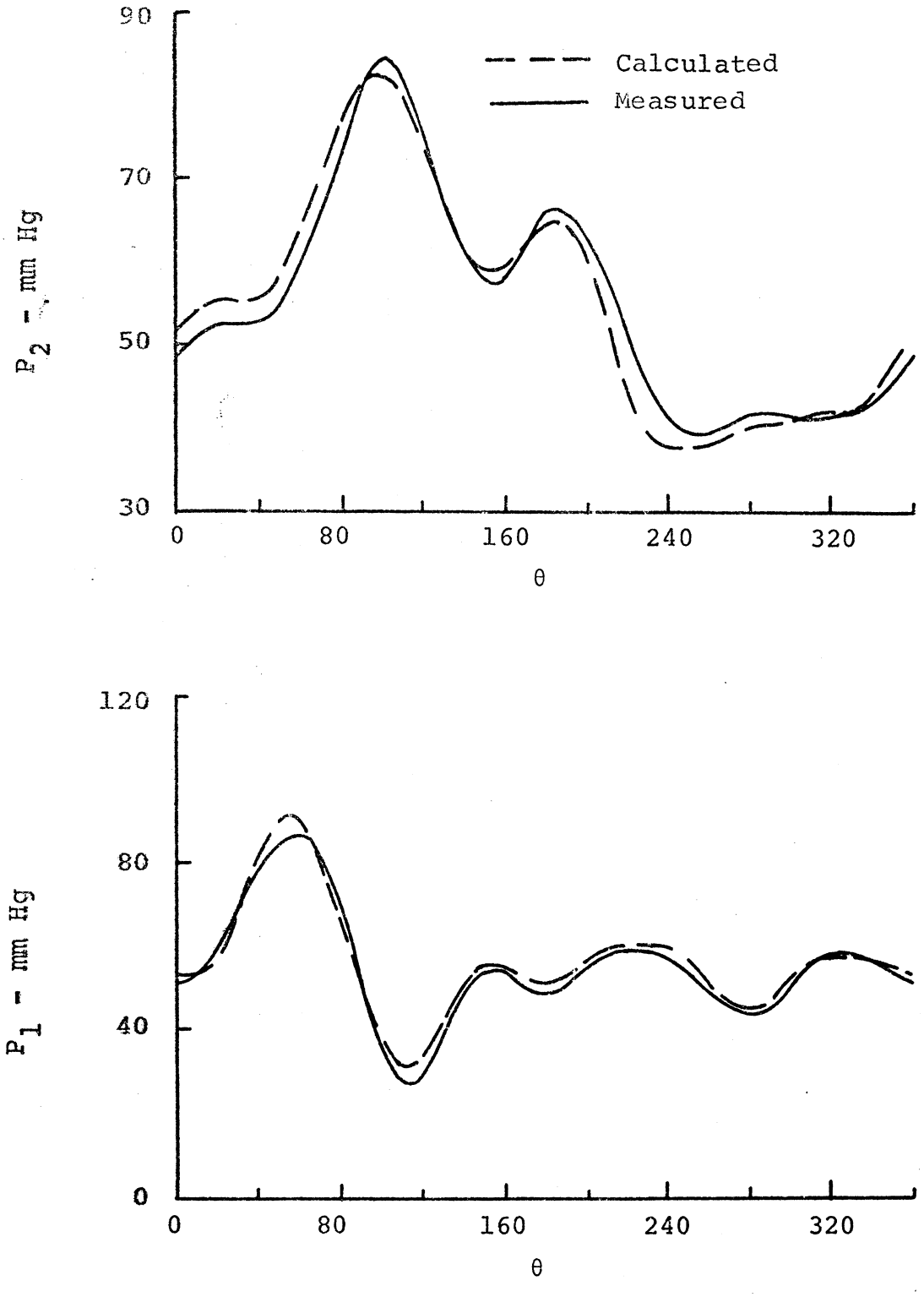

Figure 6.7 Comparison of Calculated to Measured Pressure - Run 47

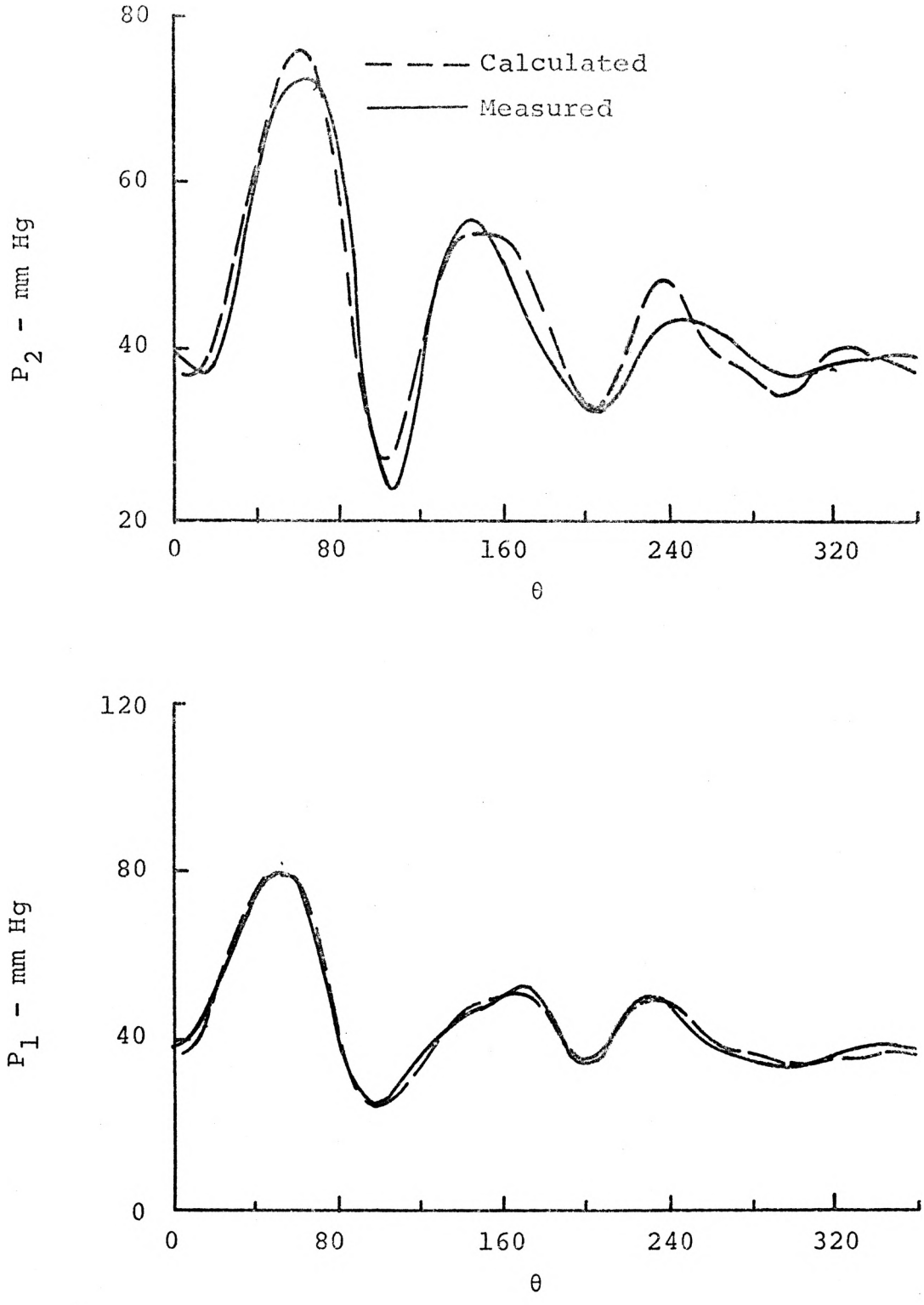

Figure 6.8 Comparison of Calculated to Measured Pressure - Run 75

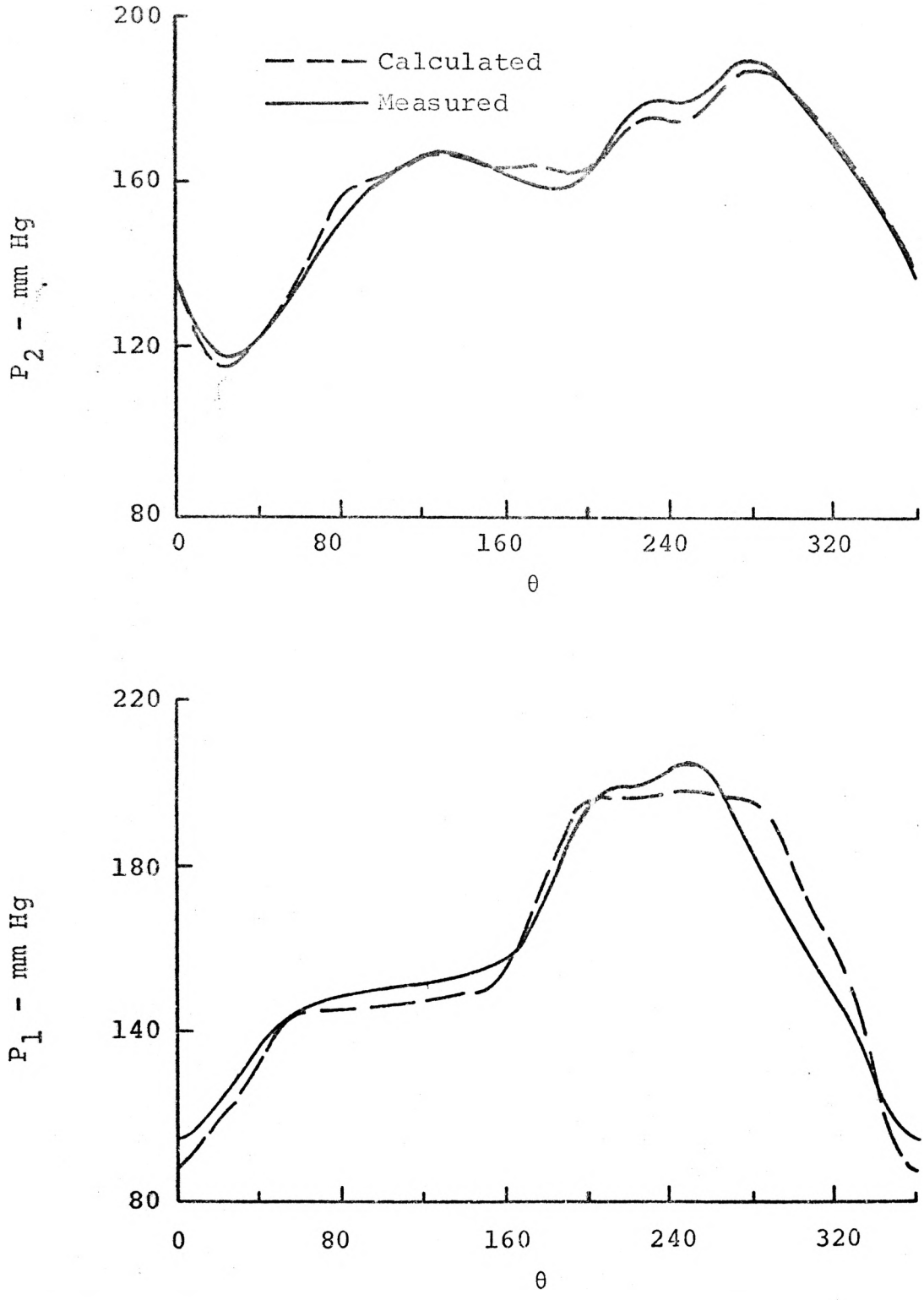

Figure 6.9 Comparison of Calculated to Measured Pressure - Run 1

of pressure-diameter relationships. First consider

$$-\frac{\partial P}{\partial z} = -E_{pk}\frac{\partial D}{\partial z} \tag{6.15}$$

where again E_{pk} is treated as only a function of the peak value. Figures 6.10 and 6.11 compare pressure gradients obtained experimentally and those calculated from equation (6.15). Again similar phase leading occurs in that the diameter gradient leads the pressure gradient. This immediately follows from the fact that two curves which lead two curves, possess a difference that also leads. Since the non-linearity of the elastic wall is not taken into account by this method, some error occurs.

When this non-linearity and phase discrepancy is taken into account, there is considerable improvement. This is shown by Figure 6.12. The data from run 45 fits extremely well over the primary portion of the cycle, and during the reflections the maximum error is less than 13%.

6.5 Calculation of Spatial Gradient from Time Derivative

It has been suggested by several authors[29, 34, 38] that the pressure gradient could be obtained from the pressure-time curve. This is most conveniently expressed as

$$-\frac{\partial P}{\partial z} = -\frac{\partial P}{\partial t} \tag{6.16}$$

However, Fry[29] critiques this relation by measuring the flow and then computes the flow from both pressure gradients

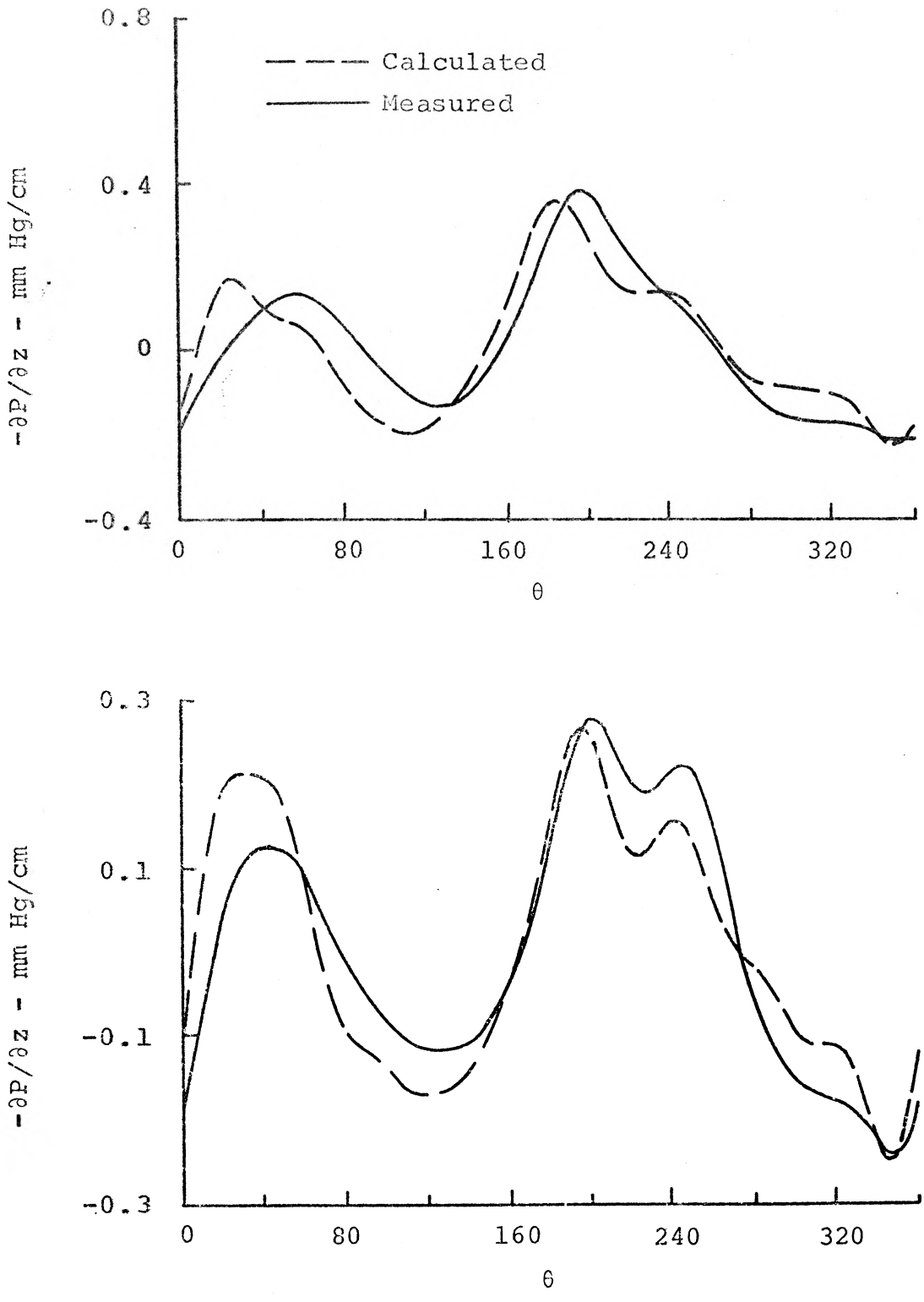

Figure 6.10 Comparison of Calculated to Measured Pressure Gradient - Run 8, 1

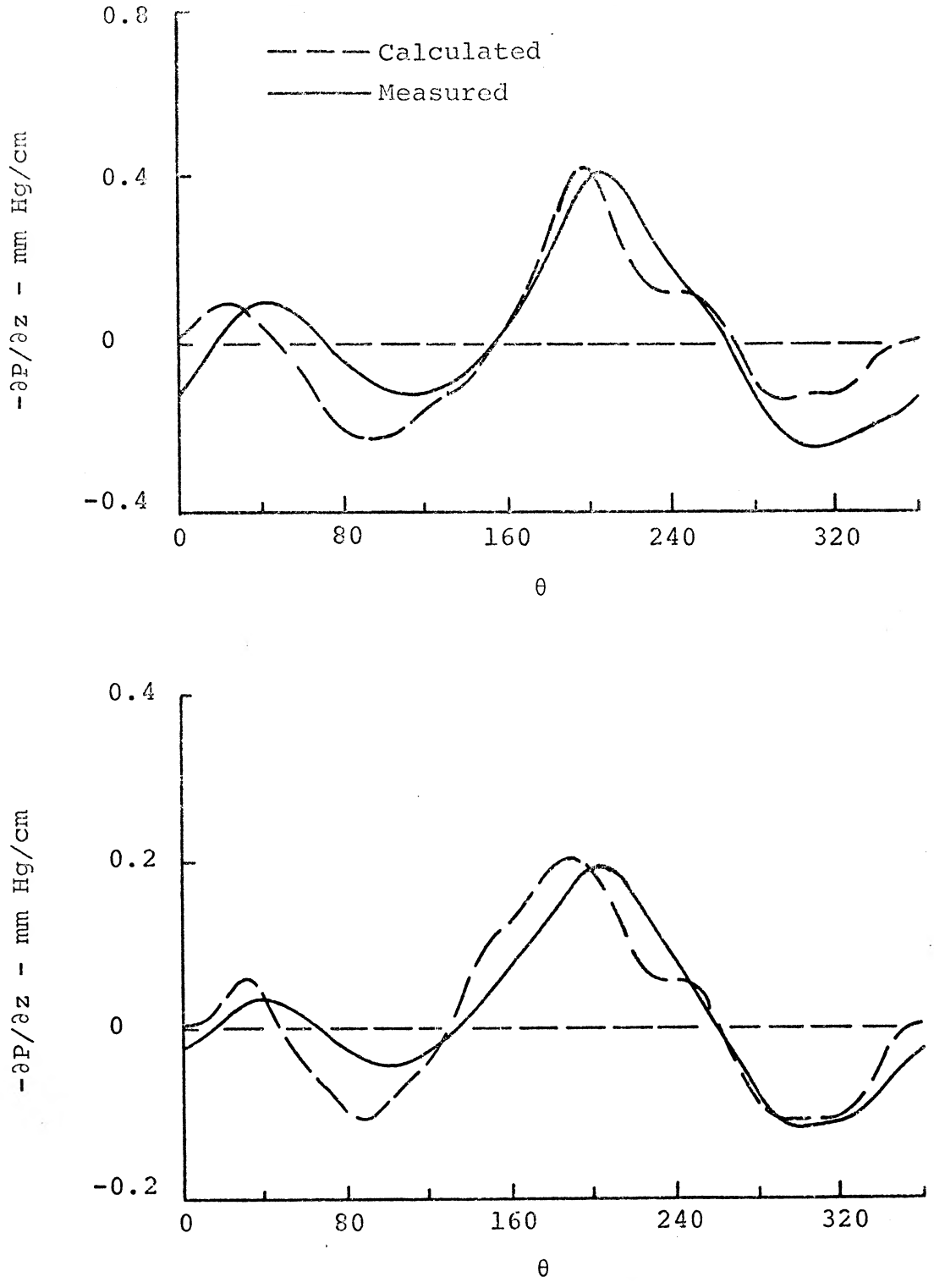

Figure 6.11 Comparison of Calculated to Measured Pressure Gradient - Run 95, 87

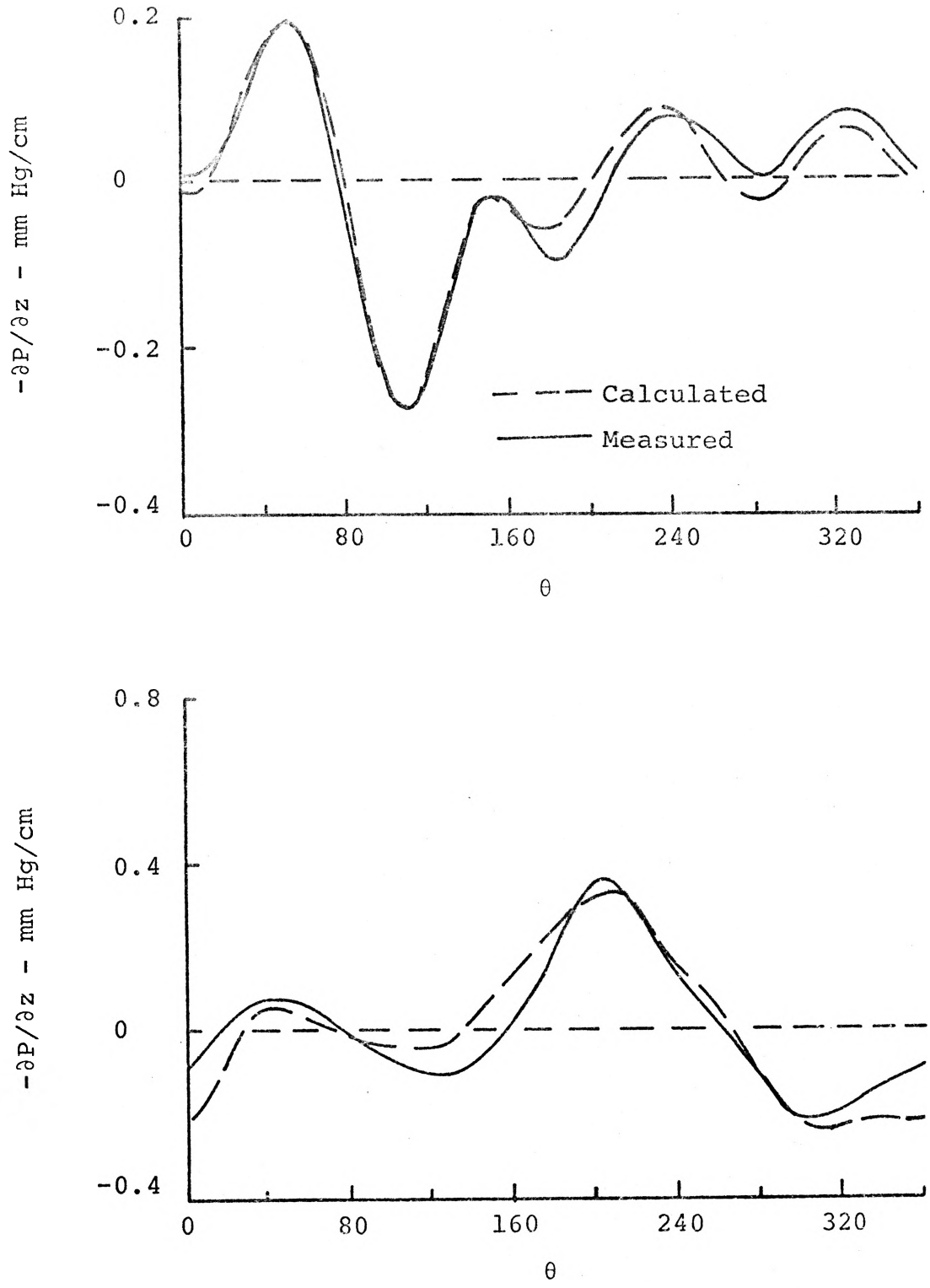

Figure 6.12 Comparison of Calculated to Measured Pressure Gradient - Run 45, 13

(i.e., the measured and the pressure time derivative). Remarkable results are obtained, but are discounted as accident rather than as a result of any relationships that might exist between the temporal and spatial derivatives of pressure. A more realistic approach would be to examine the flow conditions necessary to produce such a relationship.

Consider a traveling wave that can be represented by the following

$$P = P_1 e^{i\omega t-\gamma z} + P_2 e^{i\omega t+\gamma z} \tag{6.17}$$

where

$\gamma = \alpha+i\beta$ = propagation constant

α = damping constant

β = phase constant

and $P_1 e^{i\omega t}$ and $P_2 e^{i\omega t}$ are the disturbances creating the forward and retrograde waves, respectively. Thus

$$-\frac{\partial P}{\partial z} = -P_1 e^{i\omega t-\gamma z}(-\gamma) - P_2 e^{i\omega t+\gamma z} \tag{6.18}$$

and

$$\frac{\partial P}{\partial t} = P_1 e^{i\omega t=\gamma z}(i\omega) + P_2 e^{i\omega t+\gamma z}(i\omega) \tag{6.19}$$

Dividing by 1/c yields

$$\frac{1}{c}\frac{\partial P}{\partial t} = \gamma P_1 e^{i\omega t-\gamma z} + \gamma P_2 e^{i\omega t+\gamma z} \tag{6.20}$$

which is equal to

$$-\frac{\partial P}{\partial z} + 2\gamma P_2 e^{i\omega t+\gamma z} = \frac{1}{c}\frac{\partial P}{\partial t} \tag{6.21}$$

Therefore

$$-\frac{\partial P}{\partial z} = \frac{1}{c}\frac{\partial P}{\partial t} - 2\gamma P_2 e^{i\omega t + \gamma z} \tag{6.22}$$

This reveals the true relation between the spatial gradient and time derivative for viscous flow in the presence of reflections. For the case of no reflections (i.e., $P_2 = 0$), equation (6.22) reduces to

$$-\frac{\partial P}{\partial z} = \frac{1}{c}\frac{\partial P}{\partial t} \tag{6.23}$$

Thus, under the assumption of the form of the traveling wave, the spatial gradient is related to the time derivative through equation (6.23). However, this is only true in complex notation at this point. The real part of this equation is of primary interest as the measured time derivative of pressure will be expressed as the real part of the left hand side of equation (6.23). Thus it is necessary to examine the relationship of complex notation to order of differentiation.

It is easily shown that

$$\mathrm{Re}\left[-\frac{\partial P}{\partial z}\right] = -\frac{\partial}{\partial z}\left\{\mathrm{Re}[P]\right\} \tag{6.24}$$

$$\mathrm{Re}\left[-2\gamma P_2 e^{i\omega t + \gamma z}\right] = -2\alpha P_2 e^{\alpha z}\cos(\omega t + \beta z) + 2\beta P_2 e^{\alpha z}\sin(\omega t + \beta z) \tag{6.25}$$

and

$$R_e\left[\frac{1}{c}\frac{\partial P}{\partial t}\right] = \frac{X_1 X}{c_o} + \frac{Y_1 Y}{c_o} \tag{6.26}$$

where

$$\frac{c_o}{c} = X - iY \quad \text{[see equation (2.56)]} \tag{6.27}$$

X_1 = Real part of time derivative

Y_1 = Imaginary part of time derivative

But on the other hand

$$\frac{1}{c}\frac{\partial}{\partial t}\left\{R_e[P]\right\} = \frac{X_1 X}{c_o} - i\frac{Y_1 Y}{c_o} \tag{6.28}$$

which has a real part of

$$R_e\left[\frac{1}{c}\frac{\partial}{\partial t}\left\{R_e[P]\right\}\right] = \frac{X_1 X}{c_o} \tag{6.29}$$

Equation (6.29) is equal to equation (6.26) when either Y_1 or Y is identically zero. Since Y_1 is the imaginary part of the time derivative, it cannot be zero for all time or there would be no disturbance. Thus, when Y is zero, (i.e., no attenuation, $\alpha = 0$) equations (6.22) and (6.23) are the same regardless of whether real or complex notation is used to express the pressure. The simplest representation would then be

$$\frac{-\partial P}{\partial z} = \frac{1}{c_1} \frac{\partial P}{\partial t} \qquad (6.30)$$

where P is the measured real pressure.

This equation was used to calculate the pressure gradient with c_1 being approximated by the group velocity. The result is shown in the upper part of Figure 6.13. The calculated gradient is based on the upstream pressure which explains the fact that it leads the actual gradient in phase. The reverse would be true if the gradient was calculated from the downstream pressure. The lower curves show the same result except that the calculated gradient is based on the upstream measurement of diameter. The pressure was calculated from the dilatation, taking into account the non-linearity of the wall over the pulse cycle, plus the phase was corrected both for the diameter-pressure leading phase and the finite transmission time from the upstream point to the gradient sight. A smaller gradient is predicted than actually occurs, as the form of the equation assumes no attenuation. However, it appears to yield approximate values for the spatial gradient, and it has been shown that this similarity is a result of a fluid relationship between the temporal derivative and spatial gradient.

6.6 Comparison of Flow Theories

Three flow models were discussed in detail in Chapter II. A summary of these models was given in section

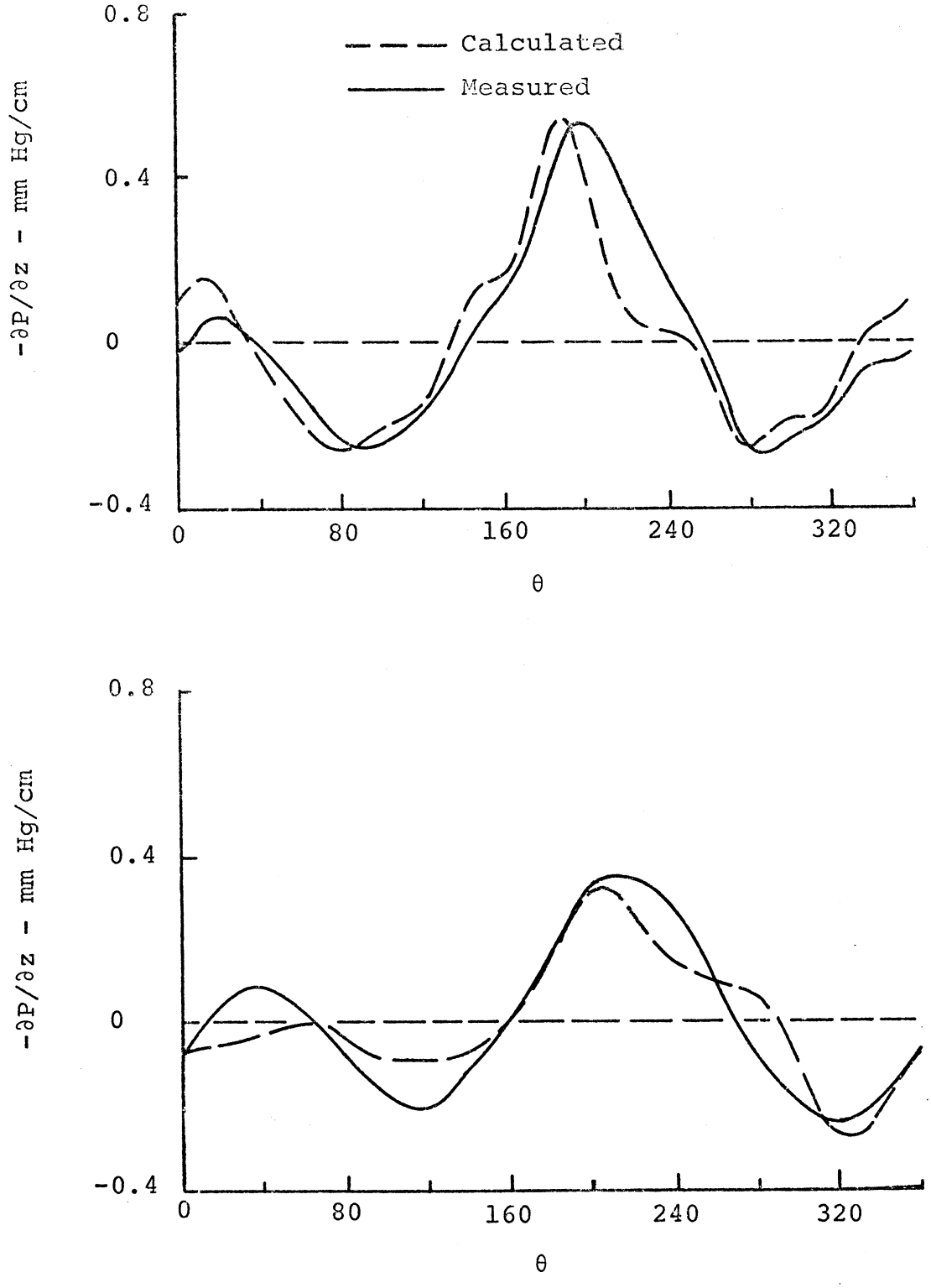

Figure 6.13 Comparison of Calculated to Measured Pressure Gradient - Run 28, 17

2.5 as well as the defining equations associated with each. Appendix C contains the computer program written to calculate the instantaneous average velocity for each of the flow models from the measured pressure gradient. Figures 6.14 through 6.17 show the result of these comparisons. Fry's model always predicts peak flows greater than that of either Womersley or Uchida. This is because the resistance used in the model has a value less than the actual resistance. Thus the flow attains a greater velocity during the cycle. Womersley's elastic model predicts greater peak values than those given by the rigid solution of Uchida. It can be shown theoretically[26] that for all positive values of Poisson's ratio this will occur. The same statements can be made about the reverse flow portion of the cycle (i.e., Fry's model predicts the largest velocity in the reverse direction).

It can be seen from the mentioned figures that the phase of the flow is almost identical for all three models and that the amplitude differs by less than 12%. This can be seen better by an examination of the Fourier series analysis of each flow curve. This is shown in Table 6.3 for run 32. The phase of each harmonic of Fry's model lags that of Womersley which in turn lags that of Uchida's. The "rigid phase" should indeed lead the "elastic phase" as some of the energy of the wave is used to distend the vessel in the elastic case. The phase predicted by Fry's model lags because the inductance used in the model is less than the actual value.

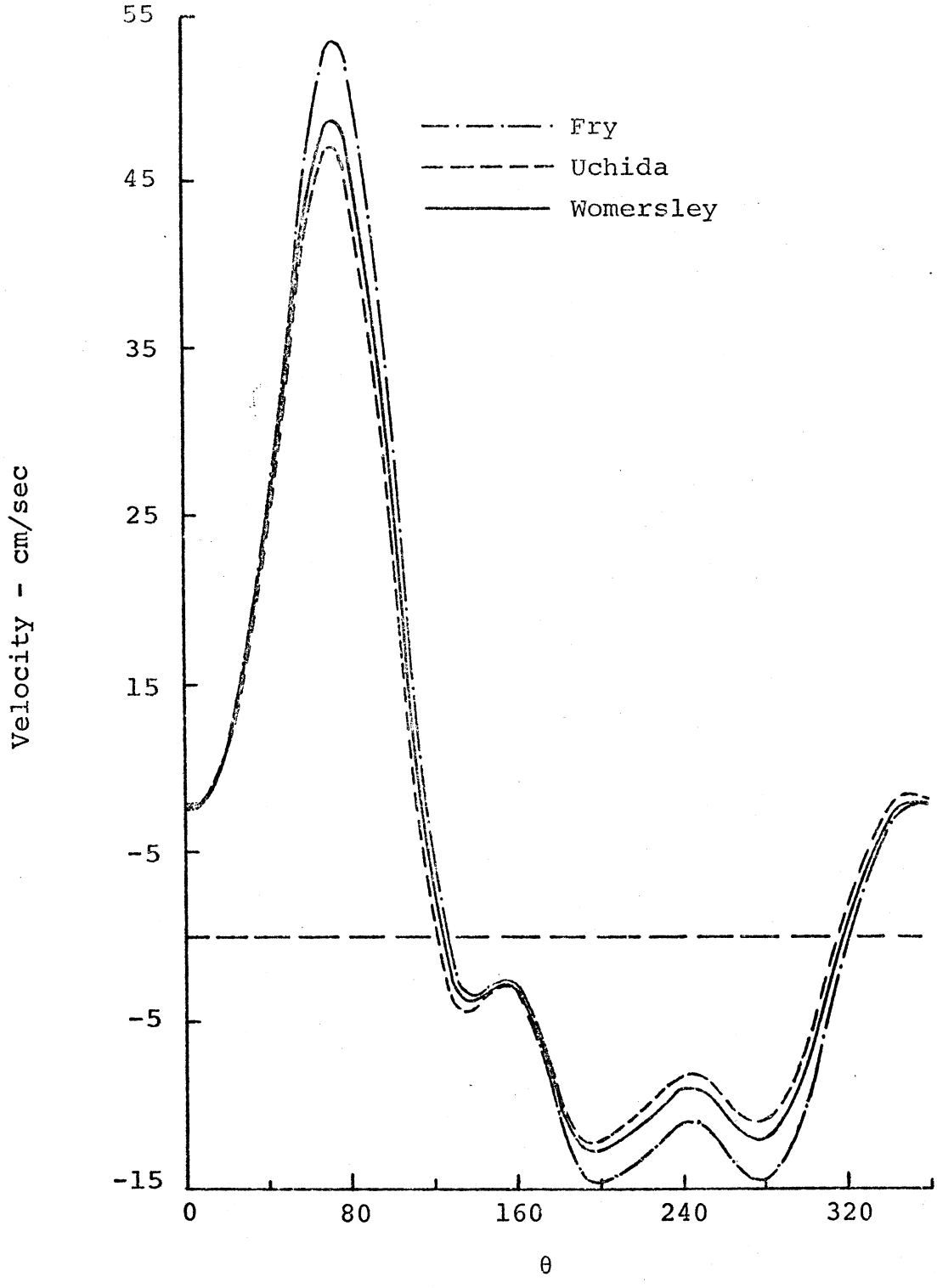

Figure 6.14 Comparison of Flow Theories - Run 32

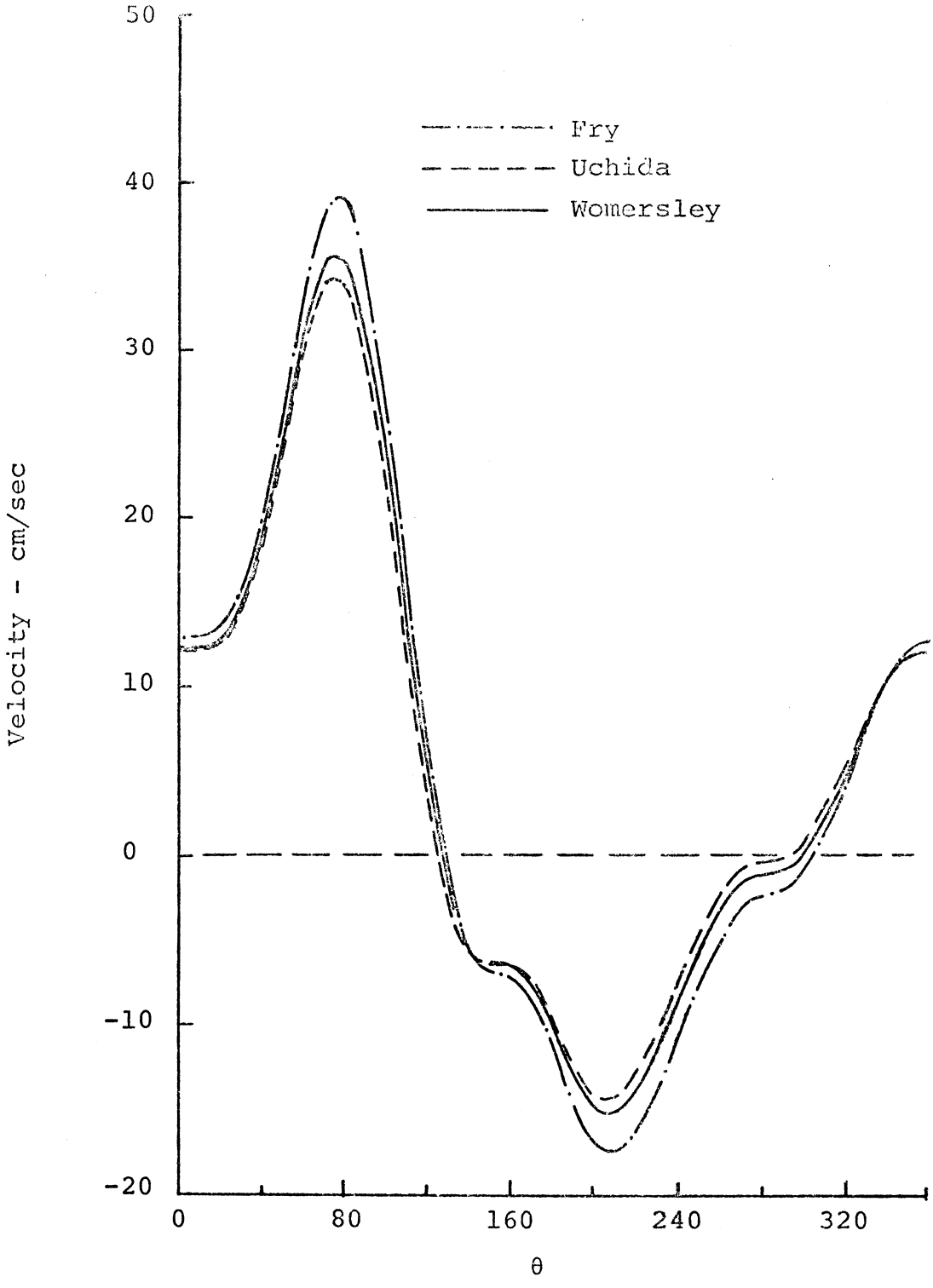

Figure 6.15 Comparison of Flow Theories - Run 47

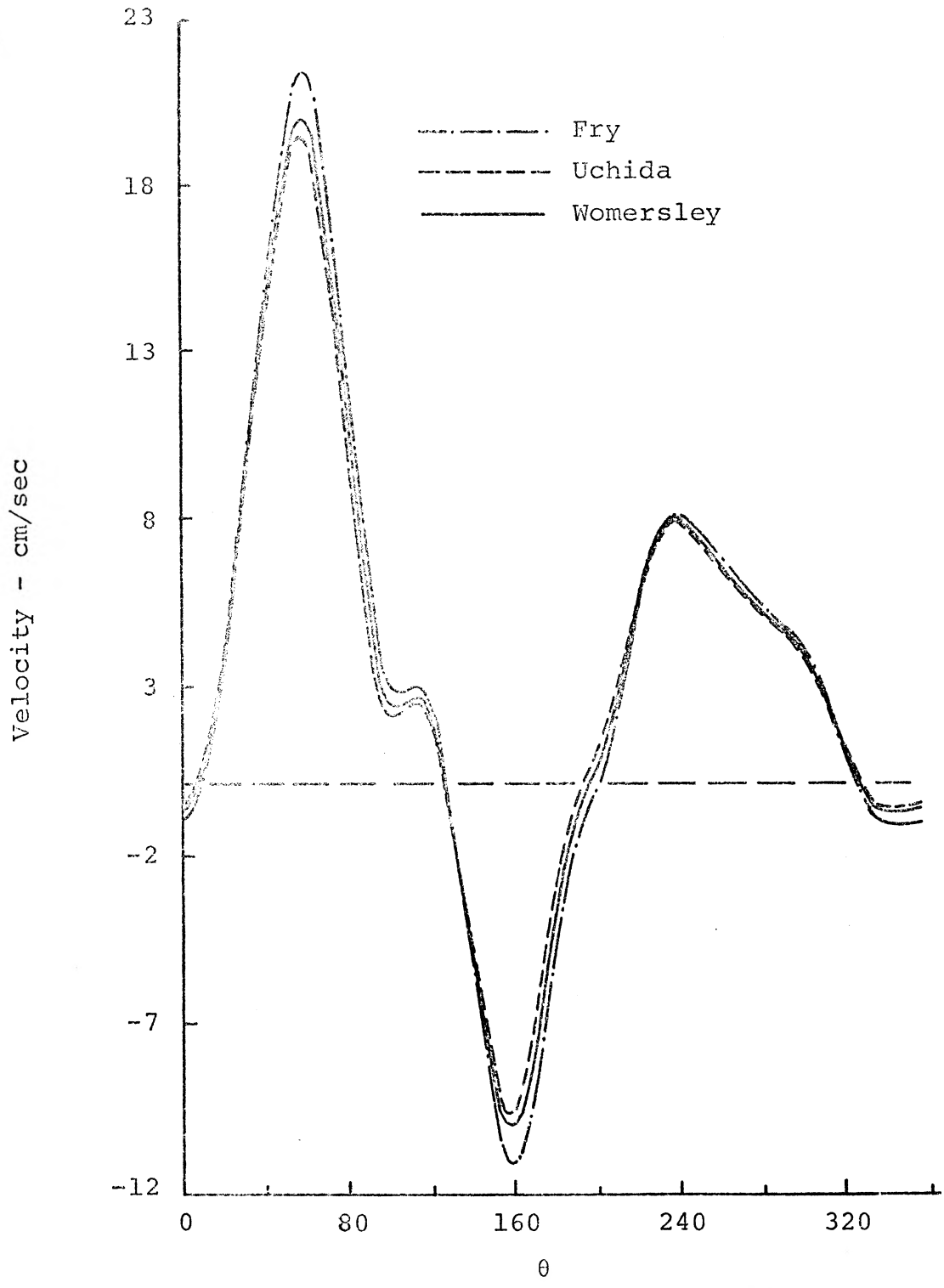

Figure 6.16 Comparison of Flow Theories - Run 75

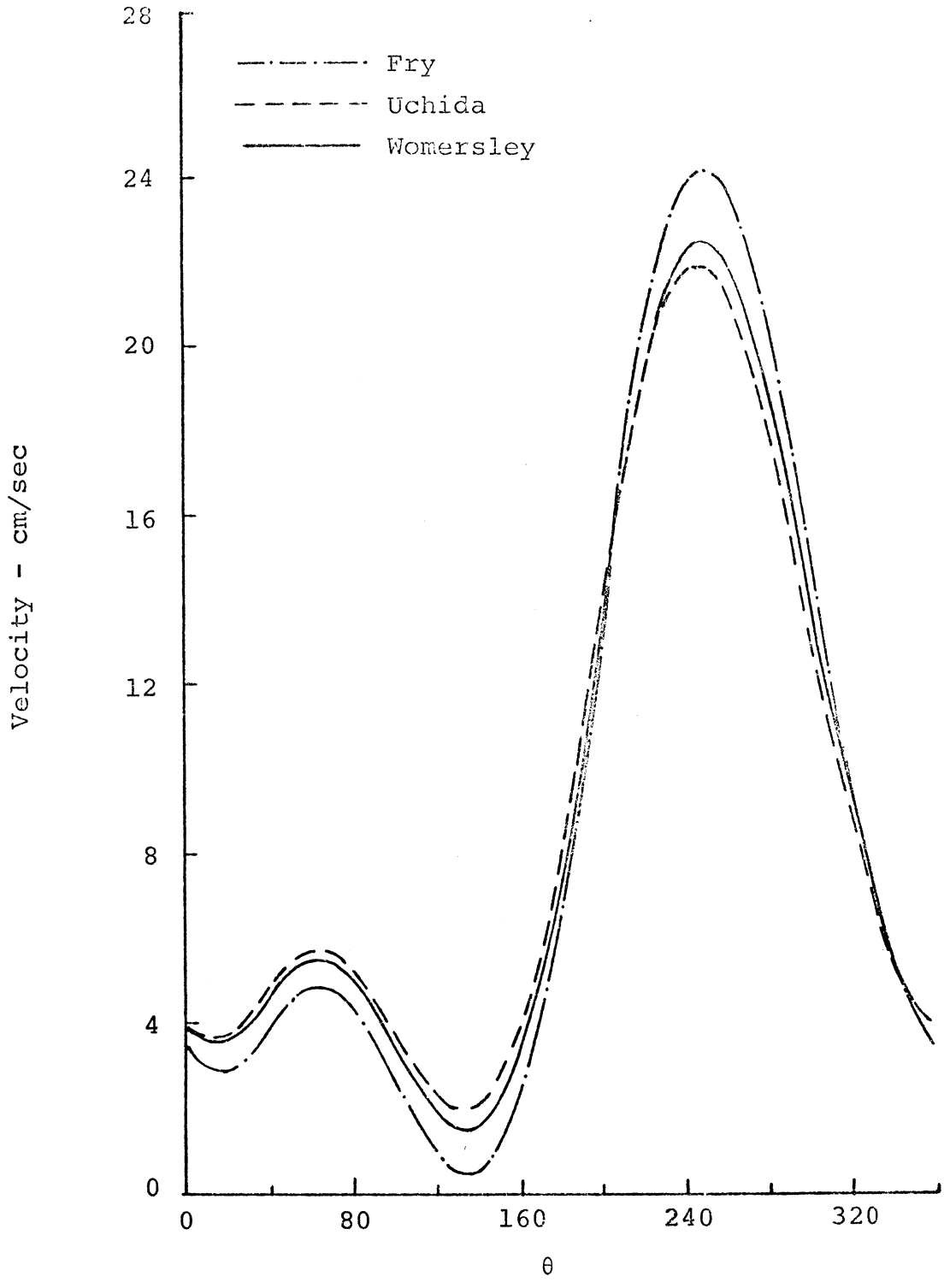

Figure 6.17 Comparison of Flow Theories - Run 87

TABLE 6.3

COMPARISON OF FLOW THEORIES

Harmonic	Model	Modulus	Phase
	Fry	25.18	325.4
1	Uchida	21.37	321.4
	Womersley	22.38	323.4
	Fry	9.82	308.9
2	Uchida	8.71	304.9
	Womersley	9.01	306.4
	Fry	6.97	304.1
3	Uchida	6.32	300.4
	Womersley	6.49	301.7
	Fry	6.08	264.6
4	Uchida	5.58	261.1
	Womersley	5.71	262.3
	Fry	1.71	289.9
5	Uchida	1.59	286.6
	Womersley	1.62	287.1

TABLE 6.3 (Continued)

Harmonic	Model	Modulus	Phase
	Fry	0.50	323.4
6	Uchida	0.46	320.4
	Womersley	0.47	321.4
	Fry	0.19	47.5
7	Uchida	0.18	44.7
	Womersley	0.18	45.6
	Fry	0.26	166.7
8	Uchida	0.25	164.0
	Womersley	0.26	164.8
	Fry	0.06	132.3
9	Uchida	0.06	129.6
	Womersley	0.06	130.4
	Fry	0.17	51.8
10	Uchida	0.16	49.2
	Womersley	0.16	50.0

Amplitude and phase correction factors have been used for the resistance and inductance by previous authors[27], e.g.,

$$R_s = (1.6)\frac{8\mu}{\pi R^4}$$

[see equation (2.93)] (6.31)

$$L = (1.1)\frac{\rho}{\pi R^2}$$

[see equation (2.44)] (6.32)

However, application of these corrections proved to exaggerate the result. The result was very near the Uchida solution for both phase and amplitude. Calculation of new correction factors from the present data yielded 1.1 ± .03 for resistance and 1.03 ± .02 for inductance. It was also found that the resistance correction factor can be approximated by the ratio of the first harmonic moduli. For example, from Table 6.3 a correction factor of 1.12 can be calculated from the first harmonic while the actual factor is 1.09. All in all, average values of 1.1 and 1.03 yield very good results.

6.7 Measurement of Flow Velocities

The instantaneous flow velocity was measured with the Doppler ultrasonic flowmeter described in section 3.5 and 3.6. Calibration details are described in section 4.1. The basic Doppler equation as it applies to the 1500 Ward Doppler Ultrasonic Flowmeter is as follows

$$F_1 - F_2 = F_d = 2 F_e \frac{\bar{v}_z}{C} \cos\theta \qquad (6.33)$$

where

F_d = Doppler frequency [cps]

F_e = Frequency of excitation [$5(10)^6$ cps]

$\bar{v}_z$ = Average velocity [cm/sec]

θ = Angle between acoustical and flow axes [60°]

C = Acoustic velocity in fluid [cm/sec]

Rewriting the Doppler equation in terms of velocity and the physical properties of the system yields

$$\bar{v}_z = 27.43\ (10)^{-3} F_d \qquad (6.34)$$

This is the theoretical coefficient of proportionality between velocity and frequency shift. A check on this, and a quick calibration technique, is to pass a known volume of liquid through the flow cuff and record the corresponding shift. These data points were then subjected to a least square analysis to determine the slope. The resulting equation is

$$\bar{v}_z = 27.57\ (10)^{-3} F_d \qquad (6.35)$$

All flow data was calculated from equation (6.35) with latex pigment producing the back scattering (see section 4.4).

After all the experimental data had been taken, some unit density, 1 μ diameter polystyrene particles became

available. The foregoing calibration data was repeated using these particles to seed the test fluid. Excellent agreement was obtained and the following equation verified that the latex particles were sufficient.

$$\bar{v}_z = 27.83\ (10)^{-3}\ F_d \qquad (6.36)$$

Pulsatile flow data could then be taken and recalibrated at any time by imposing the measured bucket velocity on the "electronic mean" of the AC components. A typical pressure gradient-flow relationship is shown in Figure 6.18. The velocity curve is reproduced from the Fourier coefficients obtained from the experimental data. This integrates out some of the higher frequency components that are present in the raw flow data. These components are due to some randomness of the particles in the control volume, turbulence and non-uniformity of the flow field. However, no major attenuation occurs when the integration time constant is below 0.03 seconds for the frequencies of interest. This can also be seen from the harmonic content of the higher harmonics. Tables 6.1 and 6.2 show 93% of the energy is 10 harmonics while the harmonic percents average 3.5% over the last 5 harmonics. Thus the average error is probably less than 5% (see section 6.1).

The measured flow velocities compared extremely well to all three flow models, as it was shown in the previous section that there is not very much difference in

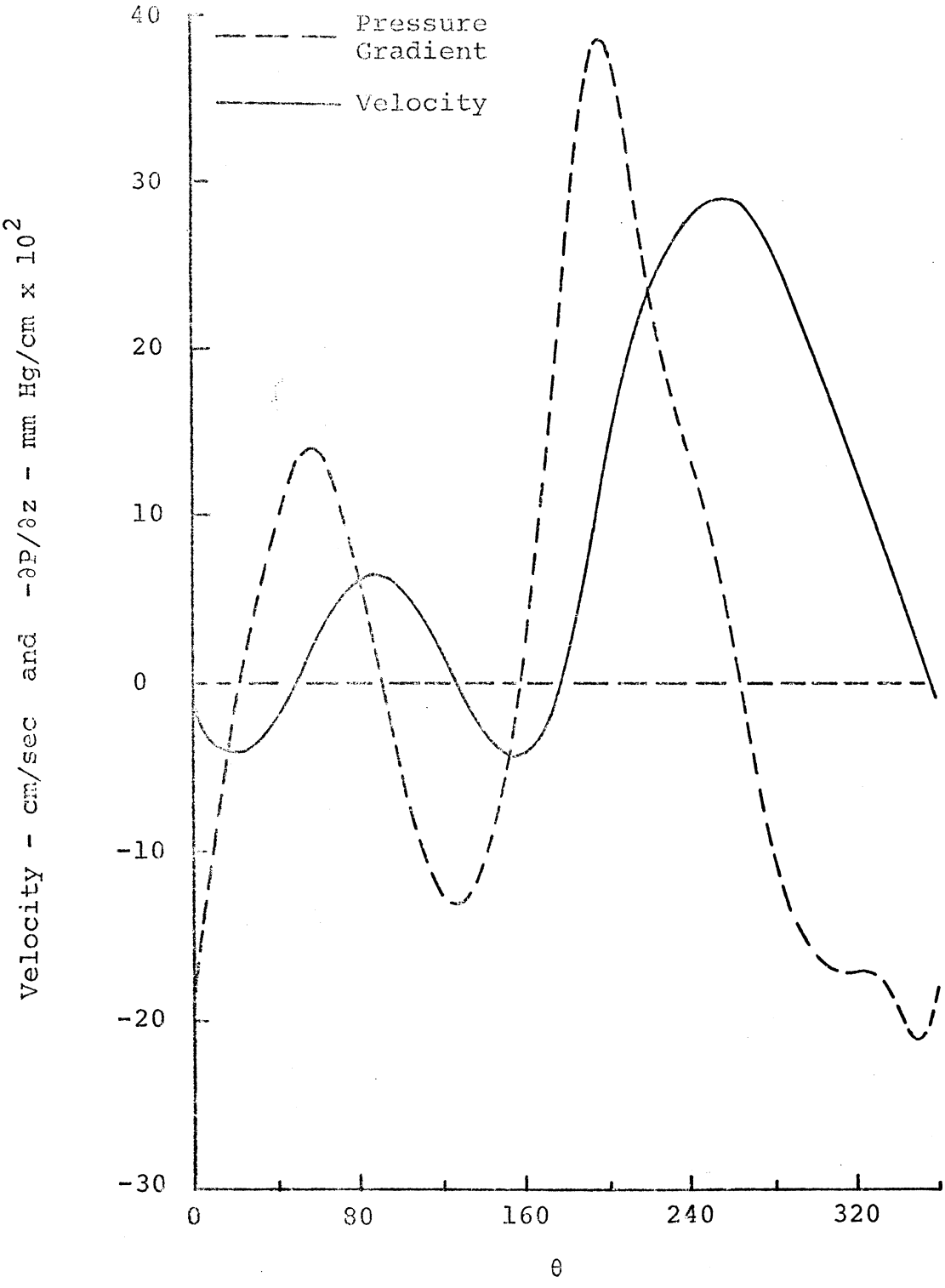

Figure 6.18 Relationship of Pressure Gradient to Velocity - Run 8

the theoretical solution. Figure 6.19 compares the measured velocity to that predicted by Womersley's theory. The theory underestimates the peak flow by some 4% and the back flow by 10%. As the pressure gradient reverses due to the upstream phase lead, the flow is retarded and then reverses. This reverse flow is increased by the retrograde wave until that pressure difference reverses (at 160° on Figure 6.2). From there through 240°, the flow is accelerated downstream due to the second reflection off the inlet (now a forward reflection). The experimental data shows that the theory underpredicts the secondary forward portion by 20 - 25%. This can best be explained by the attenuation factor of the second forward wave being unequal to the first forward damping factor. Womersley's theory assumes that the waves are attenuated the same in both directions. However on the whole, the data fits the theoretical solutions very well, especially during the primary portion of the cycle (which is of prime importance). Also the reflection coefficients present in this run (run 75) are extremely high. This gives rise to larger error than would otherwise occur. It is felt that the theory predicts the physical phenomona of the flow field as accurately as it can be measured.

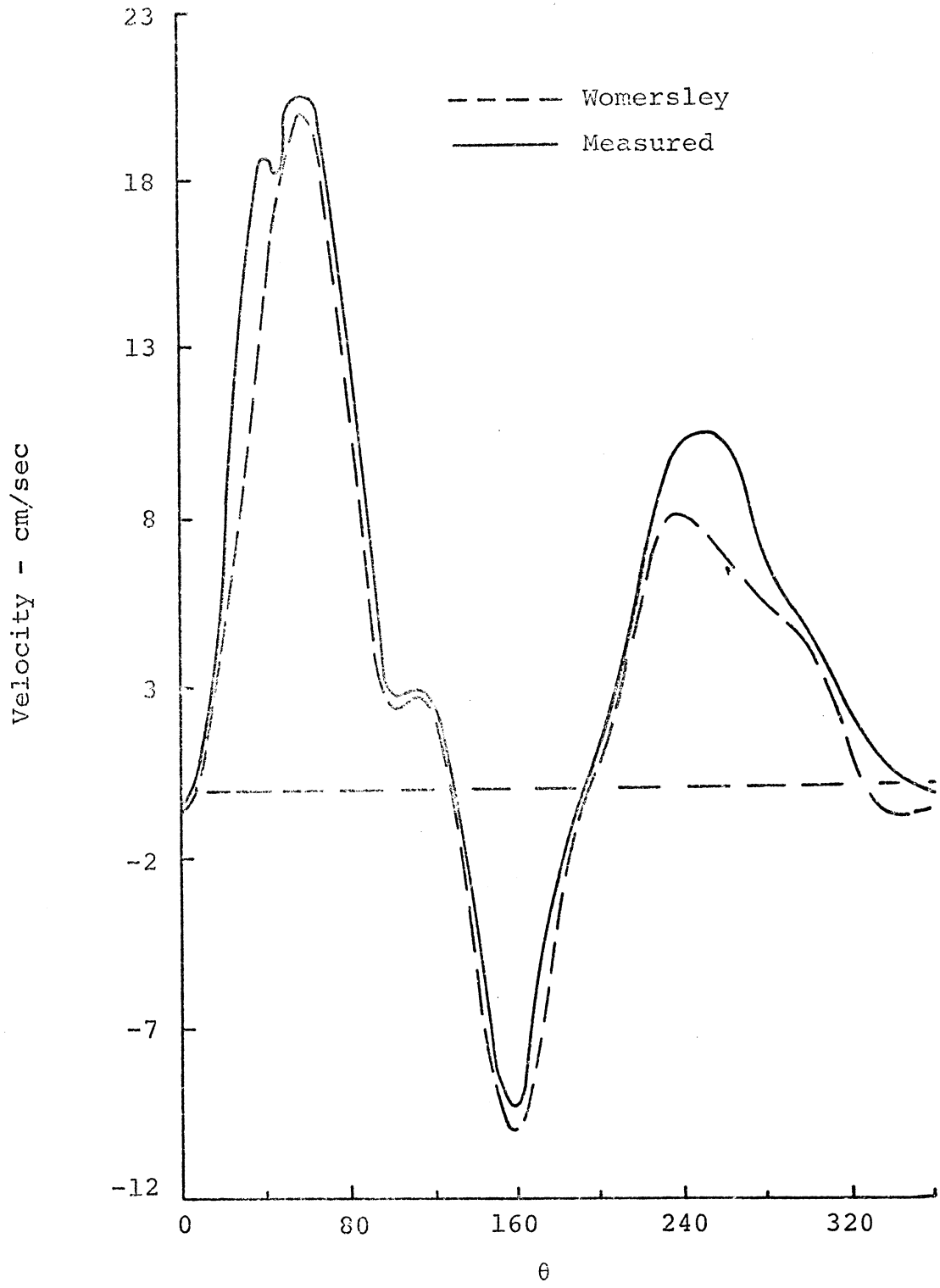

Figure 6.19 Comparison of Calculated to Measured Flow - Run 75

CHAPTER VII

CONCLUSIONS AND RECOMMENDATIONS

7.1 Introduction

The scope of this investigation was outlined in section 1.2 with the main objective being the determination of a method of obtaining the internal flow rate with an external measurement. To do this, it was first necessary to examine the current mathematical models to determine the accuracy of predicting flow fields from measured pressure gradients. Since the pressure gradient is the driving force for acceleration of the fluid, various methods were suggested to calculate this forcing function from measurement of other quantities (i.e., diameter gradient and time derivatives of both pressure and diameter). The success of these techniques were quantitatively discussed in Chapter VI, while qualitative conclusions will be listed in the next sections.

7.2 Necessity of Elasticity Model

The main consideration used to justify the need of another elasticity model was the constraint of plain strain. In the study of a tethered elastic tube, the removal of longitudinal displacement greatly disturbed the author. Quantitative justification came when pulse velocities calculated were smaller than measured counterparts. The use

of the present model improved these results, so the model was used exclusively throughout the study.

7.3 Calculation of Flow From the Models

Womersley's elastic solution accurately predicts the deviation of pulsatile flow in flexible tubes from Uchida's solution for corresponding flow in rigid tubes. Both solutions are equally laborious and difficult to apply in that they require the calculations of complex Bessel functions of both zero and first order. However, Fry's simplified model predicted surprisingly good results for all of the flow conditions tested. The error produced by the use of this model was always in the same direction and predictable correction factors were obtained to allow accurate calculations to be made. Thus, due to the excellent results obtained from Fry's model, it was concluded that the more complex theories need not be used if the average instantaneous velocity is the quantity of interest.

7.4 Calculation of Pressure From Diameter

Pressure-diameter relationships were discussed in section 6.2. It was shown the internal pressure could be determined very accurately from the external measurement of diameter. This was accomplished within 5% deviation over the complete cycle for most flow runs when the non-linearity over the pulse cycle and phase relationships were taken into account. The pressure gradient could theoretically be calculated from two external wall position measurements via

this approach. However, better accuracy is obtained if the subtractions are performed on the electronic signals rather than on the Fourier functions.

7.5 Calculation of Pressure Gradient From Diameter Gradient

A functional relationship between spatial gradients of pressure and diameter was introduced in section 6.4. It was found that the pressure gradient could be calculated within 10% from the external measurement of displacement at two locations. To do this, accurate pressure-volume data of the vessel of interest must be known to allow calculation of the coefficient of proportionality. Once this is known, the pressure gradient can be determined directly from the external measurements and used as the forcing function in the desired flow model.

7.6 Relationship of Spatial Gradient to Time Derivative

A flow relationship was shown to exist between the temporal derivative and spatial gradient of pressure. The assumptions implied in the use of the simplified real equation (equation 6.30) were outlined to determine the applicability and use of this simple relationship. Experimental results indicated that approximate gradients could be obtained in this manner when the group velocity was substituted for the phase velocity.

This technique yielded the largest error for determination of the pressure gradient, but could still be very

useful if, experimentally, there was a constraint of one physical measurement.

7.7 Summary

The basic conclusions are

(1) Womersley's elastic solution is an accurate representation of the flow field.

(2) Fry's approximation can be used for simplicity.

(3) Predictable pressure-diameter relationships exist.

(4) Pressure gradient can be obtained from diameter gradient.

(5) Pressure gradient-time derivative relationships exist and can be used to yield approximate results.

(6) Internal flow velocities can be obtained from two external measurements of wall position very accurately.

(7) One wall position will yield approximate ($< 25\%$) flow conditions.

7.8 Recommendations for Future Work

The obvious extension of this investigation would be clinical application of the techniques described here. Intermediate studies to determine pressure-volume data of the vessels of major interest, based on the elastic model presented here, could be done to further these clinical

application. The most important result of future work would be to verify any contributions contained in these techniques to simplify current clinical experimental measurement.

REFERENCES

1. Morgan, G. W., "On the Steady Laminar Flow of a Viscous Incompressible Fluid in an Elastic Tube," Bulletin of Mathematical Biophysics, Vol. 14, (1952).

2. Nishimura, Jiro, and Syoten Oka, "The Steady Flow of a Viscous Fluid through a Tapered Tube," Journal of the Physical Society of Japan, Vol. 20, No. 3 (1965).

3. Oka, Syoten, "The Steady Slow Motion of a Viscous Fluid through a Tapered Tube," Journal of the Physical Society of Japan, Vol. 19, No. 8, (1964).

4. Rashevsky, N., "A Problem in Mathematical Biophysics of Blood Circulatory; I," Bulletin of Mathematical Biophysics, Vol. 7, (1945)

5. _____, "A Problem in Mathematical Biophysics of Blood Circulatory; II," Bulletin of Mathematical Biophysics, Vol. 7, (1945).

6. Cerny, L. C., and W. P. Walawender, "The Flow of a Viscous Liquid in a Converging Tube," Bulletin of Mathematical Biophysics, Vol. 28, (1966).

7. Kuchar, N. R., and S. Ostrach, "Flows in the Entrance Regions of Circular Elastic Tubes," Biomedical Fluid Mechanics Symposium, ASME, p. 45, (1966).

8. Harris, F. D., Stability of Pulsating Incompressible Flow in Flexible-Elastic Tubes, Doctoral Dissertation, U. of Arkansas, Engineering Mechanics Department, 1966.

9. Morgan, G. W., and W. R. Ferrante, "Wave Propagation in Elastic Tubes Filled with Streaming Liquid," Journal of the Acoustical Society of America, Vol. 27, No. 4, (1955).

10. Morgan, G. W., and J. P. Kiely, "Wave Propagation in a Viscous Liquid Contained in a Flexible Tube," Journal of the Acoustical Society of America, Vol. 26, No. 3, (1954).

11. Streeter, V. L., W. F. Keitzer, and D. F. Bohr, "Pulsatile Pressure and Flow Through Distensible Vessels," Circulation Res., Vol. 13, (1963).

12. Yellin, E. L., "Laminar Turbulent Transition Process in Pulsatile Flow," Circulation Res., Vol. 19, (1966).

13. Attinger, E. O., "The Physics of Pulsatile Blood Flow with Particular Reference to Small Vessels," Investigative Ophthalmology, Vol. 4, No. 6, (1965).

14. Attinger E. O., H. Sugawara, A. Navarro, and A. Anne, "Pulsatile Flow Patterns in Distensible Tubes," Circulation Res., Vol. 18, (1966).

15. Cerny, L. C., and W. P. Walawender, "Blood Flow in Rigid Tapered Tubes," American Journal of Physiology, Vol. 210, (1966).

16. Chang, Chieh C., and H. Bulent Atabeck, "The Inlet Length for Oscillatory Flow and its Effects on the Determination of the Rate of Flow in Arteries,"

17. Hershey, Daniel, and Sung Joon Cho, "Blood Flow in Rigid Tubes: Thickness and Slip Velocity of Plasma Film at the Wall," Journal of Applied Physiology, Vol. 21, No. 1, (1966).

18. Kuchar, N. R., and S. Ostrach, "Unsteady Entrance Flows in Elastic Tubes with Application to the Vascular System," AIAA 3rd Fluid and Plasma Dynamics Conference, No. 70-786, 1970.

19. Merrill, E. W., A. M. Benis, E. R. Gilliland, T. K. Sherwood, and E. W. Salzman, "Pressure-Flow Relations of Human Blood in Hollow Fibers at Low Flow Rates," Journal of Applied Physiology, Vol. 20, No. 5, (1965).

20. Morgan, Beverly C., David H. Dillard, and Warren G. Guntheroth, "Effect of Cardiac and Respiratory Cycle on Pulmonary Vein Flow, Pressure, and Diameter," Journal of Applied Physiology, Vol. 21, No. 4, (1966).

21. Morkin, Eugene, "Analysis of Pulsatile Blood Flow and Its Clinical Implications," The New England Journal of Medicine, Vol. 277, No. 3, (1967).

22. Whitmore, Raymond L., "A Theory of Blood Flow in Small Vessels," Journal of Applied Physiology, Vol. 22, No. 4, (1967).

23. Brashears, M. R., and F. D. Harris, "Laminar Viscous Flow in Flexible-Elastic Tubes," 8th ICMBE, July, 1969.

24. Womersley, J. R., "Method for the Calculation of Velocity, Rate of Flow and Viscous Drag in Arteries When The Pressure Gradient is Known," Journal of Physiology, Vol. 127, (1955).

25. Uchida, Shigeo, "The Pulsating Viscous Flow Superposed on the Steady Laminar Motion of Incompressible Fluid in a Circular Pipe," Zamp VII, 1956.

26. Womersley, J. R., "An Elastic Tube Theory of Pulse Transmission and Oscillatory Flow in Mammalian Arteries," Wright Air Development Center, Tech. Rept. WADC-TR-56-614, 1958.

27. Fry, D. L., "The Measurement of Pulsatile Blood Flow by the Computed Pressure Gradient Technique," IRE Trans. Med. Election ME-6, 1959.

28. Greenfield, J. C., Jr., and D. L. Fry, "Relationship Between Instantaneous Aortic Flow and the Pressure Gradient," Circulation Res., Vol. 17, (1965).

29. _____, "A Critique: Relationship of the Time Derivative of Pressure to Blood Flow," Circulation Res., Vol. 20, (1965).

30. Skalak, R., "Wave Propagation in Blood Flow," Biomechanics Symposium, ASME Annual Meeting, November, 1966.

31. Barnett, C. O., A. J. Malles, and A. Shapiro, "Relationship between Aortic Pressure and Diameter in the Dog," Journal of Applied Physiology, Vol. 16, (1961).

32. Love, A. E. H., "A Treatise on Mathematical E Elasticity, 3rd ed. Cambridge University Press, 1927.

33. Bergel, D. H., "The Static Elastic Properties of the Arterial Wall," Journal of Physiology (London), Vol. 156, 1961.

34. Attinger, E. O., Pulsatile Blood Flow, Pulsatile Blood Flow Symposium, McGraw-Hill, New York, 1963.

35. Cox, R. H., "Wave Propagation Through a Newtonian Fluid Contained Within a Thick-Walled, Viscoelastic Tube," Biophysical Journal, Vol. 8, (1968).

36. Attinger, E. O., A. Anne, and D. A. McDonald, "Use of Fourier Series for the Analysis of Biological Systems," Biophysical Journal, Vol. 6, (1966).

37. Hjelmfelt, A. T., "Motion of Discrete Particles in a Turbulent Fluid," Applied Science Research, Vol. 16

38. McDonald, D. A., Blood Flow in Arteries, Edward Arnold LTD., London, 1960.

39. Courant, R., and D. Hilbert, Methods of Mathematical Physics, Interscience Publishers, Inc., New York, 1953.

40. Abramowitz, M., and I. A. Stegun, Handbook of Mathematical Functions, National Bureau of Standards, Washington, D. C., 1970.

A P P E N D I C E S

APPENDIX A

ANALOG TO DIGITAL PROCESS

The analog magnetic tape contains six signals to be digitized. The tape is inputed to the SEL 840A by a Hewlet-Packard model 3514A reproducer. The machine language A/D program monitors a control channel (channel 7 on the analog tape) and upon detection of a positive voltage begins sampling channels 1 through 6. The results are treated as simultaneous digital points on all six channels. However, in actuality, a constant time line is skewed in the real time domain by 25 sec. per channel. This gives rise to a total shift of 150 sec. from channel 1 through channel 6. This shift can be neglected as the sampling rate is selected to yield approximately one hundred digital points per data cycle, and for the lowest frequency (a period of 1 sec.), the time spacing from point to point is 0.01 sec., which is much greater than the total skew. Therefore, point 1 of channel 1 corresponds directly to point 1 on any other channel.

The control channel contains a 1.5 volt square wave of one-half the fundamental frequency of the data signals. This allows digitalization of one complete cycle of data during the time the positive portion of the square wave is being reproduced. This square wave is produced by the

electrical circuit shown in Figure 3.8, and is controlled by a micro-switch that follows the motion of the connecting rod of the pulsatile pump (see Figure 3.4). Thus, one complete cycle of the pump (which is the fundamental frequency of the system) produces either a positive or negative 1.5 volts.

A flow chart of the entire process is shown in this appendix.

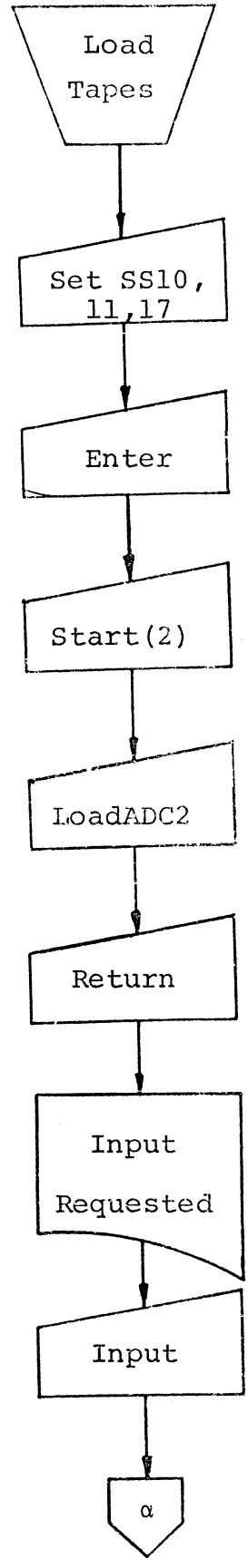
Load
Tapes
Set SS10,
11,17
Enter
Start(2)
LoadADC2
Return
Input
Requested
Input
α

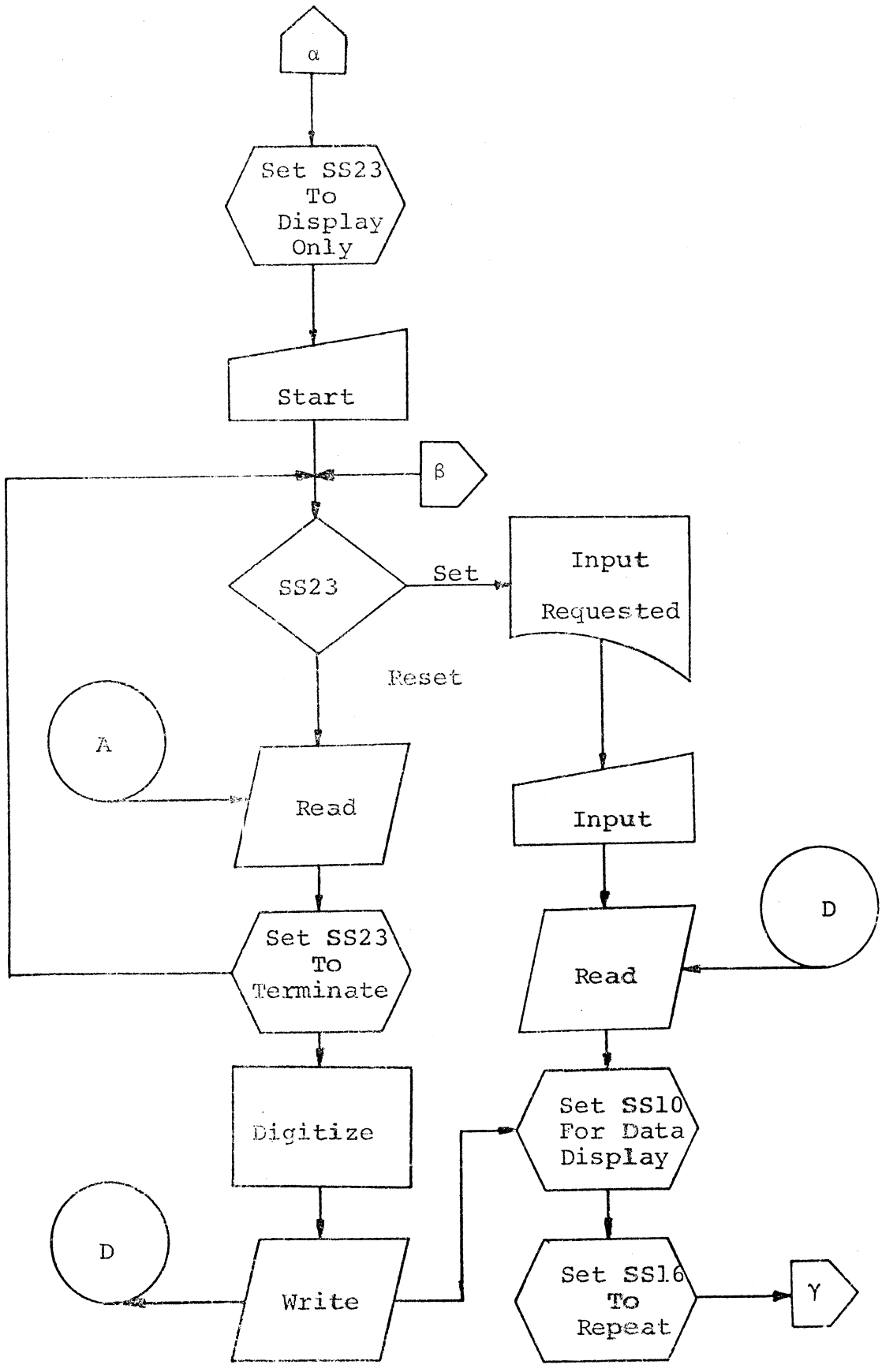
α
Set SS23 To Display Only
Start
β
SS23
Set
Input Requested
Reset
A
Read
Input
D
Read
Set SS23 To Terminate
Digitize
Set SS10 For Data Display
D
Write
Set SS16 To Repeat
γ

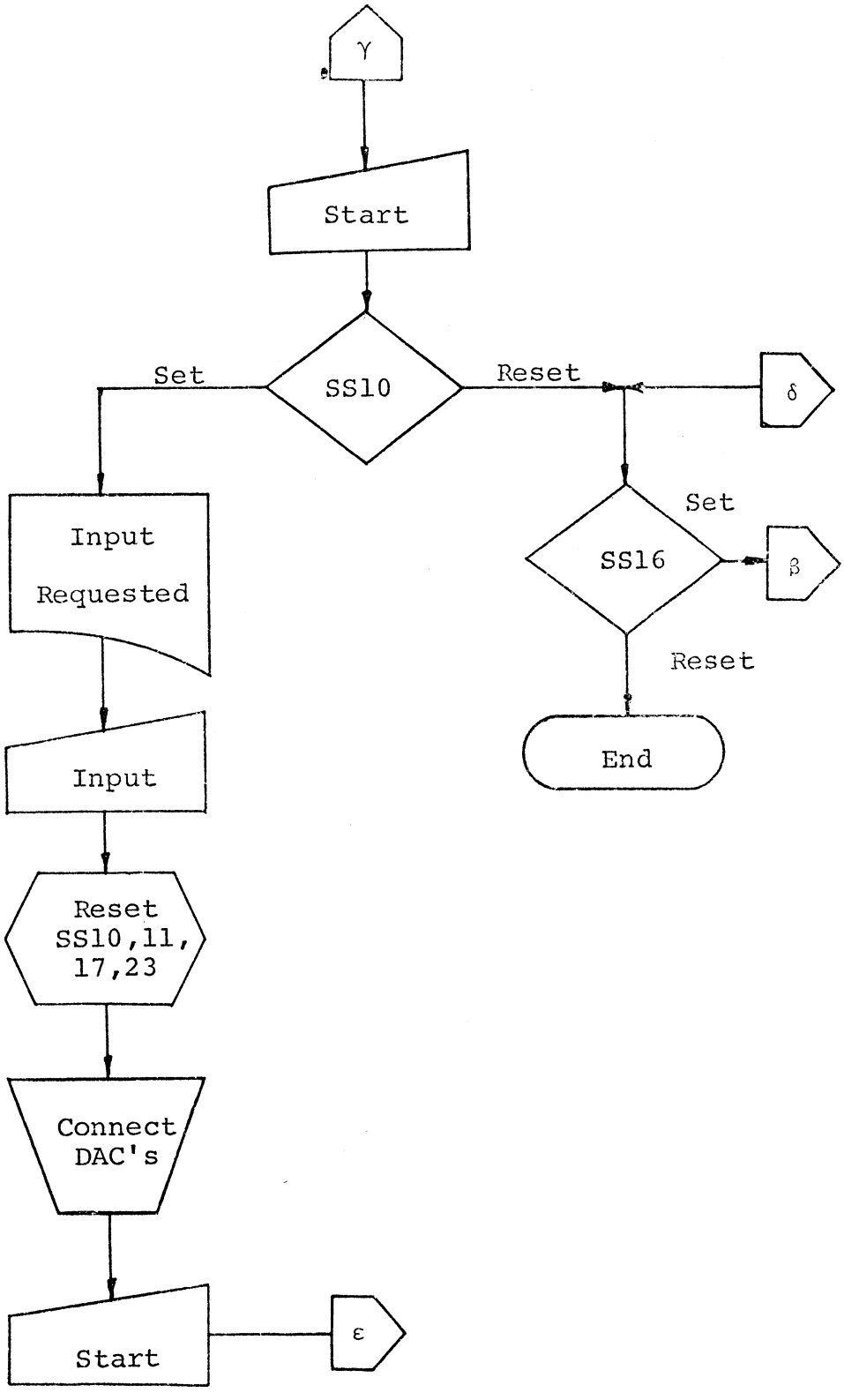
γ
Start
SS10
Set
Reset
δ
Input
Requested
SS16
Set
β
Reset
End
Input
Reset
SS10,11,
17,23
Connect
DAC's
Start
ε

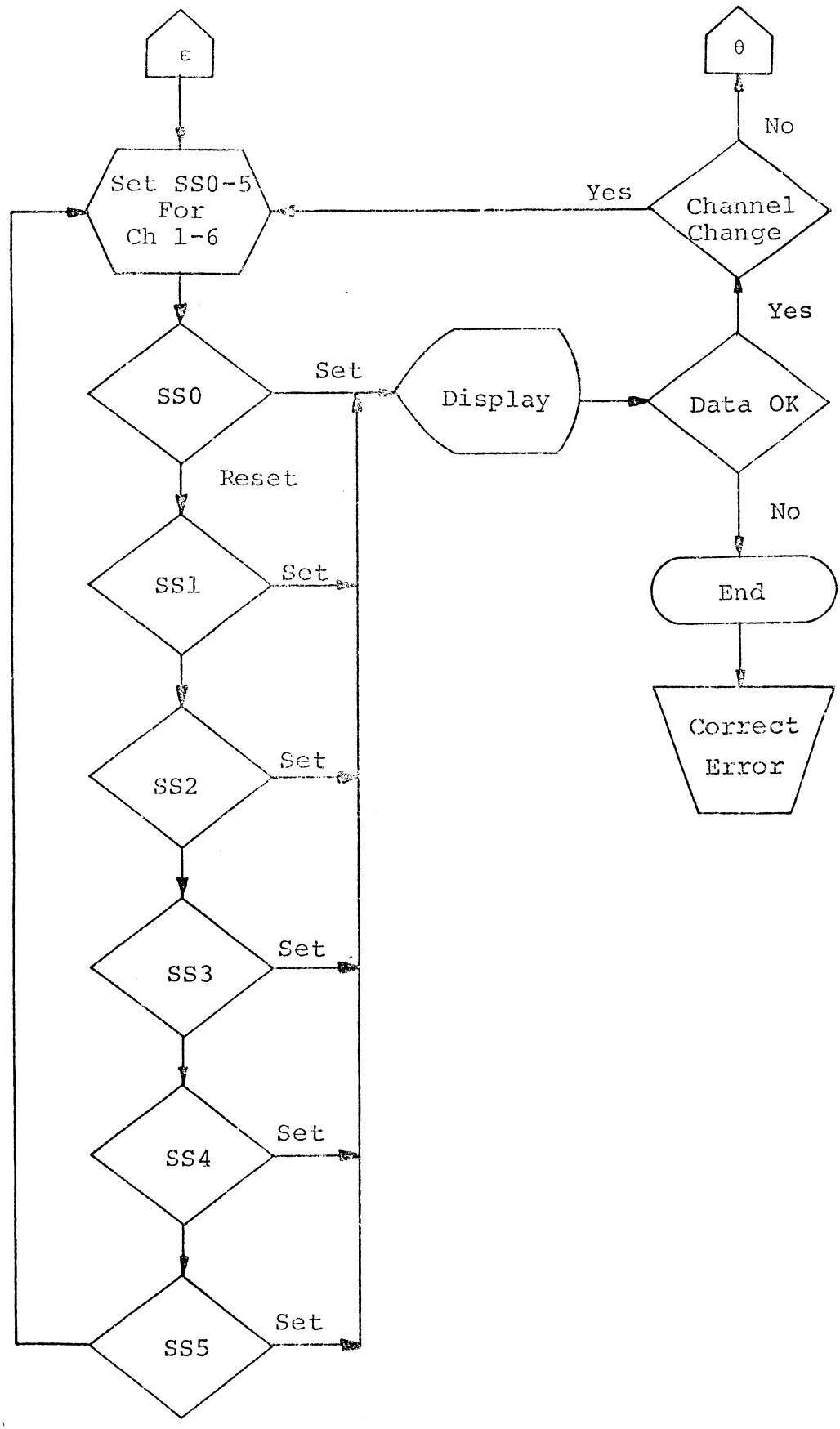
ε
θ
No
Set SS0-5 For Ch 1-6
Yes
Channel Change
Yes
SS0
Set
Display
Data OK
Reset
No
SS1
Set
End
SS2
Set
Correct Error
SS3
Set
SS4
Set
SS5
Set

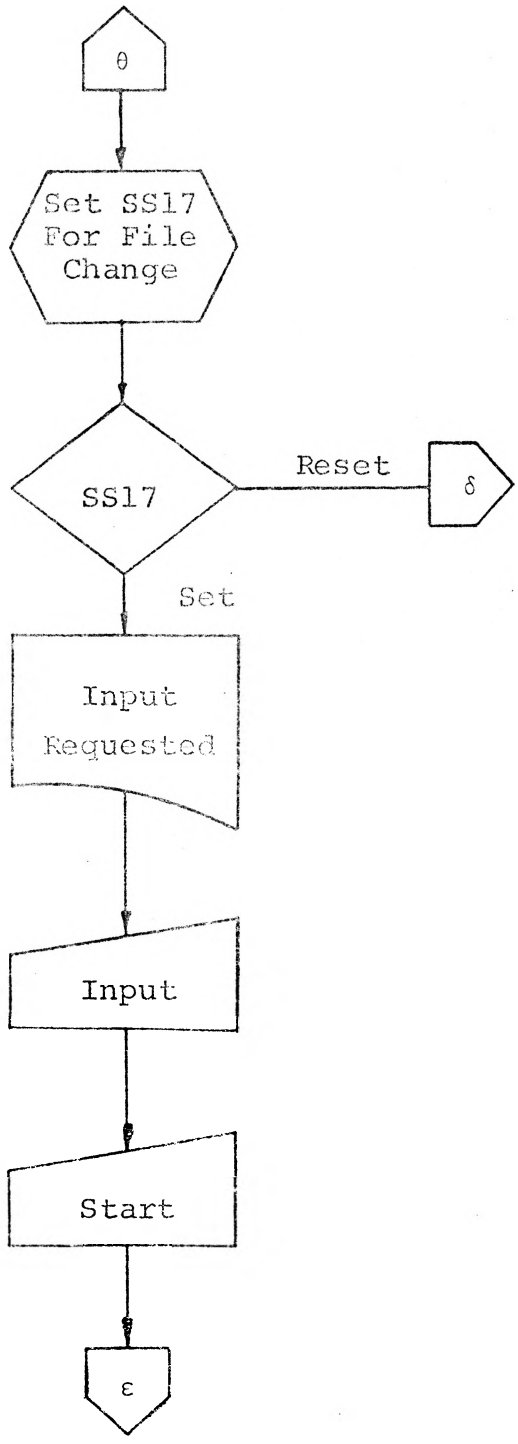
θ
Set SS17 For File Change
SS17
Reset
δ
Set
Input Requested
Input
Start
ε

```
$PIC45   UPDATED ADC PROGRAM UTILIZING BTC@S**R W L**C4
      *MAY 70**
      ORG  0200
STRT  CALL MAGT          INITIALIZE MAG TAPE
      LIX  ONRD,1        CLEAR DATA FILE STORAGE COUNTER
      LAA  ZERO
      STA  DTFL&200,1
      IIB  *-1,1         UPDATE STORAGE COUNTER
      LIX  ZERO,3        SET-UP FILE COUNTER
BLAG  CALL CRLF          OUTPUT CARR RETN AND LINE FEED
      CALL ASRO          ASK FOR BLOCK SIZE
      DAC  MES7
      CALL ASRI          INPUT BLOCK SIZE
      SNS  19            IF SET, RE-ENTER VALUE
      BRU  BLAG          SET--DO IT AGAIN
      BAP  CNT1          CHECK FOR NO INPUT ERROR
      CALL ERR1          OUTPUT MESSAGE OF INPUT ERROR
      DAC  BLAG
CNT1  CMA  TOFE          CHECK FOR VALUE LE 2048
      BRU  CNT2          OK
      BRU  CNT2          OK
      CALL ERR2          OUTPUT MESSAGE OF VALUE TC LARGE
      DAC  BLAG
CNT2  STA  TTOC          SAVE VALUE AS BLOCK SIZE
      AMA  INO1
      STA  STA1          CREATE INSTRUCT TO CLEAR ARRAY-1
      LAA  TTOC
      AMA  INO2
      STA  STA2          CREATE INSTRUCT TO CLEAR ARRAY-2
      LAA  TTOC          LOAD BLOCK SIZE
      MOA  MAK1          ADD TERMINATE BIT
      STA  WCTP          STORE FOR USE BY TAPE WC BTC
INAG  CALL CRLF          OUTPUT CARR RETN AND LINE FEED
      CALL ASRO          ASK FOR NUMBER OF CHANNELS
      DAC  MES5
      CALL ASRI          INPUT NUMBER OF CHANNELS
      SNS  19            IF SET, RE-ENTER VALUE
      BRU  INAG          SET--DO IT AGAIN
      BAP  CNT3          CHECK FOR NO INPUT ERROR
      CALL ERR1          OUTPUT MESSAGE OF INPUT ERROR
      DAC  INAG
CNT3  BAZ  INAG          ZERO NOT ALLOWED
      CMA  EGHT          CHECK FOR MAXIMUM CHANNEL SCAN E
      *XCEEDED
      BRU  CNT4          OK
      BRU  CNT4          OK
      CALL ERR2          OUTPUT MESSAGE OF VALUE TC LARGE
      DAC  INAG
CNT4  STA  CHNL          SAVE VALUE
INT2  CALL CRLF          OUTPUT CARR RETN AND LINE FEED
      CALL ASRO          ASK FOR OCTAL DATA CHANNELS
      DAC  MES6
```

```
      LAA   CHNL          SET-UP INPUT COUNTER
      NEG
      TAI   ,1
      NEG                 CREATE STORE A ACC INSTRUCTION
      AMA   MUXS
      STA   ST01
      STA   ST02
      CALL  CRLF          OUTPUT CARRIAGE RETN AND LINE FE
      *ED
LP01  CALL  OCTI          INPUT 2 OCTAL DIGITS
ST01  ZZZ                 STORE INSTRUCTION PUT HERE
      IIB   LP01,1        UPDATE INPUT COUNTER
      HLT                 PAUSE
      SNS   19            IF SET, RE-ENTER VALUE
      BRU   INT2
      LAA   CNTN          INSERT CONTROL CHANNEL
ST02  ZZZ
      LAA   CHNL          GET CORRECT CHANNEL COUNT
      AMA   ONE
      MOA   MAK1          ADD TERMINATE BIT
      STA   @63           SET MUX WC
      STA   @65           SET DATA WC
      LAA   ADDR          SET MUX CWA
      STA   @62
      LAA   BUF1          SET DATA CWA
      STA   @64
      CLA                 CALCULATE NUMBER OF PROGRAM LOOP
      *S
      LBA   TTOC
      DIV   CHNL          LOOPS # BLOCK SIZE/NUMBER OF CHA
      *NNELS
      NEG
      STA   NLOP          SAVE INDEX VALUE
      STB   TEMP          SAVE REMAINDER
      CALL  CRLF          OUTPUT CARR RETN AND LINE FEED
      LAA   TEMP          LOAD REMAINDER
      CALL  ASRD          OUTPUT REMAINDER
      CALL  ASRD          OUTPUT MESSAGE OF UNUSED WORDS A
      *T END
      DAC   MESH
      LAA   TEMP          LOAD REMAINDER
      BAZ   LP02          SKIP IF ALL OF ARRAY WILL BE USE
      *D
      NEG
      TAI   ,1            SET-UP STORAGE COUNTER
      CLA
STA1  ZZZ                 SET AREA IN ARRAY-1 TO 0
STA2  ZZZ                 SET AREA IN ARRAY-2 TO 0
      IIB   *-2,1         UPDATE STORAGE COUNTER
LP02  CALL  CRLF          OUTPUT CARR RETN AND LINE FEED
      CALL  ASRD          ASK FOR NUMBER OF FILES TO SKIP
      DAC   MES1
```

```
      CALL  ASRI        INPUT NUMBER OF FILES
      SNS   19          IF SET, RE-ENTER VALUE
      BRU   LP02        SET--DO IT AGAIN
      BAP   CNT5        CHECK FOR NO INPUT ERROR
      CALL  ERR1        OUTPUT MESSAGE OF INPUT ERROR
      DAC   LP02
CNT5  STA   FILL        SAVE NUMBER OF FILES SAVED
      BAZ   DOIA        SKIP IF NO FILES ARE TO BE SAVED
      CALL  FILEFW      SKIP NUMBER OF FILES SAVED
DOIA  CALL  CRLF        OUTPUT CARR RETN AND LINE FEED
      CALL  ASRO        ASK FOR SAMPLING RATE
      DAC   MES2
      CALL  ASRI        INPUT SAMPLING RATE
      STA   TEMP        SAVE INPUT VALUE
      BAP   CNT6        CHECK FOR NO INPUT ERROR
      CALL  ERR1        OUTPUT MESSAGE OF INPUT ERROR
      DAC   DOIA
CNT6  CALL  ASRO        OUTPUT MESSAGE OF ACTUAL RATE
      DAC   MES3
      LAA   TEMP        LOAD VALUE
      CMA   THRE        CHECK FOR RATE LESS THAN 3
      BRU   *&3
      BRU   *&2
      BRU   CONT
      LAA   DCMX        SET RATE TO SLOWEST POSSIBLE VAL
      *UE
      STA   SAMP
      LAA   THRE        PREPARE TO OUTPUT A 3
      CALL  ASRD        OUTPUT MINIMUM DECIMAL RATE
      BRU   OUTD        BRANCH AND CONTINUE
CONT  CLA
      LBA   OSTS        LOAD 160,000 INTO B ACC
      DIV   TEMP        DIVIDE TO GET INT TMR CONTROL VA
      *LUE
      STA   SAMP        STORE VALUE AT CONTROL LOCATION
      CLA               CHECK FOR REMAINDER GE .5
      MPY   TWO
      DIV   TEMP
      BAZ   *&2         IF 0, DO NOT INCREMENT
      IMS   SAMP        INCREMENT SAMPLING RATE BY ONE
      CLA               CALCULATE ACTUAL RATE
      LBA   OSTS        LOAD 160,000 IN B ACC
      DIV   SAMP        DIVIDE BY CONTROL VALUE
      STB   TEMP        SAVE REMAINDER
      CALL  ASRD        OUTPUT INTEGER PORTION OF THE RA
      *TE
      LAA   DCPT        OUTPUT DECIMAL POINT
      AOP   1,W
      CLA
      LBA   TEMP        LOAD REMAINDER
      MPY   TEN         MULTIPLY BY TEN
      DIV   SAMP        DIVIDE BY SAMPLING CONTROL VALUE
```

```
      AMA   TSTY          ADD @260 TC GET TTYP CODE
      LSL   16            SHIFT FOR OUTPUT
      AOP   1,W
OUTD  HLT
      SNS   19            IF SET, RE-ENTER VALUE
      BRU   DOIA          NO-DO IT AGAIN
      LAA   SAMP          MAKE CORRECTION ALLOWANCE FOR IN
      *TERRUPT
      SMA   TWO           TIME, BRANCH TIME, AND RESTART O
      *F INTERVAL
      STA   SAMP          TIMER
      CALL  CHCK          CHECK FOR MAXIMUM CHANNEL CAPACI
      *TY EXCEEDED
      DAC   CHNL
      DAC   SAMP
      DAC   TTOC
      DAC   DOIA
      LAA   BUF1          SET-UP MAG TAPE CWA
      STA   @66
      LAA   WCTP          SET-UP MAG TAPE WC
      STA   @67
      LAA   ITIR          SET-UP INTERVAL TIMER BRANCH
      STA   @123
      LAA   DBIR          SET-UP END OF DATA BTC BRANCH
      STA   @127
      CALL  CRLF          OUTPUT CARRIAGE RETN AND LINE FE
      *ED
      CALL  ASRO          TELL TC PRESS START TO BEGIN EXE
      *CUTION
      DAC   MES4
      HLT
      SNS   20            CHECK FOR DISPLAY ONLY
      BRU   DUMP          NO A/D WANTED, BRANCH TO DISPLAY
      PID   @77777,1      DISABLE ALL GROUP 1 INTERRUPTS
      PIE   @100,1        ENABLE DATA INTERRUPT
BEGN  LIX   NLOP,1        SET-UP LOOP COUNTER
      LIX   ZERO,2        CLEAR RECORDS PER FILE COUNTER
      CEU   @77           INITIALIZE ADC INTERFACE
      DATA  @30
      BRU   *-2
      MOP   @77           SET UP CHANNEL @10
      DATA  @10
      BRU   *-2
CKSC  AIP   @77           INPUT CONTROL SAMPLE
      BRU   *-1
      BAP   TRNT          SIGNAL WAS POSITIVE, CHECK FOR T
      *RANSIENT
      SNS   23            IF SET, TERMINATE ROUTINE
      BRU   DUMP          BRANCH AND TERMINATE
      BRU   CKSC          RECHECK CONTROL CHANNEL
TRNT  LAA   FIVE          LOAD SIGNAL CHECK VALUE
      STA   TEMP
```

```
      AIP   @77            INPUT A CONTROL SIGNAL
      BRU   *-1
      BAN   CKSG           BRANCH ON NEGATIVE CONTROL SIGNA
      *L
      IMS   TEMP           INCREMENT CONTROL SIGNAL COUNTER
      BRU   *-4
PIEC  PIE   @4,1           ENABLE INTERVAL TIMER INTERRUPT
      BRU   TIMR           BEGIN TO SAMPLE
WAIT  BRU   *-0            WAIT POSITION
*
*---BEGIN SAMPLING ROUTINE
*
TIMR  MOP   @12            START INTERVAL TIMER
SAMP  ZZZ                  CONTROL VALUE PUT HERE BY PROGRA
      *M
      BRU   *-2
      PIR   *&1            RESET INTERVAL TIMER INTERRUPT L
      *ATCH
      DAC   *&1
      CEU   @77            INITIALIZE MUX AND DATA BTC@S
      DATA  @40000030
      BRU   *-2
      LAA   CHNL           UPDATE DATA BTC CWA BY CHNL
      BRU   *-0            WAIT FOR END OF DATA INTERRUPT
DBTC  PIR   *&1            RESET DATA INTERRUPT LATCH
      DAC   *&1
      AAM   @64
      SMP*  @64            CHECK FOR POSITIVE CONTROL SIGNA
      *L
      BRU   ENBK           SIGNAL +0, GO TO END OF BLOCK
      IIB   WAIT,1         UP-DATE LOOP COUNTER
      LIX   NLOP,1         RESTORE LOOP COUNTER
      IIB   *&1,2          INCREMENT RECORDS PER FILE COUNT
      *ER
      CLA                  SET LAST WORD IN ARRAY TO 0
      STA*  @64
      CALL  WRTE           WRITE THE RECORD ON TAPE
      LAA   BUF1           INTERCHANGE BUFFER AREAS
      LBA   BUF2
      STA   BUF2
      STB   BUF1
      STB   @64            CHANGE DATA BTC CWA
      STB   @66            CHANGE TAPE BTC CWA
      BRU   WAIT           RETURN AND WAIT FOR TIMER INTERR
      *UPT
ENBK  PID   @4,1           DISABLE INTERVAL TIMER INTERRUPT
      IIB   *&1,1          UPDATE LOOP COUNTER
      IIB   *&1,2          INCREMENT RECORDS PER FILE COUNT
      *ER
      STI   TEMP,2         SAVE RECORDS PER FILE COUNTER
      LIX   ZERO,2         SET COUNTER TO ZERO
      LAA   TEMP           FETCH VALUE
```

```
      STA   DTFL,3          SAVE VALUE
      IIB   *&1,3           INCREMENT FILES WRITTEN COUNTER
      STI   TEMP,1          FIND THE NUMBER OF SPACES IN BLO
      *CK TO BE
      LAA   TEMP                  SET TC ZERO
      BAZ   WRIT            SKIP THIS SECTION IF ZERO
      MOA   MAK2            SET FIRST 9 BITS TC 1
      NEG                   FIND NUMBER OF LOOPS LEFT
      TAB
      CLA
      MPY   CHNL            MULTIPLY BY NUMBER OF CHANNELS U
      *SED
      TBA
      NEG
      AMA   ONE
      TAI   ,1              SET-UP REMAINDER COUNTER
      NEG
      AMA   @64             ADDRESS ABOVE CURRENT BLOCK
      AMA   STA             CREATE STA  ADDR,1  INSTRUCTION
      STA   STZO            SAVE INSTRUCTION
      CLA                   SET-UP ZERO DATA WORD
STZO  ZZZ                   STA INSTRUCTION PUT HERE BY PROG
      *RAM
      IIB   *-1,1           UPDATE REMAINDER COUNTER
WRIT  CALL  WRTE            WRITE DATA BLOCK ON TAPE
      CALL  WEOF            WRITE EOF ON TAPE
      LAA   BUF1            SET-UP NEW DATA BTC CWA
      STA   @64
      STA   @66             CHANGE TAPE BTC CWA
      SNS   22              IF SET, HALT PROGRAM
      HLT
      BRU   BEGN            BRANCH TO START OF SAMPLING ROUT
      *INE
*
*---DUMP FILE TABLE
*
DUMP  CALL  CRLF            OUTPUT A CARR RETN AND LINE FEED
      CALL  ASRO            OUTPUT NUMBER OF FILES SAVED ON
      *TAPE MESSAGE
      DAC   MESA
      LAA   FILL            LOAD NUMBER OF FILES SAVED
      CALL  ASRD            OUTPUT NUMBER SAVED
      STI   NUMB,3          SAVE FILES WRITTEN COUNTER
      LAA   LAA1            CREATE AND INDEXED LOAD INSTRUCT
      *ION
      AMA   NUMB            ADD NUMBER OF FILES WRITTEN
      STA   LAA             SAVE INSTRUCTION
      LAA   NUMB            GET NUMBER OF NEW FILES WRITTEN
      BAZ   *&2             CHECK FOR NO NEW FILES WRITTEN
      BRU   DTFL            FILES WERE WRITTEN, OUTPUT RECOR
      *D
      LAA   FILL            PREPARE TO OUTPUT NUMBER OF FILE
```

```
      *S ON TAPE
      STA   NUMB
      BRU   GOON              OUTPUT
OTFL  NEG
      TAI   ,3                SET-UP FILE OUTPUT COUNTER
      LAA   FILL
      STA   NUMB              SET CURRENT FILE INDEX POINTER
LOP3  CALL  CRLF              OUTPUT CARR RETN AND LINE FEED
      CALL  ASRO              OUTPUT FILE MESSAGE
      DAC   MES8
      IMS   NUMB              UPDATE CURRENT FILE POINTER
      LAA   NUMB              LOAD CURRENT VALUE
      CALL  ASRD              OUTPUT FILE NUMBER
      CALL  ASRO              OUTPUT RECORD MESSAGE
      DAC   MES9
LAA   ZZZ                     LOAD RECORD VALUE FROM TABLE
      CALL  ASRD              OUTPUT RECORDS IN THE FILE
      CALL  ASRO
      DAC   MESG
      IIB   LOP3,3            HAVE ALL NEW FILES BEEN LISTED
GOON  CALL  CRLF              OUTPUT CARR RETN AND LINE FEED
      CALL  ASRO              OUTPUT TOTAL FILES ON TAPE MESSA
      *GE
      DAC   MES8
      LAA   NUMB              LOAD NUMBER OF FILES NOW ON TAPE
      CALL  ASRD              OUTPUT NUMBERS OF FILES ON TAPE
DSPY  CALL  CRLF              OUTPUT CARR RETN AND LINE FEED
      CALL  ASRO              ASK FOR FILE DISPLAY OR NOT
      DAC   MESC
      HLT
      SNS   10                CHECK FOR DISPLAY
      BRU   *&2               SET, ENTER DISPLAY ROUTINE
      BRU   EXEC              LOAD AND RETURN CONTROL TO SYSTE
      *M EXEC
      LAA   TTOC              LOAD BLOCK SIZE
      AMA   BUF1              ADD STARTING ADDRESS
      STA   ADRS              SAVE ADDRESSING VALUE
      AMA   LAAN              CREATE LOAD INSTRUCTION
      STA   LOAD              SAVE INSTRUCTION
      LAA   ADRS              LOAD ADDRESSING VALUE
      AMA   STA               CREATE STOR INSTRUCTION
      STA   STOR              SAVE INSTRUCTION
      LAA   BUF1              SET TAPE BTC ChA
      STA   @66
      CLA                     PREPARE TO FIND X-AXIS INCREMENT
      LBA   PNTS              LOAD NUMBER OF X-AXIS SPACES
      DIV   TTOC              DIVIDE BY BLOCK SIZE
      TAB
      MPY   CHNL              MULTIPLY BY NUMBER OF DATA CHANN
      *ELS
      STB   INCR              SAVE X-AXIS INCREMENT VALUE
      LAA   NUMB              SET PRESENT FILE POSITION TO FIL
```

```
      *ES SAVED
      STA  CURF              & FILES WRITTEN & 1
      IMS  CURF
      BAZ  LDEX              IF NO FILES ON TAPE, LOAD EXEC
BGDY  SNS  23                CHECK FOR LOAD EXEC
      BRU  EXEC              SET, LOAD EXEC
      CALL CRLF              OUTPUT CARR RETN AND LINE FEED
      CALL ASRO              ASK FOR FILE TO DISPLAY
      DAC  MESD
      CALL ASRI              INPUT FILE TO BE DISPLAYED
      BAZ  BGDY              CHECK FOR FILE ZERO-ILLEGAL
      STA  FEDY              SAVE REQUESTED FILE VALUE
      BAP  CNT7              CHECK FOR NO INPUT ERROR
      CALL ERR1              OUTPUT MESSAGE OF INPUT ERROR
      DAC  BGDY
CNT7  CMA  NUMB              CHECK FOR THIS FILE ON TAPE
      BRU  CNT8              ON TAPE
      BRU  CNT8              ON TAPE
      CALL CRLF              OUTPUT CARR RETN AND LINE FEED
      CALL ASRO              OUTPUT MESSAGE OF THAT FILE NOT
      *PRESENT
      DAC  MESE
      BRU  BGDY              INPUT NEW FILE REQUEST
CNT8  CMA  CURF              DETERMINE WHICH WAY TO GO ON TAP
      *E
      BRU  BACK              BACK-SPACE TAPE TO CORRECT FILE
      BRU  REED              AT CORRECT FILE
      BRU  FOWD              ADVANCE TAPE TO CORRECT FILE
BACK  TAB                    SAVE REQUESTED FILE
      SMA  CURF              GET NUMBER OF FILES TO BACK-SPAC
      *E
      NEG
      AMA  ONE
      STB  CURF              UPDATE CURRENT FILE LOCATION
      CALL FILEBW            BACK-SPACE CORRECT NUMBER OF FIL
      *ES
      BRU  REED              BRANCH AND READ RECORDS
FOWD  TAB                    SAVE REQUESTED FILE
      SMA  CURF              GET NUMBER OF FILES TO ADVANCE
      CALL FILEFW            ADVANCE CORRECT NUMBER OF FILES
      STB  CURF              UPDATE CURRENT FILE LOCATION
REED  CALL READ              READ A RECORD FROM TAPE
      BAZ  CNTA              BRANCH ON NO EOF INDICATION
      IMS  CURF              INDICATE WE HAVE ENTERED NEXT FI
      *LE PAST AN EOF
      SNS  17                CHECK FOR NEW FILE
      BRU  BGDY              INPUT NEW FILE
      LAA  MONE              DECREMENT FILE INDICATION
      AAM  CURF
      LAA  TWO
      LBA  FEDY              LOAD REQUESTED FILE VALUE
      CALL FILEBW            BACKSPACE ONE FILE AND REDISPLAY
```

```
      BRU   REED          BRANCH AND READ A RECORD
CNTA  LAA   TTOC          SET-UP SHIFT COUNTER
      NEG
      TAI   ,1
LOAD  ZZZ                 LOAD DATA
      RSL   13            SHIFT DATA
STOR  ZZZ                 STORE DATA
      IIB   *-3,1         HAS ALL DATA BEEN SHIFTED
FIND  LAA   CHNL          LOAD NUMBER OF DATA CHANNELS
      NEG                 NEGATE
      TAI   ,1            USE AS SEARCH SWITCH COUNTER
      STI   TEMP,0        CLEAR CHANNEL INDICATOR
      LCS                 LOAD CONTROL SWITCHES
      BAN   CNTB          IS SWITCH SET
      LSL   1             NO, SHIFT LEFT AND CHECK NEXT ON
      *E
      IMS   TEMP          INCREMENT CHANNEL INDICATOR
      IIB   *-3,1         HAVE ALL ACTIVATED SWITCHES BEEN
      * CHECKED
      SNS   16            CHECK FOR NEW FILE DISPLAY
      BRU   *&2
      BRU   FIND          RECHECK CONTROL SWITCHES
      IMS   CURF          INCREMENT CURRENT FILE LOCATION
      LAA   ONE
      CALL  FILEFW        ADVANCE TO NEXT FILE
      BRU   BGOY          BRANCH AND INPUT NEW FILE REQUES
      *T
CNTB  LAA   LAAN          CREATE A LOAD INSTRUCTION FOR DI
      *SPLAY
      AMA   @66           ADD FIRST ADDRESS OF DISPLAY ARR
      *AY
      AMA   TEMP          ADD CHANNEL INDICATOR
      STA   LOD1          SAVE INSTRUCTION
CNTC  LIX   NLOP,2        SET-UP LOOP COUNTER
      LIX   ZERO,1        CLEAR WORD SKIP COUNTER
      LAA   STXA          SET START X-AXIS VALUE
      STA   XAXS
CNTC  CEU   @76,W         RESET DAC SEQUENCER CONTROL
      DATA  0
      LAA   XAXS          FETCH X-AXIS VALUE
      AOP   @76,W         OUTPUT X-AXIS VALUE ON DAC-1
      AMA   INCR          UPDATE X-AXIS VALUE
      STA   XAXS
LOD1  ZZZ                 FETCH Y-AXIS VALUE
      AOP   @76,W         OUTPUT Y-AXIS VALUE ON DAC-2
      AMX   CHNL,1        UPDATE WORD SKIP COUNTER
      IIB   CNTD,2        HAVE ALL DATA BEEN OUTPUTTED
      SNS   18            CHECK FOR RE-DISPLAY
      BRU   *&2           BRANCH AND WAIT FOR RESET TO REA
      *D RECORD
      BRU   FIND          CHECK CONTROL SWITCHES
SWTC  SNS   18            WAIT FOR SWITCH TO BE RESET
```

```
      BRU  *-1            NOT RESET YET
      BRU  REED           READ A NEW RECORD
*
*    RELOAD SYSTEM EXEC AND TRANSFER CONTROL
*
LDEX CALL CRLF
      CALL ASRO
      DAC  MESF
EXEC LAA  DCWA           SET-UP DISC BTC
      STA  @60
      LAA  DWC
      STA  @61
      CEU  @13           SEEK %HEAD,TRACK< #%0,C<
      DATA @10
      BRU  *-2
      TEU  @13           WAIT FOR SEEK COMPLETE
      DATA @02C00000
      BRU  *-2
      CEU  @13           READ SYSTEM LOADER
      DATA @40C00001
      BRU  *-2
      TEU  @13           WAIT FOR READ COMPLETE
      DATA @2
      BRU  *-2
      BRU  @100          BRANCH TO SYSTEM LOADER
*
*---DATA WORDS
*
CURF ZZZ
LAAN LAA  0,1
ADRS ZZZ
INCR ZZZ
PNTS DATA 2048
STXA DATA -1024
DCWA DATA @100
DWC  DATA @40C00100
NUMB ZZZ
XAXS ZZZ
FILL ZZZ
TOFE DATA 2048
DCPT DATA @53400000
TEN  DATA 10
ONRD DATA -200
FIVE DATA -5
THRE DATA 3
TSTY DATA @260
DCMX DATA @177777
DOOC DAC  *&1
CHNL ZZZ
DTFL BSS  200
ZERC DATA 0
ONE  DATA 1
```

```
MAK1  DATA @40000000
MAK2  DATA @77700000
ADDR  DAC  *&1
MUX   BSS  9
EGHT  DATA 8
MUXS  STA  MUX,1
IN01  STA  DAT1,1
IN02  STA  DAT2,1
CNTN  DATA @10
BUF1  DAC  *&1
DAT1  BSS  2049
BUF2  DAC  *&1
DAT2  BSS  2049
NLOP  ZZZ
TTOC  ZZZ
OSTS  DATA 160000
TWO   DATA 2
TEMP  ZZZ
WCTP  ZZZ
ITIR  BRU  TIMR
DBIR  BRU  DBTC
STA   STA  0,1
LAA1  LAA  DTFL,3
MONE  DATA -1
FEDY  ZZZ
MES1  DATA @@NUMBER OF FILES TO SKIP # $@@
MES2  DATA @@SAMPLING RATE # $@@
MES3  DATA @@   ACTUAL RATE # $@@
MES4  DATA @@PRESS START TO BEGIN EXECUTION$@@
MES5  DATA @@NUMBER OF DATA CHANNELS # $@@
MES6  DATA @@INPUT 2 DIGIT OCTAL CH NUM  $@@
MES7  DATA @@BLOCK SIZE # $@@
MES8  DATA @@FILE NUMBER$@@
MES9  DATA @@   CONTAINS$@@
MESA  DATA @@OLD NUMBER OF FILES ON TAPE SAVED # $@@
MESB  DATA @@TOTAL FILES NOW ON TAPE # $@@
MESC  DATA @@SET SSIO FOR DATA DISPLAY$@@
MESD  DATA @@DISPLAY FILE  $@@
MESE  DATA @@FILE NOT ON TAPE, INTER NEW VALUE$@@
MESF  DATA @@NO FILES ON TAPE, LOADING EXEC$@@
MESG  DATA @@ RECORDS$@@
MESH  DATA @@ ZERO WORDS AT END OF EACH DATA BLOCK$@@
      END
$PID        ERROR MESSAGE OUTPUT ROUTINES
      NAME  ERR1,ERR1
      NAME  ERR2,ERR2
ERR1  ZZZ
      CALL  CRLF            OUTPUT CARR RETN AND LINE FEED
      CALL  ASRO            OUTPUT MESSAGE OF INPUT ERROR
      DAC   MES1
      LAA*  ERR1            GET PROPER RETURN ADDRESS
      STA   ERR1            SAVE VALUE
```

```
      BRU* ERR1            RETURN
ERR2  ZZZ
      CALL CRLF            OUTPUT CARR RETN AND LINE FEED
      CALL ASRO            OUTPUT MESSAGE OF INPUT VALUE TO
      * LARGE
      DAC  MES2
      LAA* ERR2            GET PROPER RETURN ADDRESS
      STA  ERR2            SAVE VALUE
      BRU* ERR2            RETURN
MES1  DATA @@ERROR IN INPUT DATA--RE-ENTER VALUE$@@
MES2  DATA @@INPUT VALUE TO LARGE--RE-ENTER VALUE$@@
      END
$PIC        CHANNEL CAPACITY CHECK
      NAME CHCK,CHCK
CHCK  ZZZ
      LAA  FOUR            ROUTINE IS NOT YET AVAILABLE
      AAM  CHCK
      BRU* CHCK
FOUR  DATA 4
      END
$
$
```

```
$PIC45   MAG TAPE HANDLING ROUTINES
      NAME MAGT,MAGT
      NAME FILEFW,FOWD
      NAME FILEBW,BACK
      NAME WRTE,WRTE
      NAME READ,READ
      NAME WEOF,WEOF
MAGT  ZZZ
      CEU  6              REWIND TAPE UNIT 6,2 CHAR/WORD
      DATA @01000062
      BRU  *-2
      TEU  6              TEST FOR BUSY
      DATA  @4C000000
      BRU  *-2
LOP1  TEU  6              TEST FOR WRITE RING PRESENT
      DATA @00400000
      BRU  *&2            OUTPUT MESSAGE OF NO RING
      BRU* MAGT           RETURN
      CALL CRLF           OUTPUT CARR RETN AND LINE FEED
      CALL ASRO           OUTPUT NO RING PRESENT
      DAC  MES1
      HLT
      BRU  LOP1           CHECK FOR RING AGAIN
FOWD  ZZZ
      NEG                 SET-UP FILES TO SKIP COUNTER
      TAI  ,1
LOP2  CEU  6              ADVANCE 1 FILE
      DATA @02000100
      BRU  *-2
      TEU  6              TEST FOR BUSY
      DATA @40C00000
      BRU  *-2
      IIB  LOP2,1         UPDATE FILE COUNTER
      BRU* FOWD           RETURN
BACK  ZZZ
      NEG                 SET-UP FILES TO BACK SPACE COUNT
      *ER
      TAI  ,1
LOP3  CEU  @6             BACKSPACE A FILE
      DATA @02C00020
      BRU  *-2
      TEU  @6             TEST FOR BUSY
      DATA @40000000
      BRU  *-2
      IIB  LOP3,1         HAVE ALL FILES BEEN BACKSPACED
      TBA                 CHECK FOR FIRST FILE
      CMA  ONE            IS THIS THE FIRST FILE
      BRU* BACK           YES, RETURN
      BRU* BACK           YES, RETURN
      CEU  @6             ADVANCE PAST EOF MARKER
      DATA @02000100
      BRU  *-2
```

```
      TEU  @6              TEST FOR BUSY
      DATA @40000000
      BRU  *-2
      BRU* BACK            RETURN
WRTE  ZZZ
      TEU  6               TEST FOR BUSY
      DATA @40000000
      BRU  *-2
      CEU  6               WRITE A RECORD
      DATA @43000000
      BRU  *-2
      BRU* WRTE            RETURN
READ  ZZZ
      TEU  6               TEST FOR BUSY
      DATA @40000000
      BRU  *-2
      CEU  6               READ A RECORD
      DATA @42200000
      BRU  *-2
      TEU  @6              WAIT IF BUSY
      DATA @40000000
      BRU  *-2
      CLA                  SET NO EOF INDICATOR
      TEU  @6              TEST FOR EOF
      DATA @20000000
      LAA  *-1             EOF FOUND, SET INDICATOR
      BRU* READ            RETURN
WEOF  ZZZ
      TEU  6               TEST FOR BUSY
      DATA @40000000
      BRU  *-2
      CEU  6               WRITE END OF FILE ON TAPE
      DATA @02400000
      BRU  *-2
      BRU* WEOF            RETURN
MES1  DATA @@INSERT WRITE RING AND PRESS START$@@
ONE   DATA 1
      END
$PIC45   ASR-33 I/O ROUTINES
      NAME CRLF,ENT
      NAME ASRI,ASRI
      NAME ASRC,ASRO
      NAME ASRD,ASRD
      NAME OCTI,OCTI
ENT   ZZZ                  CARRIAGE RETURN AND LINE FEED RO
      *UTINE
      LAA  CRLF
      AOP  1,W             CARR RETN
      LSL  8
      AOP  1,W             LINE FEED
      BRU* ENT             RETURN
ASRC  ZZZ                  MESSAGE OUTPUT ROUTINE
```

```
      LAA*  ASRO          GET ADDRESS OF MESSAGE
      IMS   ASRO          SET-UP RETURN ADDRESS
      AMA   LBA           CREATE A LOAD B ACC INSTRUCTION
      STA   LOAD          STORE INSTRUCTION
      LIX   FOUR,1        SET-UP SHIFT COUNTER
LOAC  ZZZ                 LOAD DATA WORD
      CLA                 CLEAR A ACC
      FLL   6             SHIFT ONE CHARACTER
      CMA   DRSG          CHECK FOR $
      BRU   *&2           NOT A $
      BRU*  ASRO          $-RETURN
      CMA   FRTY          CHECK TO ADD @200 OR @300
      AMA   ONRD          ADD @100 NOW, @200 LATER
      NOP
      AMA   TNRD          ADD @200 NOW
      LSL   16            SHIFT FOR OUTPUT
      AOP   1,W           OUTPUT CHARACTER
      IIB   LOAD&1,1      UPDATE SHIFT COUNTER
      IMS   LOAD          ADD ONE TO MESSAGE ORIGIN
      BRU   LOAD-1        BRANCH BACK AND OUTPUT MORE CHAR
ASRI  ZZZ                 DECIMAL INPUT ROUTINE
      CEU   1,W           CLEAR ASR-33 BUFFERS
      DATA  @00400000
      CEU   1,W           SET TTYP TO KEYBOARD MODE
      DATA  @01000000
      LIX   SIX,1         SET MAXIMUM CHARACTER INPUT AT 6
      CLA                 CLEAR B ACC
      TAB
INPT  AIP   1,W           INPUT A CHARACTER
      CMA   CRTN          CHECK FOR CARR RETN TO TERMINATE
      BRU   *&2           CONTINUE INPUT
      BRU   RETN          CARR RETN, TERMINATE
      LSL   16            SHIFT FOR OUTPUT
      AOP   1,W           OUTPUT A CHARACTER
      RSL   16            SHIFT FOR CHECK
      SMA   TSTY          SUBTRACT FOR DIGIT
      BAN   ERR           LESS THAN 0, ERROR RETURN
      CMA   NINE          CHECK FOR DIGIT
      BRU   CNIN          LESS THAN 9-OK
      BRU   CNIN          EQUAL TO 9-OK
      BRU   ERR           ERROR-ERROR RETURN
CNIN  STA   TEMP          CONVERT TO OCTAL-SAVE VALUE
      MPY   TEN           MULTIPLY BY 10
      TBA                 UPDATE SUM OF INPUT DIGITS
      AMA   TEMP
      TAB
      IIB   INPT,1        UPDATE MAX INPUT COUNTER
      BRU   ERR           MAXIUM CHAR COUNT EXCEEDED
RETN  TBA                 PUT INPUT VALUE INTO A ACC
      BRU*  ASRI          RETURN
ERR   LAA   ARUP          LOAD TTYP ERROR INDICATOR
      AOP   1,W           OUTPUT
```

```
      LAA   MONE          LOAD ERROR RETURN INDICATOR
      BRU*  ASR1          RETURN
ASRD  ZZZ                 TTYP DECIMAL OUTPUT ROUTINE
      TAB                 PUT VALUE INTO B ACC
      LIX   FIVE,1        SET-UP STORAGE COUNTER
      LAA   BLNK          LOAD A BLANK
      STA   TABL&5,1      STORE A BLANK
      IIB   *-1,1         UPDATE BLANK COUNTER
      LIX   MONE,1        SET-UP WORD STORAGE
LOP1  CLA
      DIV   TEN           GET DIGIT
      BAZ   INTI          TERMINATE CONVERSION
      IAB
      AMA   TSTY          CONVERT TO TTYP CODE
      LSL   16            SHIFT FOR OUTPUT
      STA   TABL&5,1      SAVE RESULT
      AMX   MONE,1        UPDATE STORAGE COUNTER
      BRU   LOP1          DO IT AGAIN
INTI  IAB
      AMA   TSTY          CONVERT TO TTYP CODE
      LSL   16            SHIFT FOR OUTPUT
      STA   TABL&5,1      SAVE VALUE
      LIX   FIVE,1        SET-UP OUTPUT COUNTER
      LAA   TABL&5,1      GET WORD
      AOP   1,W           OUTPUT WORD
      IIB   *-2,1         UPDATE COUNTER
      BRU*  ASRD          RETURN
OCTI  ZZZ
      CEU   1,W           CLEAR ASR-33 BUFFERS
      DATA  @00400000
      CEU   1,W           SET TTYP TO KEYBOARD MODE
      DATA  @01C00000
      LBA   ZERO          CLEAR B ACC
      LIX   MTWO,3        SET COUNTER FOR 2 CHAR INPUT
INOC  AIP   1,W           INPUT A CHARACTER
      LSL   16            SHIFT FOR OUTPUT
      AOP   1,W           OUTPUT A CHARACTER
      LSL   5             SHIFT OFF @260
      FRL   3             ROTATE INTO B ACC
      IIB   INOC,3        UPDATE COUNTER
      LAA   COMM          OUTPUT A COMMA
      AOP   1,W
      TBA
      BRU*  OCTI          RETURN
CRLF  DATA  @43305000
DRSC  DATA  @44
LBA   LBA   0
FOUR  DATA  -4
TSTY  DATA  @26C
NINE  DATA  9
ARUP  DATA  @67400000
CRTN  DATA  @215
```

```
ONRD  DATA @100
TNRD  DATA @200
FRTY  DATA @40
SIX   DATA -6
TEMP  ZZZ
TEN   DATA 10
BLNK  DATA @50000000
TWO   DATA 2
TABL  BSS  5
FIVE  DATA -5
ZERO  DATA 0
MONE  DATA -1
MTWO  DATA -2
COMM  DATA @53000000
      END
$
$
$
```

APPENDIX B

FOURIER SERIES ANALYSIS

An arbitrary periodic function of time can be represented by a Fourier series (see section 2.8) as follows:

$$f(t) = a_o + \sum_{n=1}^{J} a_n \cos n\omega t + b_n \sin n\omega t \qquad (B.1)$$

where

$$a_o = \frac{1}{T} \int_{-T/2}^{T/2} f(t)dt \qquad (B.2)$$

$$a_o = \frac{2}{T} \int_{-T/2}^{T/2} f(t) \cos n\omega t dt \qquad (B.3)$$

$$a_n = \frac{2}{T} \int_{-T/2}^{T/2} f(t) \sin n\omega t dt \qquad (B.4)$$

This can also be written in modulus and phase form as

$$f(t) = c_o + \sum_{n=1}^{J} c_n \cos(n\omega t - \phi_n) \qquad (B.5)$$

where

$$c_o = a_o \qquad (B.6)$$

$$c_n = \sqrt{a_n^2 + b_n^2} \qquad (B.6)$$

$$\phi_n = \tan^{-1} b_n/a_n \qquad (B.8)$$

To curve fit a set of K + 1 data points via Fourier series the coefficients must first be found by numerical integration. The scheme used in this study was area determination by the trapezoidal rule. A brief description will be given to transform equations (B.2) - (B.4) into discrete form.

First let

$$\theta_i = \omega t_i = \frac{2\pi i}{K} \quad i = 0,K \tag{B.9}$$

and

$$h = \Delta t = \frac{T}{K} = \frac{1}{fK} = \frac{2\pi}{\omega K} \tag{B.10}$$

In general, the single step form for trapezoidal integration is

$$\int_{t_k}^{t_{k+1}} F(t)dt \simeq \frac{h}{2} \left(F_k(t) + F_{k+1}(t)\right) \tag{B.11}$$

i.e., the area of the trapezoid of base h.
When an integral over more than one step is required, the range T is divided into a number of equal intervals Δt (equation (B.10)) and equation (B.11) is applied K times. The result is

$$\int_{t_0}^{t_{k+1}} F(t)dt \simeq \frac{h}{2} \left(F_0+2F_1+2F_2+\ldots+2F_K+F_{K+1}\right) \tag{B.12}$$

Therefore, the equation for a_n can be written as

$$a_n = \frac{2}{T}\frac{\Delta t}{2}\left(f_0\cos n\theta_0 + 2f_1\cos n\theta_1 + \ldots + 2f_K\cos n\theta_K + f_{K+1}\right) \qquad (B.13)$$

This can be rearranged to yield

$$a_n = \frac{1}{K}\sum_{i=0}^{K-1} f_i\cos 2n\pi\frac{i}{K} + f_{i+1}\cos 2n\pi\left(\frac{i+1}{K}\right) \qquad (B.14)$$

Similar equations can be derived for the remaining coefficients.

$$b_n = \frac{1}{K}\sum_{i=0}^{K-1} f_i\sin 2n\pi\frac{i}{K} + f_{i+1}\sin 2n\pi\left(\frac{1+1}{K}\right) \qquad (B.15)$$

$$a_o = \frac{1}{2K}\sum_{i=0}^{K-1} f_i + f_{i+1} \qquad (B.16)$$

Consequently the discrete points, a result of the analog to digital process, are inputed to the program shown in this appendix. This program performs the numerical integration necessary to calculate the Fourier coefficients. The program also calibrates the digital points (see section 4.1) upon input. This is done by a sorting routine to determine the maximum and the minimum value per cycle per channel. This difference is then set equal to the known pulse value (from the chart recorder) and all points are then scaled accordingly. The error between each digital point and the corresponding Fourier ordinate is then computed to determine the percent difference for use in determining the accuracy of the fit. Also various plotting routines are employed for visual data display in graphical form.

```
C THIS PROGRAM INPUTS DIGITAL POINTS VIA MAGNETIC TAPE,
C COMPUTES THE COEFFICIENTS OF A FOURIER SERIES EXPAN-
C SION BY TRAPEZOIDAL NUMERICAL INTEGRATION,PUNCHES THE
C OUTPUT ON CARDS AND DISPLAYS THE RESULTS GRAPHICALLY.
C SUBROUTINES NEEDED WITH THIS PROGRAM ARE AMAX1,AMIN1,
C FPLOT AND SKIP
C
      INTEGER*2 ENDFIL
      INTEGER*2 A(6,300)
      DIMENSION FU(300),FA(300),FB(300),D(6,300)
      DIMENSION AF(15),B(15),PR(15),PD(15),C(15)
      DIMENSION UNITPP(6),DC(6),CAL(6),SUBDC(6)
      DIMENSION PM(15),VAR(15)
      DIMENSION AR(800)
      LOGICAL*1 LR(400)
      REAL NT,NTD(300),NTDE
      INTEGER DATANO,DAY,YR
C INPUT TOTAL NUMBER OF DATA SHEETS
      NDS=7
      DO 260 IT=1,NDS
C INPUT DATA SHEET NUMBER,DATE,NUMBER OF DATA CHANNELS
C AND NUMBER OF POINTS PER RECORD
      READ(5,1)DATANO,MO,DAY,YR,NDCH,NPTS
    1 FORMAT(6I5)
      NCURVE=NDCH
      NCT=2
      READ(1,2,END=3)((A(I,J),I=1,NDCH),J=1,NPTS),ENDFIL
    2 FORMAT(6(200A2))
      GO TO 5
    3 CONTINUE
    5 CONTINUE
      WRITE(6,7)((A(I,J),J=1,NPTS),I=1,NDCH)
    7 FORMAT(10I10)
      DO 20 J=1,NPTS
      DO 17 I=1,NDCH
      ISUMT=0
      DO 15 IJ=1,NDCH
      ISUM=A(IJ,J)
      ISUMT=ISUMT+ISUM
   15 CONTINUE
      IF(ISUMT.EQ.0)GO TO 25
      D(I,J)=-A(I,J)/3200.
   17 CONTINUE
   20 CONTINUE
   25 CONTINUE
      K=J-1
      READ(5,9)K
C INPUT PULSE VALUES FOR CALIBRATICN OF SEL OUTPUT
    9 FORMAT(I3)
      READ(5,10)(UNITPP(M),M=1,NDCH)
   10 FORMAT(6F10.7)
C INPUT MEAN VALUES
```

```
      READ(5,11)(DC(M),M=1,NDCH),J
   11 FORMAT(6F10.7,I5)
      DO 200 II=1,NCURVE
      CALL SKIP
      WRITE(6,27)DATANO,MO,DAY,YR
   27 FORMAT(1X,'DATA SHEET NUMBER'2X,I6,5X,'DATE'2X,I2,
     *'/'I2,'/'I2////)
      WRITE(6,28)II
   28 FORMAT(1X,'CHANNEL'I2,1X,'FOURIER ANALYSIS'//)
      KK=K
      DO 30 M=1,K
      FU(M)=D(II,M)
   30 CONTINUE
C FIND PEAK TO PEAK VALUES
      SMALL=FU(1)
      BIG=FU(1)
      DO 35 M=2,K
      BIG=AMAX1(FU(M),BIG)
      SMALL=AMIN1(FU(M),SMALL)
   35 CONTINUE
      VOLTPP=BIG-SMALL
C CALIBRATE INPUT
      CAL(II)=UNITPP(II)/VOLTPP
      DO 36 M=1,K
      FU(M)=FU(M)*CAL(II)
   36 CONTINUE
      KP=K+1
      K1=K-1
      PI=4.*ATAN(1.)
C BEGIN FOURIER ANALYSIS
      HH=2./K
      HHH=1./K
      FA(KP)=FU(1)
      FA(1)=FU(1)
      FB(1)=0.
      FB(KP)=0.
      FU(KP)=FU(1)
      DO 50 N1=1,J
      DO 40 N2=1,K1
      ARG=N1*2.*PI*N2/K
      FA(N2+1)=FU(N2+1)*COS(ARG)
      FB(N2+1)=FU(N2+1)*SIN(ARG)
   40 CONTINUE
      AF(N1)=0.
      B(N1)=0.
      DO 41 N2=1,K
      TERMA=FA(N2)+FA(N2+1)
      TERMB=FB(N2)+FB(N2+1)
      AF(N1)=AF(N1)+TERMA
      B(N1)=B(N1)+TERMB
   41 CONTINUE
      AF(N1)=HH*AF(N1)/2.
```

```
      B(N1)=HH*B(N1)/2.
      PR(N1)=ATAN(B(N1)/AF(N1))
      IF(AF(N1))44,44,42
C COMPUTE PHASE
   42 IF(B(N1))43,43,48
   43 PR(N1)=PR(N1)+2.*PI
      GO TO 48
   44 PR(N1)=PR(N1)+PI
   48 CONTINUE
      PD(N1)=180.*PR(N1)/PI
C COMPUTE MODULUS
      C(N1)= SQRT(AF(N1)**2+B(N1)**2)
   50 CONTINUE
C INTEGRATE TO FIND DC LEVEL
      A0=0.
      DO 60 N3=1,K
      TERM0=FU(N3)+FU(N3+1)
      A0=A0+TERM0
   60 CONTINUE
      A0=A0*HHH/2.
      SUBDC(II)=A0
      A0=DC(II)
      VARS=0.0
      DO 66 N4=1,J
      WRITE(6,65)N4,AF(N4),B(N4),C(N4),PR(N4),PD(N4)
   65 FORMAT(1X,'HARMONIC' I2,3X,'A='F12.8,3X,'B='F12.8,
     *3X,'C='F12.8,3X,
     *'PHASE (RAD)=',F7.3,3X,'PHASE (DEG)=',F8.1)
      PM(N4)=200.*C(N4)/UNITPP(II)
      VART=.5*C(N4)**2
      VARS=VARS+VART
      VAR(N4)=VARS
   66 CONTINUE
      WRITE(6,68)A0
   68 FORMAT(/13X,'MEAN VALUE IS',F8.4///)
      WRITE(7,69)A0,(AF(M),M=1,7)
   69 FORMAT(8E10.4)
      WRITE(7,69)(AF(M),M=8,J)
      WRITE(7,71)(B(M),M=1,7)
   71 FORMAT(10X,7E10.4)
      WRITE(7,69)(B(M),M=8,J)
      VARC=0.0
      DO 85 M=1,K
      VART=((FU(M)-SUBDC(II))**2)/K
      VARC=VARC+VART
   85 CONTINUE
      DO 80 M=1,J
   80 VAR(M)=100.*VAR(M)/VARC
      WRITE(6,87)VARC,(VAR(N4),N4=1,J)
   87 FORMAT(//1X,'TOTAL ENERGY='F12.8,5X,'ACCUMALATED V
     *ARIANCE RATIOS'5
     *X,10F6.1//)
```

```
      WRITE(6,88)UNITPP(II),(PM(N4),N4=1,J)
   88 FORMAT(2X,'PULSE VALUE='F12.8,10X,'HARMONIC PERCEN
     *TS'5X,10F6.1)
      CALL SKIP
      WRITE(6,74)II,DATANO
   74 FORMAT(1X,'ERROR COMPARISON FOR CHANNEL'I2,1X,'OF
     *DATA SHEET'I6//)
C COMPUTE DIGITAL VALUES FROM FOURIER COEFFICIENTS
      DO 75 M=1,K
      FF=A0
      AODC=FF
      WT=2*PI*(M-1)/K
      WTD=360.*(M-1)/K
      DO 70 N=1,J
      ANG=N*WT-PR(N)
      SUM=C(N)*COS(ANG)
   70 FF=FF+SUM
C INTEGRATE OUT THE DC LEVEL AND ADD TRUE MEAN VALUE
      FU(M)=FU(M)-SUBDC(II)+AODC
      IF(ABS(FU(M)).LT..00000001)PERC=0.
      IF(ABS(FU(M)).LT..00000001)GO TO 73
C COMPUTE PERCENT ERROR
      PERC=100.*(FU(M)-FF)/FU(M)
   73 CONTINUE
      WRITE(6,72)WTD,FU(M),FF,PERC
   72 FORMAT(1X,'THETA='F5.1,5X,'EXPERIMENTAL VALUES='F1
     *3.7,5X,'FOURIER
     1VALUES='F13.7,5X,'PERCENT DIFFERENCE='F10.4)
      IF(M-1)78,77,78
   77 FFE=FF
   78 CONTINUE
   75 CONTINUE
      IF(ABS(FU(1)).LT..00000001)PERC=0.
      IF(ABS(FU(1)).LT..00000001)GO TO 76
      PERC=100.*(FU(1)-FFE)/FU(1)
   76 CONTINUE
      SUMT=A0
      DO 81 N=1,J
      SUM=AF(N)
   81 SUMT=SUMT+SUM
      NTDE=360.
      WRITE(6,72)NTDE,FU(1),FFE,PERC
      DO 200 N=1,KK
      SUMT=A0
      NT=2.*PI*(N-1)/KK
      NTD(N)=180.*NT/PI
      DO 95 N1=1,J
      SUM=C(N1)*COS(NT*N1-PR(N1))
   95 SUMT=SUMT+SUM
  100 CONTINUE
      IF(N-1)90,89,90
   89 D(II,KK+1)=SUMT
```

```
      NTD(KK+1)=360.
   90 CONTINUE
  200 D(II,N)=SUMT
      CALL SKIP
C PLOT RESULTS
      KK=KK+1
      NPLOTS=NCURVE/NCT
      M1=1
      M2=NCT
      DO 255 L=1,2
      CALL SKIP
      IPNT=0
      ISTOP=0
      DO 250 N=1,KK
      IF(N.EQ.KK)ISTOP=1
      DO 240 N1=M1,M2
      IF(N1.EQ.M2)NC=2
      IF(N1.EQ.M1)NC=1
      CALL FPLOT(800,IPNT,AR,LR,ISTOP,NC,NCT,NTD(N),D(N1
     *,N))
  240 CONTINUE
  250 CONTINUE
      M1=M1+2
      M2=M2+2
  255 CONTINUE
      DO 257 L=5,6
      CALL SKIP
      IPNT=0
      ISTOP=0
      DO 256 N=1,KK
      IF(N.EQ.KK)ISTOP=1
      CALL FPLOT(800,IPNT,AR,LR,ISTOP,1,1,NTD(N),D(L,N))
  256 CONTINUE
  257 CONTINUE
  260 CONTINUE
      CALL SKIP
      STOP
      END
```

APPENDIX C

CALCULATIONS OF FLOW SOLUTIONS

To make use of Uchida's and Womersley's theoretical solution, the constant F_{10} must be evaluated [see sections (2.2) and (2.3)]. This requires the calculation of zero and first order complex Bessel functions of the first kind. The equation to do this is given by

$$F_{10} = \frac{2}{\alpha i^{3/2}} \frac{J_1\left(\alpha i^{3/2}\right)}{J_o\left(\alpha i^{3/2}\right)} \tag{C.1}$$

Since α can vary over a large range ($1<\alpha<20$), it is not feasible to calculate F_{10} by the same method for all values. For small α, ($\alpha \leq 7$), the defining power series[40] for Bessel functions was used. This is

$$J_\nu(z) = \left(\frac{z}{2}\right)^\nu \sum_{k=0}^{\infty} \frac{\left(-\frac{1}{4}z^2\right)^K}{K!\Gamma(\nu+K+1)} \tag{C.2}$$

In the numerical calculation of this series, truncation occurs when the relative percentage change in the K + 1 term is less than a specified tolerance. For flow calculations, 10^{-4} was used as this tolerance.

For $\alpha>7$, an asymptotic expansion was used for the calculation of F_{10}. This expansion is given by

$$J_\nu(z) = \sqrt{\frac{2}{\pi z}} \left[P(\nu,z) \cos \chi - Q(\nu,z) \sin \chi \right] \qquad (C.3)$$

for $\left(| \arg z | \right) < \pi$

where

$$P(\nu,z) \simeq \sum_{K=0}^{\infty} \frac{(-1)^k (\nu,2K)}{(2z)^{2K}} = \qquad (C.4)$$

$$1 - \frac{(\mu-1)(\mu-9)}{2!(8z)^2} + \frac{(\mu-1)(\mu-9)(\mu-25)(\mu-49)}{4!(8z)^4}$$

$$Q(\nu,z) \simeq \sum_{K=0}^{\infty} (-1) \frac{(\nu,2K+1)}{2z} = \qquad (C.5)$$

$$\frac{\mu-1}{8z} - \frac{(\mu-1)(\mu-9)(\mu-25)}{3!(8z)^3}$$

and $\mu = 4\nu^2$

The error for P and Q does not exceed the K + 1 term; thus the program checks consecutive terms and determines the relative percentage change. Here the cutoff tolerance used in the program was 10^{-5}.

All the calculations mentioned here were carried out in complex arithmetic on the computer. The program to do this is shown in this appendix.

```
C THIS PROGRAM COMPARES THE MATHEMATICAL MODELS OF FRY,
C UCHIDA AND WOMMERSLEY FROM THE INPUTTED FOURIER
C COMPONENTS OF THE PRESSURE GRADIENT. THE RESULTING
C HARMONIC CONTENT IS THEN PUNCHED OUT ON CARDS FOR
C FUTURE USE. SUBROUTINES NEEDED WITH THIS PROGRAM ARE
C SKIP AND FPLOT.
C
      DIMENSION AF(10),B(10),C(10),PD(10),PR(10),THETA(1
     *0)
      DIMENSION WCOM(10),VCOM(10),THETAR(10),S(150,4),FR
     *Y(10),AR(800)
      DIMENSION XM(3),XA(10,3),XB(10,3),PRF(10)
      COMPLEX COC,G,H1,I,I32,J0,J1,ARGC,SUM0,SUM1,XS,CSQ
     *RT,COM,F10
      COMPLEX Z,PH,QH,SUMP,SUMQ,CCOS,CSIN,CI,NG,WCOM,VCO
     *M,CEXP
      REAL K1,KB,M0,M1,M1OR,M10,NT,NTD,MU,MOD,LL,NTDD(10
     *0)
      INTEGER DATANO,DAY,YR
      LOGICAL*1 LR(400)
      CALL SKIP
C INPUT NUMBER OF PRESSURE GRADIENTS.
      NDS=1
C INPUT FLUID DENSITY,DIAMETER,POISSON'S RATIO,WALL
C THICKNESS,WEIGHTED VOLUME OF WALL AND SPRING CONSTANT
C OF SURROUNDING MATERIAL.
      READ(5,5)P,D,U,PW,H,HB,KB
    5 FORMAT(7F7.3)
C INPUT VISCOSITY COEFFICIENTS.
      READ(5,11)V0,V1,V2,V3,V4,V5
   11 FORMAT(6E10.3)
C INPUT STRESS COEFFICIENTS.
      READ(5,12)S0,S1,S2,S3,S4,S5
   12 FORMAT(6E10.3)
      DO 360 IT=1,NDS
      CALL SKIP
      READ(5,15)PM,DM
   15 FORMAT(2F10.3)
C INPUT FLOW TIME,VISCOSITY TIME AND TEMPERATURE.
      READ(5,6)VTIME,VITIME,TEMP
    6 FORMAT(3F10.2)
      TIMEW=V0+V1*TEMP+V2*TEMP**2+V3*TEMP**3+V4*TEMP**4+
     *V5*TEMP**5
      V=(721.1/TEMP+.215)*10.**(-6.)*929.03*VITIME/TIMEW
C INPUT DATA SHEET NUMBER AND DATE.
      READ(5,1)DATANO,MO,DAY,YR
    1 FORMAT(4I5)
C INPUT NUMBER OF DIGITAL POINTS,NUMBER OF HARMONICS AND
C SAMPLING RATE.
      READ(5,10)K,J,SAMPRT
   10 FORMAT(2I5,F10.1)
C INPUT PRESSURE GRADIENT.
```

```
      READ(5,20)A0,(AF(MA),MA=1,J)
   20 FORMAT(8E10.4)
      READ(5,21)(B(MA),MA=1,7)
   21 FORMAT(10X,7E10.4)
      READ(5,20)(B(MA),MA=8,J)
      R=D/2.
      RM=DM/2.
      ST=PM*R/(H*51.71)
      SLOPE=S1+2.*S2*ST+3.*S3*ST**2+4.*S4*ST**3+5.*S5*ST
     ***4
      E=(10.**6)/(SLOPE*14.5)
      F=SAMPRT/K
      WRITE(6,2)DATANO,MO,DAY,YR
    2 FORMAT(1X,'DATA SHEET NUMBER'2X,I6,5X,'DATE'2X,I2,
     *'/'I2,'/'I2////)
      WRITE(6,3)V,F,P,R,E,U,PW,H
    3 FORMAT(1X,'DATA'2X,'V='F10.8,2X,'F='F6.3,2X,'DENSI
     *TY='F6.2,2X,'R='
     *F6.3,2X,'E='F10.1,2X,'POISSONS RATIO='F5.3,2X,'PW=
     *'F6.2,2X,'H='F7.
     *5////)
      PI=4.*ATAN(1.)
      NPC=K
C NPC IS NUMBER OF POINTS ON OUTPUT PLOT.
      NPC=72
C NFLOW EQUAL 0 FOR VELOCITY,1 FOR VOLUMETRIC FLOW.
      NFLOW=0
C CORRECTION COEFFICIENTS FOR FRY'S THEORY.
      CR=1.
      CL=1.
      FLOW=2639./VTIME
      AVEL=FLOW/(PI*R**2)
      WRITE(6,8)FLOW,AVEL
    8 FORMAT(1X,'BUCKET FLOW RATE='F7.3,5X,'BUCKET VELOC
     *ITY='F7.3)
      K11=K-1
      MU=V*P
      GC=1.
      GG=980.66
C CHANGE UNITS OF PRESSURE GRADIENT TO G/CM**2/CM.
      UNITPG=1.35947
      RS=CR*8.*MU/(GG*PI*(R**4))
      LL=CL*P/(GG*PI*(R**2))
      TAU=RS/LL
      CO=SQRT(H*E*GC/(2.*R*P))
      WRITE(6,35)CO,RS,LL,TAU,CR,CL
   35 FORMAT(/1X,'PULSE VELOCITY='F7.1,5X,'RESISTANCE='E
     *12.4,5X,'INDUCTA
     *NCE='E12.4,5X,'TIME CONSTANT='F6.3,5X,'CL='F4.2,5X
     *,'CR='F4.2///)
      EPS=0.0001
      DO 50 N1=1,J
```

```
      IF(AF(N1).EQ.0.)PR(N1)=PI/2.
      IF(AF(N1).EQ.0.)GO TO 41
      PR(N1)=ATAN(B(N1)/AF(N1))
   41 CONTINUE
      IF(AF(N1))44,44,42
   42 IF(B(N1))43,43,48
   43 PR(N1)=PR(N1)+2.*PI
      GO TO 48
   44 PR(N1)=PR(N1)+PI
   48 CONTINUE
      PD(N1)=180.*PR(N1)/PI
      C(N1)= SQRT(AF(N1)**2+B(N1)**2)
   50 CONTINUE
      DO 66 N4=1,J
      WRITE(6,65)N4,AF(N4),B(N4),C(N4),PR(N4),PD(N4)
   65 FORMAT(1X,'HARMONIC' I2,3X,'A='F8.4,3X,'B='F8.4,3X
     *,'C='F8.4,5X,
     *'PHASE (RAD)=',F7.4,3X,'PHASE (DEG)=',F8.1)
      C(N4)=C(N4)*UNITPG
   66 CONTINUE
      WRITE(6,68)A0
   68 FORMAT(/13X,'MEAN VALUE IS',F8.4///)
      A0=A0*UNITPG
      WRITE(7,71)A0,(AF(M),M=1,J)
   71 FORMAT(8E10.4)
      WRITE(7,72)(B(M),M=1,7)
   72 FORMAT(10X,7E10.4)
      WRITE(7,71)(B(M),M=8,J)
      CALL SKIP
      I=(0.,1.)
C COMPUTE ALPHA.
      A=R*SQRT(2.*PI*F/V)
      AA=A
      I32=COS(3.*PI/4.)+SIN(3.*PI/4.)*(0.,1.)
      VWE=GG*R*R*A0/(8.*MU)
      VUE=GG*R*R*A0/(8.*MU)
      VFE=A0/(RS*PI*R*R)
      XM(1)=VFE
      XM(2)=VUE
      XM(3)=VWE
      IF(NFLOW.EQ.0) GO TO 74
      VFE=VFE*PI*R*R
      VUE=VUE*PI*R*R
      VWE=VWE*PI*R*R
   74 CONTINUE
      WRITE(6,75)A,VFE,VWE
   75 FORMAT(1X,'FUNDAMENTAL VALUE OF ALPHA IS'F5.2,5X,'
     *MEAN VELOCITY FO
     *R FRYS THEORY-'F8.3,3X,'FOR UCHIDA AND WOMERSLEY-'
     *F8.3/)
      DO 255 N5=1,J
C     CALCULATE BESSEL FUNCTIONS FOR A<7.
```

```
      IF(A-7.)69,69,95
   69 CONTINUE
      JO=(1.,0.)
      J1=(A/2.)*(1.,0.)
      SUMO=0.
      SUM1=0.
      KK=0
      L=1
   70 KK=KK+1
      JO=JO+SUMO
      J1=J1+SUM1
      COM=(((-1.)**KK)*(I**(3*KK)))/L
      SUMO=(COM*(A/2.)**(2*KK))/L
      SUM1=(COM*(A/2.)**(2*KK+1))/(L*(KK+1))
      L=(KK+1)*L
      IF((ABS(CABS(JO+SUMO)-CABS(JO))/CABS(JO+SUMO))-EPS
     *)80,80,70
   80 IF((ABS(CABS(J1+SUM1)-CABS(J1))/CABS(J1+SUM1))-EPS
     *)90,90,70
   90 CONTINUE
      J1=J1*I32
      F10=(2.*J1)/(A*I32*JO)
      GO TO 130
C     CALCULATE BESSEL FUNCTIONS FOR A>7.
   95 CONTINUE
      N3=0
      Z=A*I32
      UV=0.
  100 PH=1.
      QH=(UV-1.)/(8.*Z)
      FP=1.
      N=1
  101 CONTINUE
      NP=2*N-1
      PP=1.
      QQ=1.
      DO 102 M=1,NP,2
      PRODP=(UV-(2.*M-1.)**2)*(UV-(2.*M+1.)**2)
      PRODQ=(UV-(2.*M+1.)**2)*(UV-(2.*M+3.)**2)
      PP=PRODP*PP
      QQ=PRODQ*QQ
  102 CONTINUE
      N2=2*N
      N1=N2-1
      DO 105 M=N1,N2
      FP=FP*M
  105 CONTINUE
      FQ=FP*(N2+1.)
      SUMP=((-1.)**N)/(FP*(8.*Z)**(2*N))
      SUMQ=(UV-1.)*((-1.)**N)/(FQ*(8.*Z)**(2*N+1))
      PH=PH+SUMP*PP
      QH=QH+SUMQ*QQ
```

```
      N=N+1
      IF(CABS(SUMP*PP)-0.00001)110,110,101
  110 IF(CABS(SUMQ*QQ)-0.00001)111,111,101
  111 CONTINUE
      IF(N3-1)113,112,112
  112 CI=Z-(.5+.25)*PI
      J1=CSQRT(2./(PI*Z))*(PH*CCOS(CI)-QH*CSIN(CI))
      GO TO 115
  113 CI=Z-PI/4.
      J0=CSQRT(2./(PI*Z))*(PH*CCOS(CI)-QH*CSIN(CI))
      N3=N3+1
      UV=4.
      GO TO 100
  115 CONTINUE
      J0=J0/(10.**40)
      J1=J1/(10.**40)
      F10=(2.*J1)/(A*I32*J0)
      J0=J0*(10.**40)
      J1=J1*(10.**40)
  130 CONTINUE
      K1=(HB*PW/(R*P))*(1.-KB*GC/(PW*HB*((2.*N5*PI*F)**2
     *)))
      H1=(1.+2.*K1)/(1.-F10)-1.
      G=(1.25-U)/(1.-F10)+(K1/2.)+U-.25
      XS=(G+CSQRT((G**2)-(1.-U*U)*H1))/(1.-U*U)
      NG=2./(XS*(F10-2.*U))-(1.-2.*U)/(F10-2.*U)
      CO=SQRT(H*E*GC/(2.*R*P))
      COC=CSQRT((1.-U*U)*(XS/2.))
      X=REAL(COC)
      Y=-AIMAG(COC)
      COCCOR=X/CO
      COCCOI=Y/CO
      PHASEV=CO/X
      ATTEN=EXP(-2.*PI*Y/X)
      WAVEL=PHASEV/(N5*F)
      ARGC=1.+NG*F10
      M10=CABS(ARGC)
      E10=ATAN(AIMAG(ARGC)/REAL(ARGC))
      MOD=GG*C(N5)*R*R*M10/(MU*A*A)
      THETA(N5)=E10-PR(N5)-PI/2.
      WCOM(N5)=MOD
      AW=MOD*COS(THETA(N5))
      BW=-MOD*SIN(THETA(N5))
      CW=SQRT(AW*AW+BW*BW)
      PRW=ATAN(BW/AW)
      IF(AW)144,144,142
  142 IF(BW)143,143,148
  143 PRW=PRW+2.*PI
      GO TO 148
  144 PRW=PRW+PI
  148 CONTINUE
      PDW=360.*PRW/(2.*PI)
```

```
      WCOM(N5)=WCOM(N5)*CEXP(I*THETA(N5))
      M1OR=CABS(1.-F1O)
      E1OR=ATAN(AIMAG(1.-F1O)/REAL(1.-F1O))
      MOD=GG*C(N5)*R*R*M1OR/(MU*A*A)
      THETAR(N5)=E1OR-PR(N5)-PI/2.
      VCOM(N5)=MOD
      AU=MOD*COS(THETAR(N5))
      BU=-MOD*SIN(THETAR(N5))
      CU=SQRT(AU*AU+BU*BU)
      PRU=ATAN(BU/AU)
      IF(AU)154,154,152
  152 IF(BU)153,153,158
  153 PRU=PRU+2.*PI
      GO TO 158
  154 PRU=PRU+PI
  158 CONTINUE
      PDU=360.*PRU/(2.*PI)
      VCOM(N5)=VCOM(N5)*CEXP(I*THETAR(N5))
      RL=C(N5)/(RS*RS+(N5*2.*PI*F*LL)**2)
      AFF=RL*(RS*COS(PR(N5))-N5*2.*PI*F*LL*SIN(PR(N5)))
      BF=RL*(RS*SIN(PR(N5))+N5*2.*PI*F*LL*COS(PR(N5)))
      CF=SQRT(AFF*AFF+BF*BF)
      PRN=ATAN(BF/AFF)
      IF(AFF)174,174,172
  172 IF(BF)173,173,178
  173 PRN=PRN+2.*PI
      GO TO 178
  174 PRN=PRN+PI
  178 CONTINUE
      PRF(N5)=PRN
      PDN=PRN*180./PI
      AFF=AFF/(PI*R*R)
      BF=BF/(PI*R*R)
      CF=CF/(PI*R*R)
      AN=AFF
      BN=BF
      CN=CF
      IF(NFLOW.EQ.0) GO TO 189
      AN=AFF*PI*R*R
      BN=BF*PI*R*R
      CN=CF*PI*R*R
      AU=AU*PI*R*R
      BU=BU*PI*R*R
      CU=CU*PI*R*R
      AW=AW*PI*R*R
      BW=BW*PI*R*R
      CW=CW*PI*R*R
  189 CONTINUE
      IF(N5.EQ.7)CALL SKIP
      WRITE(6,190)N5
  190 FORMAT(/1X,'HARMONIC'I2)
      WRITE(6,200)AN,BN,CN,PRN,PDN
```

```
200 FORMAT(1X,'FRY'10X,'A='F8.4,3X,'B='F8.4,3X,'C='F8.
    *4,5X,'PHASE (RAD
    *)='F7.4,3X,'PHASE (DEG)='F8.1)
     WRITE(6,201)AU,BU,CU,PRU,PDU
201 FORMAT(1X,'UCHIDA'7X, 'A='F8.4,3X,'B='F8.4,3X,'C='
    *F8.4,5X,'PHASE (
    *RAD)='F7.4,3X,'PHASE (DEG)='F8.1)
     WRITE(6,202)AW,BW,CW,PRW,PDW
202 FORMAT(1X,'WOMERSLEY'4X,'A='F8.4,3X,'B='F8.4,3X,'C
    *='F8.4,5X,'PHASE
    * (RAD)='F7.4,3X,'PHASE (DEG)='F8.1)
     WRITE(6,210)PHASEV,ATTEN,WAVEL
210 FORMAT(/14X,'PHASE VELOCITY='F9.2,5X,'ATTENUATION
    *PER WAVELENGTH='
    *F7.5,3X,'WAVELENGTH='F7.2/)
     AG=N5
     A=AA*SQRT(AG+1.)
     FRY(N5)=CF
     XA(N5,1)=AN
     XB(N5,1)=BN
     XA(N5,2)=AU
     XB(N5,2)=BU
     XA(N5,3)=AW
     XB(N5,3)=BW
255 CONTINUE
     DO 257 N6=1,3
     WRITE(7,20)XM(N6),(XA(N5,N6),N5=1,J)
     WRITE(7,21)(XB(N5,N6),N5=1,7)
     WRITE(7,20)(XB(N5,N6),N5=8,J)
257 CONTINUE
     CALL SKIP
     WRITE(6,260)
260 FORMAT(///1X,'VELOCITY AND PRESSURE GRADIENT AS A
    *FUNCTION OF THET
    *A FOR ONE CYCLE'///)
     KK=NPC
     DO 270 N6=1,KK
     NT=2.*PI*(N6-1.)/KK
     T=NT/(2.*PI*F)
     WT=GG*R*R*AO/(8.*MU)
     VT=GG*R*R*AO/(8.*MU)
     VFT=AO/(RS*PI*R*R)
     IF(NFLOW.EQ.0) GO TO 265
     WT=WT*PI*R*R
     VT=VT*PI*R*R
     VFT=VFT*PI*R*R
265 CONTINUE
     PGT=AO
     PGT=PGT/UNITPG
     NTD=NT*180./PI
     NTDD(N6)=NTD
     DO 269 N7=1,J
```

```
      W=REAL(WCOM(N7)*CEXP(I*N7*NT))
      VR=REAL(VCOM(N7)*CEXP(I*N7*NT))
      VF=FRY(N7)*COS(N7*NT-PRF(N7))
      IF(NFLOW.EQ.0) GO TO 268
      W=W*PI*R*R
      VR=VR*PI*R*R
      VF=VF*PI*R*R
  268 CONTINUE
      WT=WT+W
      VT=VT+VR
      VFT=VFT+VF
      PG=C(N7)*COS(N7*NT-PR(N7))
      PG=PG/UNITPG
      PGT=PGT+PG
  269 CONTINUE
      IF(N6-1)280,279,280
  279 CONTINUE
      S(KK+1,1)=VFT
      S(KK+1,2)=VT
      S(KK+1,3)=WT
      S(KK+1,4)=PGT
      S(KK+1,4)=PGT*100.
  280 CONTINUE
      S(N6,4)=PGT
      S(N6,4)=PGT*100.
      WRITE(6,300)NTD,S(N6,4),VFT,VT,WT
  300 FORMAT(1X,'THETA='F5.1,2X,'PRESSURE GRADIENT='F7.2
     *,2X,'VELOCITY(FR
     *Y)='F8.3,2X,'VELOCITY(UCHIDA)='F8.3,2X,'VELOCITY(W
     *OMERSLEY)='F8.3)
      S(N6,1)=VFT
      S(N6,2)=VT
      S(N6,3)=WT
  270 CONTINUE
      NTD=360.0
      WRITE(6,300)NTD,S(KK+1,4),S(KK+1,1),S(KK+1,2),S(KK
     *+1,3)
      CALL SKIP
      IPNT=0
      ISTOP=0
      KK=KK+1
      NTDD(KK)=360.
      DO 360 L=1,KK
      IF(L.EQ.KK)ISTOP=1
      DO 350 N=1,4
  350 CALL FPLOT(800,IPNT,AR,LR,ISTOP,N,4,NTDD(L),S(L,N)
     *)
  360 CONTINUE
      CALL SKIP
      STOP
      END
```

APPENDIX D

TIME DERATIVES

It was mentioned in section 1.2 that the time derative of a function was going to be related to the axial gradient. This can be done the following way

$$\frac{\Delta F(t)}{\Delta z} \approx \frac{\Delta F(t)}{\Delta t} \frac{\Delta t}{\Delta z} \tag{D.1}$$

but $\Delta z/\Delta t$ is the speed at which the pulse way propagates -c. Therefore

$$-\frac{\Delta F}{\Delta z} = \frac{1}{c} \frac{\Delta F}{\Delta t} \tag{D.2}$$

It has been shown that c can be approximated by the group velocity. The standard method of computing the group velocity is to determine the time required for the foot of the wave to travel from recording point one to the second point, and divide this difference into the distance between the sites. This is done in the computor program shown in this appendix. A set of two Fourier coefficients are read in and the digital points are recalculated by series expansion.

A sorting routine is used to determine the minimum value of both waves. Given this time difference between these minimum values, the group velocity is found by one

division. The time derative is then calculated using equation (D.2) and the results shown in graphical form.

```
C THIS PROGRAM COMPUTES SPATIAL GRADIENTS FROM TEMPORAL
C DEVIVATIVE. THE GROUP VELOCITY IS FOUND BY DETERMINING
C THE TIME DIFFERENCE BETWEEN THE FOCT OF THE WAVE ON
C TWO CURVES.SUBROUTINES NEEDED ARE SKIP,AMIN1 AND FPLOT
C
      DIMENSION A(15,6),B(15,6),C(15,6),PR(15,6),PRD(15,
     *6),A0(6),
     *APV(15),GROUPV(6)
      DIMENSION F1(200),F2(200)
      DIMENSION D(200,6),AR(800)
      DIMENSION A1(10,4),B1(10,4),A2(10,4),B2(10,4)
      REAL NTDD(200)
      REAL NT,NTD
      LOGICAL*1 LR(400)
      REAL NT1,NT2
C INPUT NUMBER OF DATA SHEETS
      NDS=1
      DO 120 KK=1,NDS
C INPUT NUMBER OF DIGITAL POINTS,SAMPLING RATE,GRADIENT
C DISTANCE,NUMBER OF DATA CHANNELS AND NUMBER OF
C HARMONICS.
      READ(5,5)K,SAMRAT,DIST,NDCH,J
    5 FORMAT(I10,2F10.2,2I5)
      DIST=DIST*30.48
      PI=4.*ATAN(1.)
      F=SAMRAT/K
      W=2.*PI*F
      DO 4 II=1,NDCH
C INPUT UPSTREAM AND DOWNSTREAM FUNCTIONS TO BE
C DIFFERENTIATED.
      READ(5,1)A0(II),(A(I,II),I=1,7)
    1 FORMAT(8E10.4)
      READ(5,1)(A(I,II),I=8,J)
      READ(5,2)(B(I,II),I=1,7)
    2 FORMAT(10X,7E10.4)
      READ(5,1)(B(I,II),I=8,J)
      DO 3 N1=1,J
      C(N1,II)=SQRT(A(N1,II)**2+B(N1,II)**2)
      PR(N1,II)=ATAN2(B(N1,II),A(N1,II))
      PRD(N1,II)=PR(N1,II)*180./PI
      IF(PR(N1,II).LT.0.)PR(N1,II)=PR(N1,II)+2.*PI
      IF(PRD(N1,II).LT.0.)PRD(N1,II)=PRD(N1,II)+360.
    3 CONTINUE
    4 CONTINUE
      K1=K+1
      DO 50 II=1,3,2
      DO 20 N=1,K
      SUMT1=A0(II)
      SUMT2=A0(II+1)
      NT=2.*PI*(N-1)/K
      DO 9 N1=1,J
      SUM1=C(N1,II)*COS(NT*N1-PR(N1,II))
```

```
      SUM2=C(N1,II+1)*COS(NT*N1-PR(N1,II+1))
      SUMT1=SUMT1+SUM1
      SUMT2=SUMT2+SUM2
    9 CONTINUE
      F1(N)=SUMT1
      F2(N)=SUMT2
   20 CONTINUE
      SMALL1=F1(1)
      SMALL2=F2(1)
      DO 30 M=2,K
      SMALL1=AMIN1(F1(M),SMALL1)
      SMALL2=AMIN1(F2(M),SMALL2)
      IF(SMALL1.EQ.F1(M))NT1=M
      IF(SMALL2.EQ.F2(M))NT2=M
   30 CONTINUE
      DELTAT=(NT2-NT1)/K
      GROUPV(II)=DIST/DELTAT
      GROUPV(II+1)=GROUPV(II)
      CALL SKIP
      DO 40 N1=1,J
      APV(N1)=-DIST*W/(PR(N1,II)-PR(N1,II+1))
      WRITE(6,35)C(N1,II),PRD(N1,II),C(N1,II+1),PRD(N1,I
     *I+1),APV(N1)
   35 FORMAT(1X,'FOURIER MODULUS 1=',F12.8,2X,'PHASE='F6
     *.1,2X,'FOURIER M
     *ODULUS 2=',F12.8,2X,'PHASE='F6.1,2X,'APPARENT PHAS
     *E VELOCITY='F9.1
     *)
   40 CONTINUE
      WRITE(6,45)A0(II),A0(II+1)
   45 FORMAT(/13X,'MEAN VALUE 1=',F8.4,5X,'MEAN VALUE 2=
     *',F8.4)
      WRITE(6,46)GROUPV(II)
   46 FORMAT(/13X,'GROUP VELOCITY IS',F7.1/////)
   50 CONTINUE
      CALL SKIP
      I3=5
      DO 95 II=1,4
      CALL SKIP
      IF(II.EQ.3)I3=6
      DO 90 N=1,K1
      SUMT=A0(I3)
      SUMDT=A0(I3)
      NT=2.*PI*(N-1)/K
      NTD=(N-1)*360./K
      NTDD(N)=NTD
      DO 78 N1=1,J
      SUM=C(N1,I3)*COS(NT*N1-PR(N1,I3))
      SUMT=SUMT+SUM
      SUMD=(N1*W/GROUPV(II))*C(N1,II)*COS(NT*N1-PR(N1,II
     *)+PI/2.)
      SUMDT=SUMDT+SUMD
```

```
 78 CONTINUE
    DIFF=(SUMT-SUMDT)*100./SUMT
    D(N,II)=SUMDT
    IF(II.EQ.2)D(N,II+3)=SUMT
    IF(II.EQ.4)D(N,II+2)=SUMT
    WRITE(6,75)NTD,SUMT,SUMDT,DIFF
 75 FORMAT(1X,'THETA='F6.1,2X,'ACTUAL GRADIENT='F12.8,
   *2X,'DIFFERENTIAT
   *ED GRADIENT='F12.8,2X,'PERCENT DIFFERENCE='F8.2)
 90 CONTINUE
 95 CONTINUE
    CALL SKIP
    I=4
    DO 110 II=1,3,2
    WRITE(6,99)
 99 FORMAT(18X,'ACTUAL UPSTREAM', 4X,'ACTUAL DOWNSTREA
   *M' 3X,'ACTUAL GR
   *ADIENT' 5X,'CALC UPSTREAM', 6X,'CALC DOWNSTREAM'//
   */)
    IF(II.EQ.3)I=3
    DO 109 N1=1,J
    CP1=N1*W*C(N1,II)/GROUPV(II)
    CP2=N1*W*C(N1,II+1)/GROUPV(II+1)
    P1=(PR(N1,II)-PI/2.)*180./PI
    P2=(PR(N1,II+1)-PI/2.)*180./PI
    IF(P1.LT.0.)P1=P1+360.
    IF(P2.LT.0.)P2=P2+360.
    A1(N1,II)=CP1*SIN(P1)
    B1(N1,II)=CP1*COS(P1)
    A2(N1,II+1)=CP2*SIN(P1)
    B2(N1,II+1)=CP2*COS(P2)
    WRITE(6,100)C(N1,II),C(N1,II+1),C(N1,II+I),CP1,CP2
100 FORMAT(1X,'MODULI',3X,5F20.8)
    WRITE(6,101)PRD(N1,II),PRD(N1,II+1),PRD(N1,II+I),P
   *1,P2
101 FORMAT(1X,'PHASES',3X,5(F13.1,7X)/)
109 CONTINUE
    WRITE(6,111)
111 FORMAT(////)
    CALL SKIP
110 CONTINUE
    IA=5
    DO 125 II=1,2
    WRITE(7,1)A0(IA),(A1(N1,II),N1=1,J)
    WRITE(7,2)(B1(N1,II),N1=1,7)
    WRITE(7,1)(B1(N1,II),N1=8,J)
    WRITE(7,1)A0(IA),(A2(N1,II+1),N1=1,J)
    WRITE(7,2)(B2(N1,II+1),N1=1,7)
    WRITE(7,1)(B2(N1,II+1),N1=8,J)
    IA=IA+1
125 CONTINUE
    II=1
```

```
      L2=3
      DO 160 L=1,2
      IPNT=0
      ISTOP=0
      DO 150 N=1,K1
      NC=0
      DO 140 N1=L1,L2
      NN=N1
      IF(N1.EQ.3)NN=5
      IF(L.EQ.2)NN=N1
      IF(N1.EQ.5)NN=6
      NC=NC+1
      IF(N.EQ.K1)ISTOP=1
      CALL FPLOT(800,IPNT,AR,LR,ISTOP,NC,3,NTCC(N),D(N,N
     *N))
  140 CONTINUE
  150 CONTINUE
      L1=L1+2
      L2=L2+2
      CALL SKIP
  160 CONTINUE
  120 CONTINUE
      STOP
      END
```

APPENDIX E

CALCULATION OF STRESS-STRAIN RELATIONSHIPS

The elasticity models shown in sections 2.6 and 5.1 require the input of pressure versus diameter data. This digital data is inputted to the program shown in this appendix and stress-strain data is calculated for all five models. The strains in all three directions are computed along with the axial and hoop stress. The curves are all fitted with fifth order polynomials for determination of the slope (Young's Modulus) at each point. The output is then plotted in graphical form for comparison of the various models.

```
C THIS PROGRAM INPUTS PRESSURE-VOLUME DATA,COMPUTES
C STRESS-STRAIN RELATIONSHIPS OF FIVE MODELS AND LEAST
C SQUARE FITS THE RESULTING INFORMATION. SUBROUTINES
C REQUIRED FOR USE OF THIS PROGRAM ARE SKIP,LSQ
C AND FPLOT.
C
      DIMENSION SZ(50),ST(50)
      DIMENSION X(50),Y(50)
      DIMENSION YY(50),XX(50)
      DIMENSION E(50)
      DIMENSION S(100,5),AR(800)
      DIMENSION XZ(50),EA(50),HH(50)
      LOGICAL*1 LR(400)
      DOUBLE PRECISION A(6,7),P(10),ANSWER(6)
      DIMENSION D(50),PR(50)
C INPUT CALIBRATION DATA.
      DATA NPOINT,DSCALE,PSCALE,HO,V,DO/36,C.025,1.0,0.0
     *50,C.5,0.725/
C INPUT DIAMETER AND PRESSURE DIGITAL POINTS.
      READ(5,1)(X(I),I=1,NPOINT)
      READ(5,1)(Y(I),I=1,NPOINT)
    1 FORMAT(12F6.3)
      CALL SKIP
      DH=DO/HO
      E(1)=0.
      V4=4.*V**2+3.*V-1.
      V2=2.*V**2+V-1.
      V1=V*(V+1.)
      DO 22 I=1,NPOINT
      D(I)=DSCALE*X(I)
      D(I)=D(I)+DO
      PR(I)=PSCALE*Y(I)
      X(I)=(D(I)-D(1))/D(1)
      IF(I.EQ.1)EA(1)=0.
      IF(I.EQ.1)HH(1)=HO
      IF(I.EQ.1) GO TO 12
      EA(I)=PR(I)*.5*D(I)*(1.-V**2)/(HO*X(I))
      DHI=D(I)/HO
      B=1.+(DO-D(I))*V*DHI/(D(I)-HO)+DHI-PR(I)*V4*DHI/(2
     *.*EA(I))
      AC=(PR(I)*V2/EA(I)-(DO-D(I))*V/(D(I)-HO)-1.)*(.5*P
     *R(I)*DHI**2*V1/E
     *A(I)-DHI)
      AA=V2*PR(I)/EA(I)-1.-(DO-D(I))*V/(D(I)-HO)
      HH(I)=HO*(-B+SQRT(B**2-4*AC))/(2.*AA)
   12 CONTINUE
      XZ(I)=-1.+(DO*HO-HO**2)/(D(I)*HH(I)-HH(I)**2)
      XR=HH(I)/HO-1.
      WRITE(6,13)PR(I),X(I),XZ(I),XR,EA(I)
   13 FORMAT(1X,@PRESSURE=@F6.3,2X,@TANGENTIAL STRAIN=@F
     *8.5,2X,@AXIAL ST
     *RAIN=@F8.5,2X,@RADIAL STRAIN=@F8.5,2X,@MODULUS=@F6
```

```
     *.1)
  22 CONTINUE
      CALL SKIP
      DO 24 I=1,NPOINT
      SZ(I)=2.*V*PR(I)*((D(I)/2.)**2-D(I)*HH(I)+HH(I)**2
     *)/(D(I)*HH(I)
     *-HH(I)**2)+XZ(I)*EA(I)
      ST(I)=PR(I)*(D(I)**2-4.*D(I)*HH(I)+4.*HH(I)**2)/(2
     *.*D(I)*HH(I)-HH(
     *I)**2)
      WRITE(6,8)PR(I),ST(I),SZ(I),D(I),HH(I)
    8 FORMAT(1X,@PRESSURE=@F6.3,2X,@HOOP STRESS=@F5.1,2X
     *, @AXIAL STRESS=
     *@F5.1,2X,@DIAMETER=@F5.3,2X,@WALL THICKNESS=@F6.4)
  24 CONTINUE
      DO 50 J=1,5
      CALL SKIP
      SNT=0.
      SDT=0.
      DO 40 I=1,NPOINT
      H=HH(I)
      IF(J.EQ.1)GO TO 17
      IF(J.EQ.2)GO TO 18
      IF(J.EQ.3)GO TO 19
      IF(J.EQ.4) GO TO 21
      IF(J.EQ.5) GO TO 23
  17 CONTINUE
      Y(I)=(PR(I)*D(I))/(2.*H)
      GO TO 25
  18 CONTINUE
      Y(I)=PR(I)*(D(I)**2-4.*D(I)*H+4.*H**2)/(2.*(D(I)*H
     *-H**2))
      GO TO 25
  19 CONTINUE
      Y(I)=PR(I)*(1.-V**2)*(D(I)**2-4.*D(I)*H+4.*H**2)/(
     *2.*(DO*HO-HO**2)
     *)
      GO TO 25
  21 CONTINUE
      Y(I)=PR(I)*D(I)*(1.-V**2)/(2.*H)
      GO TO 25
  23 CONTINUE
      IF(I.EQ.1)Y(1)=0.
      IF(I.EQ.1)GO TO 25
      Y(I)=PR(I)*(1.-V**2)*(D(I)**2-4.*D(I)*H+4.*H**2)/(
     *(2.*(DO*H-H**2))
     **(1.+V*X2(I)/X(I)))
      GO TO 25
  25 CONTINUE
      S(I,J)=Y(I)
      IF(I.EQ.1)GO TO 20
      E(I)=(Y(I)-Y(I-1))/(X(I)-X(I-1))
```

```
      SN=X(I)*Y(I)
      SD=X(I)*X(I)
      SNT=SNT+SN
      SDT=SDT+SD
      EMOD=SNT/SDT
   20 CONTINUE
      IF(I.EQ.1)EMOD=0.
      PRM=PR(I)*760./14.696
      WRITE(6,30)PRM,Y(I),D(I),X(I),E(I),EMOD
   30 FORMAT(1X,@PRESSURE=@F5.1,2X,@STRESS=@F5.1,2X,@DIA
     *METER=@F6.4,2X,@
     *STRAIN=@F7.5,2X,@ELASTIC MODULUS=@F6.1,2X,@LEAST S
     *QUARE MODULUS=@F
     *6.1)
   40 CONTINUE
      DO 15 JJ=1,2
      DO 47 I=1,NPOINT
      IF(JJ.EQ.2)GO TO 45
      YY(I)=Y(I)
      XX(I)=X(I)
      GO TO 47
   45 YY(I)=X(I)
      XX(I)=Y(I)
   47 CONTINUE
      DO 15 I=1,5
      CALL LSQ(YY,XX,I,24,ANSWER,NCGO,JRETRN,A,P)
      II=I+1
      WRITE(6,10)I,(ANSWER(K),K=1,II)
   10 FORMAT(@0@,1X,@DEGREE@;I3, 3X,@COEFFICIENTS ARE@/
     * @ @,6F20.10)
   15 CONTINUE
   50 CONTINUE
      CALL SKIP
      KK=NPOINT
      IPNT=0
      ISTOP=0
      DO 80 L=1,KK
      IF(L.EQ.KK)ISTOP=1
      DO 90 N=1,5
   90 CALL FPLOT(800,IPNT,AR,LR,ISTOP,N,5,X(L),S(L,N))
   80 CONTINUE
      CALL SKIP
      STOP
      END
```

APPENDIX F

CURVE FITTING PROGRAM

The program shown in this appendix fits a set of n points of y versus x to a first through fifth order polynomial both for the case of y and x each as the independent variable. The polynomial coefficients are then outputted and the input data plotted.

```
C       THIS PROGRAM CURVE FITS Y VS X AND X VS Y WITH A
C       FIRST THROUGH A FIFTH ORDER POLYNOMIAL VIA LEAST
C       SQUARE ANALYSIS.SUBROUTINES NEEDED TO DO THIS ARE
C       SKIP,LSQ,DIMILQ AND FPLOT.
C
        DIMENSION AR(100),X(100),Y(100)
        DOUBLE PRECISION A(6,7),P(10),ANSWER(6)
        LOGICAL*1 LR(400)
C INPUT NUMBER OF DIGITAL POINTS.
        READ(5,1)NPNT
      1 FORMAT(I3)
        CALL SKIP
        I1=1
        I2=12
C INPUT SCALING FACTORS AND SHIFTS.
        READ(5,5)SCX,SSX1,SSX2
      5 FORMAT(3F10.5)
C INPUT X DATA.
        DO 21 MA=1,10
        READ(5,20)(X(MB),MB=I1,I2),IEND
     20 FORMAT(12F6.3,I2)
        IF(IEND.EQ.1) GO TO 22
        I1=I1+12
        I2=I2+12
     21 CONTINUE
     22 CONTINUE
        I1=1
        I2=12
C INPUT SCALING FACTORS AND SHIFTS.
        READ(5,5)SCY,SSY1,SSY2
C INPUT Y DATA.
        DO 23 MA=1,10
        READ(5,20)(Y(MB),MB=I1,I2),IEND
        IF(IEND.EQ.1) GO TO 24
        I1=I1+12
        I2=I2+12
     23 CONTINUE
     24 CONTINUE
        DO 25 I=1,NPNT
        X(I)=(X(I)+SSX1)*SCX+SSX2
        Y(I)=(Y(I)+SSY1)*SCY+SSY2
     25 CONTINUE
        DO 36 J=1,2
        DO 32 L=1,NPNT
        HOLD=Y(L)
        Y(L)=X(L)
        X(L)=HOLD
     32 CONTINUE
     33 CONTINUE
        DO 35 I=1,5
        CALL LSQ(X,Y,I,NPNT,ANSWER,NCGO,JRETRN,A,P)
        II=I+1
```

```
      CALL SKIP
      WRITE(6,30)I,(ANSWER(K),K=1,II)
   30 FORMAT(@ @,1X,@DEGREE@,I3,3X,@COEFFICIENTS ARE@/@0
     *@,6D15.5)
      WRITE(6,37)
   37 FORMAT(///)
      DO 38 K=1,NPNT
      YF=ANSWER(1)
      DO 34 KK=2,II
      YFT=ANSWER(KK)*X(K)**(KK-1)
      YF=YF+YFT
   34 CONTINUE
      IF(Y(K).EQ.0.)PERC=0.
      IF(Y(K).EQ.0.)GO TO 31
      PERC=(Y(K)-YF)*100./Y(K)
   31 CONTINUE
      WRITE(6,40)X(K),Y(K),YF,PERC
   40 FORMAT(10X,@ABSCISSA IS@F10.5,5X,@ORDINATE IS@,F10
     *.5,5X,@FITTED OR
     *DINATE IS@F10.5,5X,@PERCENT DIFFERENCE IS@F10.5)
   38 CONTINUE
   35 CONTINUE
      CALL SKIP
      IPNT=0
      ISTOP=0
      DO 80 L=1,NPNT
      IF(L.EQ.NPNT)ISTOP=1
      CALL FPLOT(800,IPNT,AR,LR,ISTOP,1,1,X(L),Y(L))
   80 CONTINUE
      CALL SKIP
   36 CONTINUE
      CALL SKIP
      STOP
      END
```

APPENDIX G

SUBROUTINES

This appendix contains all the subroutines necessary to complete any program listed in previous appendices. Each program contains a comment card with a list of needed subroutines and all are listed here for convenience.

```
      SUBROUTINE FPLOT(M1,IPNT,AR,LR,ISTOP,NC,NCMAX,V1,V
     *2)                                                1
      LOGICAL*1 LM(2),LN(120),LP(4),LX(4),LR(1),LC(20)
      INTEGER*2 IM,IR(802),RI(2),ST(2),SG(2),IA(238),N12
     *0,N58                                             3
      DIMENSION AR(M1),N(30),RHO(30),Z(15),ICFF(2),ISP(2
     *),SF1(2),SF2(2),                                  4
     *ID(2),ISG(2),II(4)
      EQUIVALENCE (IP,LP(1)),(IM,LM(1)),(LN(1),N(1),RHO(
     *1)),(IX,LX(1)),                                   6
     *(N120,RI(1)),(N58,RI(2))
      DATA Z(1),Z(2),Z(3),Z(4),Z(5),Z(6),Z(7),Z(8),Z(9),
     *Z(10),Z(11),                                      8
     * Z(12),Z(13),Z(14),Z(15)/1.,1.25,1.5,1.75,2.,2.5,3
     *.,3.5,4.,4.5,5.,                                  9
     *6.,7.,8.,9./,ISP(1),ISP(2),IX,IP,IM/10,5,4HXXXX,4H
     *++++,0/                                          10
      DATA ID(1),ID(2),ISG(1),ISG(2)/120,58,1,-1/
      IF(ISTOP)173,172,172
172   J=IPNT+2
      IF(J.GT.M1)GO TO 173
      IPNT=J
      AR(J-1)=V1
      AR(J)=V2
      IM=NC
      J=J/2
      LR(J)=LM(2)
173   IF(NC.LT.NCMAX)RETURN
      IF(ISTOP.EQ.0)RETURN
103   READ(5,1)LN(1),(II(I),I=1,4),(LC(I),I=1,20),(LN(I)
     *,I=2,52)                                         23
    1 FORMAT(A1,2I3,2I1,71A1)
      WRITE(6,1)LN(1),(II(I),I=1,4),(LC(I),I=1,20),(LN(I
     *),I=2,52)                                        25
      DO 171 I=1,2
      RI(I)=ID(I)
      SG(I)=ISG(I)
      IF(II(I).NE.0)RI(I)=II(I)
      IF(II(I+2).EQ.1)SG(I)=-SG(I)
171   ST(I)=(RI(I)+1-SG(I)*(RI(I)-1))/2
      IF(RI(1).GT.120)RI(1)=120
      IF(RI(2).GT.238)RI(2)=238
      N30=N120/4
      N120=4*N30
      DO 3 I=1,2
      AMIN=AR(I)
      AMAX=AR(I)
      DO 7 J=I,IPNT,2
      AA1=AR(J)
      IF(AMIN.GT.AA1)AMIN=AA1
    7 IF(AMAX.LT.AA1)AMAX=AA1
      R=AMAX-AMIN
```

```
      IF(R.EQ.0.AND.AMAX.EQ.0)R=1.
      IF(R.EQ.0.AND.AMAX.LT.0)R=-AMAX
      IF(R.EQ.0.AND.AMAX.GT.0)R=AMAX
      DO 22 J=1,15
      B=ALOG10(R/(RI(I)-2)/Z(J))
      M=B
      IF(B.LT.0)M=M-1
      C=Z(J)*10.**(M+1)
      B=AMIN/Z(J)/10.**(M+1)
      I1=B
      IF(B.LT.0)I1=I1-1
      IF((RI(I)-2+I1)*C-AMIN)18,19,19
   18 C=10.*C
   19 IF(J.EQ.1)SMIN=C
   22 IF(C.LT.SMIN)SMIN=C
      SF1(I)=(1./SMIN)*SG(I)
      B=AMIN/SMIN
      M=B
      IF(B.LT.0)M=M-1
      SF2(I)=ST(I)-M*SG(I)
      RHO(I)=SF2(I)+0.5
      M=SF2(I)
      DO 25 J=1,10
      IF(M-J-((M-J)/ISP(I))*ISP(I))25,3,25
   25 CONTINUE
    3 IOFF(I)=J
      DO 101 I=1,N58
  101 IA(I)=0
      DO 102 J=1,IPNT,2
      IR(J)=SF1(1)*AR(J)+RHO(1)
      IT=SF1(2)*AR(J+1)+RHO(2)
      IF(J.NE.1)GO TO 109
      IR(IPNT+2)=2
      IR(J+1)=0
  108 I3=IT
      GO TO 102
  109 IF(IT-I3)104,105,105
  104 IR(J+1)=IR(IPNT+2)
      IR(IPNT+2)=J+1
      GO TO 108
  105 I=IT+1
  106 I=I-1
      I1=IA(I)
      IF(I1)106,106,107
  107 IR(J+1)=IR(I1)
      IR(I1)=J+1
  102 IA(IT)=J+1
      LAST=IPNT+2
      JJ=IOFF(2)
      LZH=SF2(1)
      LZV=SF2(2)
      DO 100 I=1,N58
```

```
      DO 40 J=1,N30
   40 N(J)=0
      IF((I-1)*(I-N53))140,151,140
  151 DO 141 J=1,N30
  141 N(J)=IX
  140 LN(1)=LX(1)
      LN(N120)=LX(1)
      IF(LZH.LE.0.OR.LZH.GT.N120)GO TO 131
      LN(LZH)=LP(4)
  131 NB=1
      IF(I.NE.JJ)GO TO 35
      NB=2
      JJ=JJ+5
      I3=IOFF(1)
      DO 32 J=I3,N120,10
   32 LN(J)=LP(4)
      IF(I.NE.LZV)GO TO 35
      DO 135 J=1,N30
  135 N(J)=IP
   35 I3=IA(I)
      IF(I3.EQ.0)GO TO 121
  120 LAST=IR(LAST)
      I2=IR(LAST-1)
      I1=LAST/2
      LM(2)=LR(I1)
      LN(I2)=LC(IM)
      IF(LAST.NE.I3)GO TO 120
  121 GO TO (38,41),NB
   38 WRITE(6,39)(N(J),J=1,N30)
   39 FORMAT(11H           ,30A4)
      GO TO 100
   41 AA1=I
      VALUE=(AA1-SF2(2))/SF1(2)
      WRITE(6,42)VALUE,(N(J),J=1,N30)
   42 FORMAT(1H ,1PE10.3,30A4)
  100 CONTINUE
      I3=IOFF(1)
      J=0
      DO 49 I=I3,N120,10
      J=J+1
      AA=I
   49 RHO(J)=(AA-SF2(1))/SF1(1)
      IF(IOFF(1)-5)62,62,63
   62 WRITE(6,50)(RHO(I),I=1,J)
   50 FORMAT(9X,12(1PE10.3))
      RETURN
   63 IF(J.GE.12)J=11
      WRITE(6,64)(RHO(I),I=1,J)
   64 FORMAT(15X,11(1PE10.3))
      RETURN
      END
```

```
      SUBROUTINE LSQ (X,Y,NDEG,NPTS,ANSWER,NOGO,JRETRN,A
     *,P)                    LSQ  001
      DIMENSION X(NPTS),Y(NPTS)
      DIMENSION A(1,1), ANSWER(1), P(1)
      DOUBLE PRECISION A,ANSWER,P,SUM
      NDEGX2=NDEG*2
      IF(NDEG)100,110,10
  100 JRETRN=1
      RETURN
  110 JRETRN=2
      RETURN
   10 IF (NPTS - NDEG) 130, 130, 18
  130 JRETRN = 4
      RETURN
   18 DO 12 I=1,NDEGX2
      SUM=0.
      DO 13 J=1,NPTS
   13 SUM=SUM+X(J)**I
   12 P(I)=SUM
      NEQ=NDEG+1
      DO 30 I=1,NEQ
      DO 30 J=1,NEQ
      K=I+J-2
      IF(K)29,29,28
   28 A(I,J)=P(K)
      GO TO 30
   29 A(1,1)=NPTS
   30 CONTINUE
      KONCOL=NEQ+1
      SUM=0.
      DO 21 J=1,NPTS
   21 SUM=SUM+Y(J)
      A(1,KONCOL)=SUM
      DO 22 I=2,NEQ
      SUM=0.
      DO 23 J=1,NPTS
   23 SUM=SUM+Y(J)*X(J)**(I-1)
   22 A(I,KONCOL)=SUM
      JRETRN=3
      CALL DIMILQ(NEQ,A,ANSWER,NOGO)
      RETURN
      END
```

```
      SUBROUTINE DIMILQ (N,A,X,NOGO)
      DIMENSION A(1,1), X(1)
      DOUBLE PRECISION A,X,DABS,S,D,DT,DBLE
      NOGO=0
    2 N1=N+1
      N2=N-1
      DO 3 L=1,N2
      L1=L+1
      K=L
      DO 5 J=L1,N
      IF(DABS(A(K,L))-DABS(A(J,L)))4,5,5
    4 K=J
    5 CONTINUE
      IF(A(K,L))6,18,6
    6 IF(K-L)12,12,13
   13 DO 10 J=L,N1
      S=A(K,J)
      A(K,J)=A(L,J)
   10 A(L,J)=S
   12 D=1./A(L,L)
      DO 14 J=L1,N1
   14 A(L,J)=A(L,J)*D
      DO 3 I=L1,N
      IF(A(I,L))15,3,15
   15 DT=1./A(I,L)
      DO 16 J=L1,N1
   16 A(I,J)=A(I,J)*DT-A(L,J)
    3 CONTINUE
      IF(A(N,N))17,18,17
   18 NOGO=1
      RETURN
   17 X(N)=A(N,N1)/A(N,N)
      DO 19 J=1,N2
      M=N-J
      DO 20 I=1,M
   20 A(I,N1)=A(I,N1)-X(M+1)*A(I,M+1)
   19 X(M)=A(M,N1)
      RETURN
      END
```

```
      REAL FUNCTION AMIN1(X,Y)
      IF(X.LT.Y)GO TO 1
      AMIN1=Y
      RETURN
    1 AMIN1=X
      RETURN
      END
```

```
      REAL FUNCTION AMAX1(X,Y)
      IF(X.GT.Y)GO TO 1
      AMAX1=Y
      RETURN
    1 AMAX1=X
      RETURN
      END
```

```
      SUBROUTINE SKIP
      WRITE(6,1)
    1 FORMAT('1')
      RETURN
      END
```

VITA

Melvin Richard Brashears was born in Alamogordo, New Mexico, on [redacted] the son of Gail Curtis Brashears and Robert Vaughn Brashears. He attended Mark Twain High School in Center, Missouri, and completed the requirements in May, 1963. Upon graduation he entered The University of Missouri at Columbia, and was awarded a Bachelor of Science Degree in Mechanical Engineering in June, 1967. Immediately following, he entered Graduate School at The University of Missouri at Columbia, and was employed as a Research Assistant in Mechanical Engineering. In January, 1969, he became a Teaching Assistant in the Mechanical Engineering Department and was awarded a National Science Foundation Fellowship. The following June, he earned a Master of Science Degree in Mechanical and Aerospace Engineering. He continued as a Teaching Assistant and a NSF Fellow until August, 1971. He then accepted a National Aeronautics and Space Administration Dissertation Fellowship to complete his Doctor of Philosophy Degree at The University of Missouri at Columbia.

University Libraries
University of Missouri

Digitization Information Page

Local identifier Brashears1971

Source information

Format	Book
Content type	Text
Source ID	Gift copy from department; not added to MU collection.
Notes	

Capture information

Date captured	March 2024
Scanner manufacturer	Fujitsu
Scanner model	fi-7460
Scanning system software	ScandAll Pro v. 2.1.5 Premium
Optical resolution	600 dpi
Color settings	8 bit grayscale
File types	tiff
Notes	

Derivatives - Access copy

Compression	Tiff: LZW compression
Editing software	Adobe Photoshop
Resolution	600 dpi
Color	grayscale
File types	pdf created from tiffs
Notes	Images cropped, straightened, brightened